ADVANCING CAPACITY FOR MARSH MODELING RETROSPECTIVE ANALYSIS

Elevation Mapping via Remote Sensing in Low Gradient Coastal Landscapes

CHRISTOPHER ESPOSITO, MARICEL BELTRAN BURGOS

Produced for and funded by the Gulf of America Alliance and Office for Coastal Management, National Oceanic and Atmospheric Administration

January 2026

ABOUT THE WATER INSTITUTE

The Water Institute is an independent, non-profit, applied research institution advancing science and developing integrated methods to solve complex environmental and societal challenges. We believe in and strive for more resilient and equitable communities, sustainable environments, and thriving economies. For more information, visit www.thewaterinstitute.org.

SUGGESTED CITATION

Advancing Capacity for Marsh Modeling Retrospective Analysis: Elevation Mapping via Remote Sensing in Low Gradient Coastal Landscapes (2026). The Water Institute. Prepared for and funded by the Gulf of America Alliance and Office for Coastal Management, National Oceanic and Atmospheric Administration. Baton Rouge, LA.

PREFACE

This study was conducted by The Water Institute (the Institute) for the Gulf of Americal Alliance (GOAA) as a component of efforts to develop the data foundation for retrospective numerical modeling in coastal marshes. The report is a deliverable of the "Advancing Capacity for Marsh Modeling Retrospective Analyses in the Gulf of Mexico" project under subgrant FG-122347. The project manager for GOAA was Kate Harrison. Christopher Esposito led the execution of this task and the writing of the report for the Institute. This report describes the development and implementation of a methodology to produce digital elevation models (DEMs) in coastal wetlands from satellite remote sensing inputs.

EXECUTIVE SUMMARY

High quality digital elevation models (DEMs) did not exist in coastal wetlands prior to the widespread adoption of aerial LiDAR for landscape surveys beginning in the early 2000s. And while LiDAR-derived DEMs are now widely available, they are expensive to produce and are not always collected at high temporal frequency. This report presents a novel method that employs satellite remote sensing data to produce DEMs in coastal marshes during periods of time when no other DEM or survey is available. Using this method, three DEMs were produced at coastal marshes along the Gulf Coast. These are at Grand Bay, MS, Apalachicola, FL, and Breton Sound, LA.

Wetland response to changing conditions is often understood as a balance between the wetland's vertical accretion rate and the rate of Relative Sea Level Rise (RSLR). But without frequent and spatially continuous elevation data, it is challenging to interpret how a wetland or region is responding. This is especially important in management settings where wetland managers seek to understand model outputs in the context of their experience, observations, history of management decisions, and perception of risk. The DEMs produced here will be the foundation of an effort to comparatively assess the performance of multiple marsh models at selected coastal marshes. They will serve as initialization conditions and valuable validation data for models that simulate the period from the early 1980s to the present.

To produce the DEMs, The Water Institute team compiled images of Landsat's Dynamic Surface Water Extent (DSWE) product that were collected within one year of an existing high-quality DEM. DSWE provides information about the presence or absence of surface water, which is used to produce maps showing inundation frequency at decadal timescales. The inundation frequency maps were then correlated to pre-existing LiDAR based DEMs to produce a function that relates inundation frequency with wetland elevation within the tidal frame. The function is then applied to the period before DEMs are widely available but during which Landsat sensors are consistent with today's standards (i.e., 1984 to the present), allowing the project team to produce DEMs that were not previously available. These are referred to as *synthetic DEMs*, and are validated with in-situ observational data as available. The method's reliance on inundation mapping is an effective strategy because inundation can be observed with remote sensing, is inherently connected to elevation, and is a useful marker of sea level in its own right.

The well organized and spatial structure of this method allows for straightforward integration with other data sets, including in-situ observations and geochronology to reduce and communicate uncertainty. An extensive code base was produced with this project, which will facilitate extension to additional coastal wetlands, and integration with numerical modeling.

TABLE OF CONTENTS

LIST OF FIGURES

1.0 INTRODUCTION

Coastal wetland management professionals frequently make decisions regarding the wetlands that they manage that will impact those areas both in the near-term and over the course of many decades. These include decisions over restoration resource allocation, informational and educational installations, and guidance to partners. In making these decisions, marsh managers can turn to predictive models to assess vulnerabilities to changing conditions and to receive guidance on the uncertainty surrounding marsh response to future conditions. While numerous predictive models are available for this purpose, there have historically been challenges in understanding the capabilities of different models, their accuracy, and how the models can appropriately be applied given different assumptions and limitations.

To assist wetland managers in choosing the model that works best for their marsh, and for their planning and communication needs, two workshops were conducted to facilitate dialogue between marsh managers and marsh modelers and to plan for more effective integration of marsh modeling into the management process. A 2018 workshop funded by the Gulf of America Alliance (GOAA) brought together coastal natural resource and fish and wildlife stewards from all five Gulf states, marsh modelers, and agencies that fund natural resource research (NOAA et al., 2018). Attendees identified the need for a retrospective analysis, in which marsh model performance is assessed against historic data to aid in understanding and applying model outputs to guide coastal management decision making. The retrospective marsh modeling effort was conceptualized to provide a platform for deeper engagement with wetland managers who have observed and personally interacted with their wetland systems across decades. Producing model outputs that corresponded with their experience, as well as with traditional validation metrics, would increase the uptake of modeling into their management practice. To plan this effort, a subsequent workshop was conducted in 2022 (Martin et al., 2022) to bring marsh modelers together to determine the most scientifically sound approach for a retrospective analysis.

In the 2022 workshop, marsh modelers were convened by the Southeast Climate Adaptation Science Center to consider the design and data needs of a marsh modeling retrospective analysis (Martin et al., 2022). Prior to the workshop organizers compiled wetland digital elevation models (DEMs), tidal datums, wetland vegetation coverage, and other relevant data dating back to the year 2000 for three representative coastal wetlands. This dataset was presented during the workshop, and marsh modelers worked from it to develop a list of data needs and identify candidate test locations for a retrospective study. Attendees decided that, due to the pace of marsh evolution, it was likely necessary to extend the retrospective analysis back to the year 1980, and that it would be possible to do this for Grand Bay, MS, Apalachicola, FL, and Breton Sound, LA. This set of sites met the needs of a retrospective analysis because 1) data are readily available at each, 2) the relevant marsh managers have a history of collaborative engagement, and 3) each location represents a different set of marsh evolution processes that contribute to the comparison and the impact of the project outcomes.

One of the key data needs that was identified as necessary to support this effort is a set of DEMs for each of the three wetland study areas that can be used to initialize a model to approximately 1980 and assess its performance through to the present. This report describes the effort to meet that need. It describes a methodology to produce DEMs of tidal wetlands during periods when Light Detection and Ranging

(LiDAR) or other directly surveyed data are not available. The methodology exploits the fact that in tidal wetlands the frequency of inundation is inherently connected to elevation, and that locations at higher elevations are inundated less frequently than those at lower elevations. Because there are vetted techniques for detecting inundation from satellite platforms, there is an opportunity to produce maps of inundation frequency that are predictive of elevation. This methodology can be used to produce DEMs as far back as 1982, when the U.S. Geological Survey (USGS) Landsat 4 mission began providing satellite remote sensing data at a spatial scale and set of imagery bands that have been consistently collected to the present day.

This report presents newly produced DEMs of wetlands in Grand Bay MS, Apalachicola, FL, and Breton Sound, LA, for each decade beginning in the 1980s. Because these DEMs differ from others that are produced from LiDAR or other direct surveying techniques, they are referred to herein as *synthetic DEMs*. The process by which synthetic DEMs are produced from remote sensing data and validated to in situ observations is described in Section 2.0, and the three sets of synthetic DEMs that were produced are presented and discussed individually in Section 3.0.

The widespread proliferation of LiDAR technology deployed either from drones or crewed aircraft has greatly expanded the availability of high quality DEMs in coastal wetlands over the past two decades. But because the relevant elevation gradients are so small, and obstacles such as vegetation are so prevalent, even the best aerial LiDAR survey is still subject to vertical errors that can be a significant component of the relief that the survey is attempting to capture. Alizad et al. (2020) documented vertical uncertainty in LiDAR surveys of microtidal wetlands on the Gulf Coast that was on the order of the entire tidal range. To account for this level of uncertainty, many practitioners in the field are improving techniques for rigorous supplemental in-situ surveys to provide more accurate correctors for the LiDAR data (Medeiros et al., 2015, 2022b).

The present study employs LiDAR-based DEMs that were collected in the previous 10 years to discern a relationship with wetland inundation frequency that can be applied to predict elevations in the decades before LiDAR was available. This process necessarily carries with it the uncertainty in the modern DEMs that are used as inputs, and it is useful to think of the uncertainty in a modern LiDAR study as a lower bound for the uncertainty in the synthetic DEMs that result from this effort. The synthetic DEMs are best used in conjunction with other datasets to ensure that they represent spatial and temporal trends of wetland elevation change in a way that comports with other observations.

Each coastal wetland that is studied is presented with a Validation to Observational Data section, and the code repository that was developed for this effort (Appendix A) is designed to facilitate a variety of comparisons to other elevation datasets. Despite the inherent uncertainty, it is important to note that there are no available DEMs of coastal wetlands prior to the early 2000s. As such, the synthetic DEMs represent a significant improvement in the availability of elevation datasets in coastal wetlands that can support numerical modeling efforts that initiate as far back as the 1980s.

An additional data product of this study are maps of wetland inundation frequency. These maps were primarily used in the synthetic DEM production workflow, but they are also likely to be useful to coastal marsh modeling efforts in their own right. These are presented in detail in the Results section.

2.0 METHODS

The synthetic DEM production workflow consisted of three essential steps. First, maps of wetland inundation frequency were produced on decadal timescales during the modern remote sensing era (1982–present). The maps of inundation frequency during the most recent decade (2010–2020) were then compared with directly surveyed DEMs representing the same time period to produce a functional relationship that uses wetland inundation frequency to predict land surface elevation within the tidal frame, where inundation frequency and elevation were expected to be correlated. The directly surveyed DEMs used in this step were typically derived from LiDAR, but any high quality spatially continuous elevation dataset would suffice. Finally, the functional relationship was applied to other time periods where remotely sensed inundation data was available to produce a map of elevation within that time period's tidal frame. These maps were then adjusted to account for changes in mean sea level to produce a synthetic DEM of that time period. Each of these three steps is described in detail below. All vertical data are presented in NAVD88 unless otherwise specified.

At each of the three study sites, a recent DEM was used to establish a relationship between inundation and elevation:

- Grand Bay: S. C. Medeiros, Alizad, et al., (2022).
- Apalachicola: S. C. Medeiros, Alizad, et al., (2022a).
- Breton: USGS (2020).

The synthetic DEMs are validated against records from surface elevation tables (SETs):

- SET data from Grand Bay and Apalachicola were obtained from the National Estuarine Research Reserve System Science Collaborative at https://nerrssciencecollaborative.org/resource/processed-surface-elevation-table-set-data-five-reserves.
- Breton: Coastwide Reference Monitoring System CRMS (2023).

The initial project plan was to produce DEMs by assessing changes to vegetation patterns in remotely sensed imagery. However, in the early phases of the project the Institute determined with NOAA that vegetation is not a sufficiently sensitive indicator of elevation, so this approach was discarded in favor of a focus on inundation frequency as a predictor. Results from the initial investigations are shown in Appendix C.

2.1. WETLAND INUNDATION FREQUENCY

The Institute team created maps of inundation frequency for every decade since 1980 by applying the USGS Landsat Collection 2 Level-3 Dynamic Surface Water Extent (DSWE) Product (Earth Resources Observation and Science Center [EROS], 2022). DSWE provides a pixel-level classification of every Landsat scene collected in the continental U.S., Alaska, or Hawaii since 1982 to indicate the presence of absence of surface water. After masking for clouds, snow, and shadow, each pixel is classified as "Water", "Not Water", or "Partial Surface Water" (Figure 1).

These classifications are made with a two-step process that takes the Landsat Surface Reflectance bands as input. In the first phase, a set of five Boolean diagnostic tests is applied to each pixel based on combinations of commonly accepted reflectance indices and thresholds. In the second phase each pixel is interpreted based on how many and which of the five tests return a True value, using a previously defined conversion table. These results are then packaged by USGS for download into an interpreted raster layer with all masks applied to it. The specific classification thresholds and band ratio combinations are described by (Earth Resources Observation and Science (EROS) Center, 2022b).

The Partial Surface Water category was developed to provide information about the presence or absence of standing surface water in the presence of vegetation (Jones, 2015, 2019), making it ideal for the task of identifying the frequency with which tidal wetlands are inundated. DSWE provides the option to use Partial Surface Water values produced by a conservative or an aggressive algorithm. For this analysis, the more aggressive estimate of Partial Surface Water coverage was used. A detailed description of the Partial Surface Water algorithms, their development, and their validation to wetlands in the Everglades can be found in the work of Jones (2015).

Landsat satellites collect data at every location on the globe approximately every 16 days. This allows for up to 22 data points to be collected each year at each pixel. This number is doubled during periods when two Landsat missions are operating simultaneously, but is reduced when pixels must be masked due to cloud cover or to known and documented data gaps in from Landsat 7 scenes (see Hossain et al., 2015 for a description of the Landsat 7 data gaps). Masking is also occasionally inconsistently applied in the Landsat record, with shorelines or other geographic transitions mistakenly masked as clouds or snow. Valid DSWE pixel availability at each site was based on the aforementioned constraints and served as an important statistical constraint on confidence in the uncertainty maps.

Maps of inundation frequency are computed for any selected time period by dividing the number of times a pixel is inundated according to DSWE by the number of times that pixel had any valid (i.e., unmasked) measurement. For this effort, the pixel was considered to be inundated if it was classified Partial Surface Water. Figure 2 shows the frequency of valid measurements at each pixel in the Grand Bay, MS study site from 2010 to 2020. This served as the denominator for the inundation frequency calculation, which was done at the level of each pixel. Note that variation in the number of valid measurements at each pixel occurred due to certain geomorphic features (e.g., shorelines) and structures. Striping is the result of a known issue with the data coverage in the Landsat 7 mission. Because the image frequency calculation was done on a pixel-by-pixel basis, this spatial variation did not affect the continuity of the inundation maps.

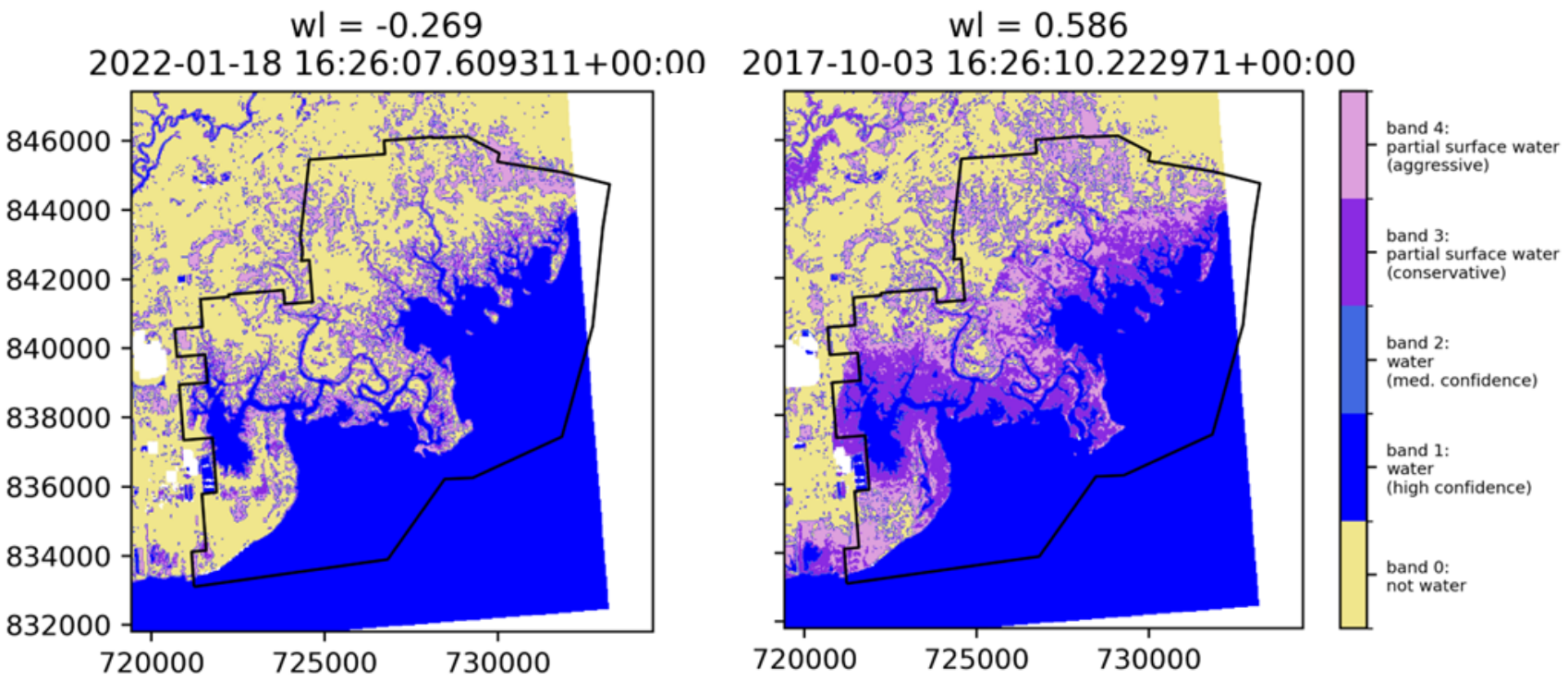

Figure 1. DSWE scenes at Grand Bay during a time of low water level (left) and high-water level (right). Note in particular the more extensive coverage of the Partial Surface Water bands during high water. Water level indicated is from the Dauphin Island gauge. The black outline represents the domain for the Grand Bay Anaysis

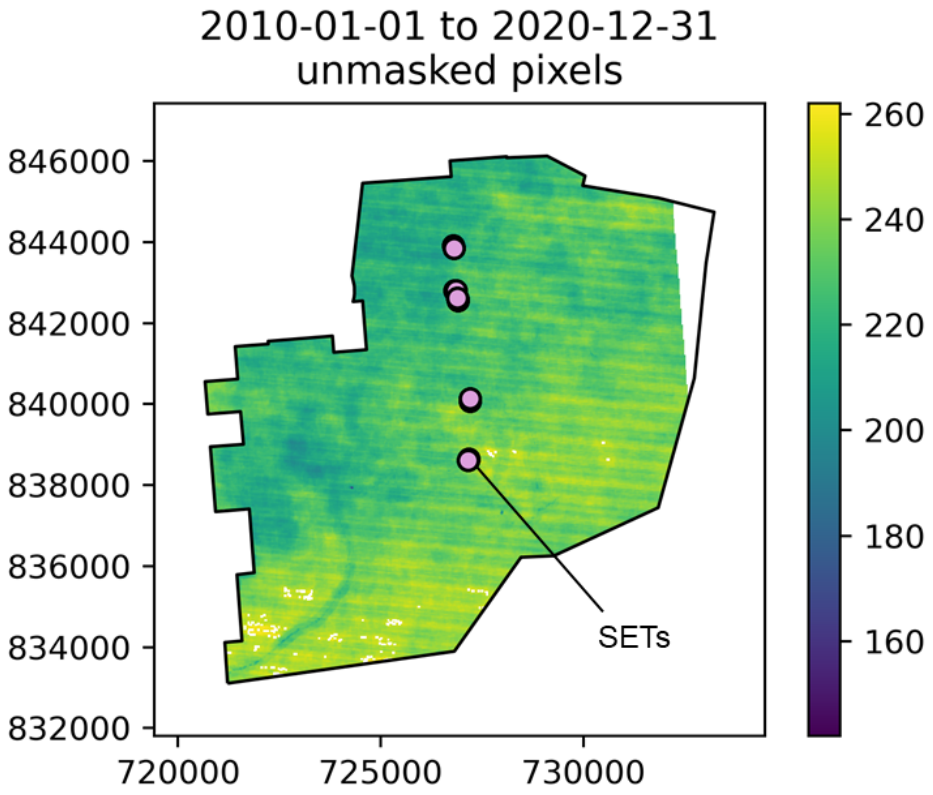

Figure 2. Frequency of valid measurements at each pixel in the Grand Bay study site during the time period 2010-01-01 to 2020-12-31.

In practice, a weighted average was necessary because the sampling time of Landsat scenes is not perfectly aligned with the tidal signal (Figure 3 and Figure 4). The weighting procedure ensured that the computed wetland inundation frequency was representative of the water levels experienced in the marsh.

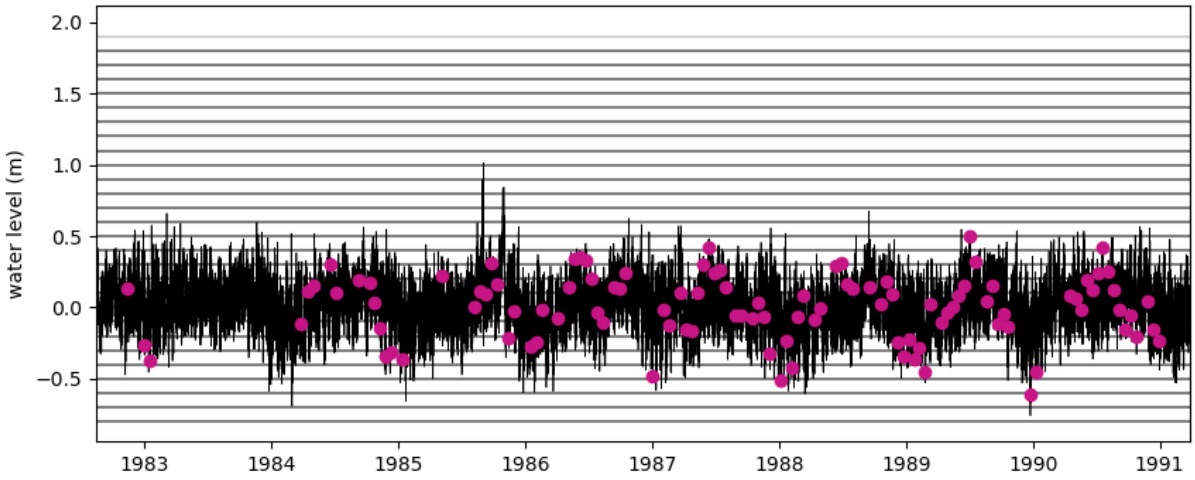

Figure 3. Landsat scenes latched to tidal signal at Grand Bay during the 1980s.

The weighting procedure, shown in Figure 4, consisted of four steps.

1. First a histogram of water levels from the tide relevant gauge was computed, binned in 10 cm increments. This showed the frequency distribution of water level at the gauge.
2. An equivalent histogram was computed for the water levels that are associated with satellite passes. Because the number of satellite passes is limited, this histogram did not match the one computed from the water level gauge directly. The goal of reweighting was to apply weights to these images so that this histogram matched the water level frequency as closely as possible. This step was completed after removing pixels that are masked by clouds or other inconsistencies.
3. For each bin, the appropriate weight was computed such that the histogram of satellite passes most nearly matches the histogram of water levels.
4. The histogram of image collection frequency was adjusted using these weights.

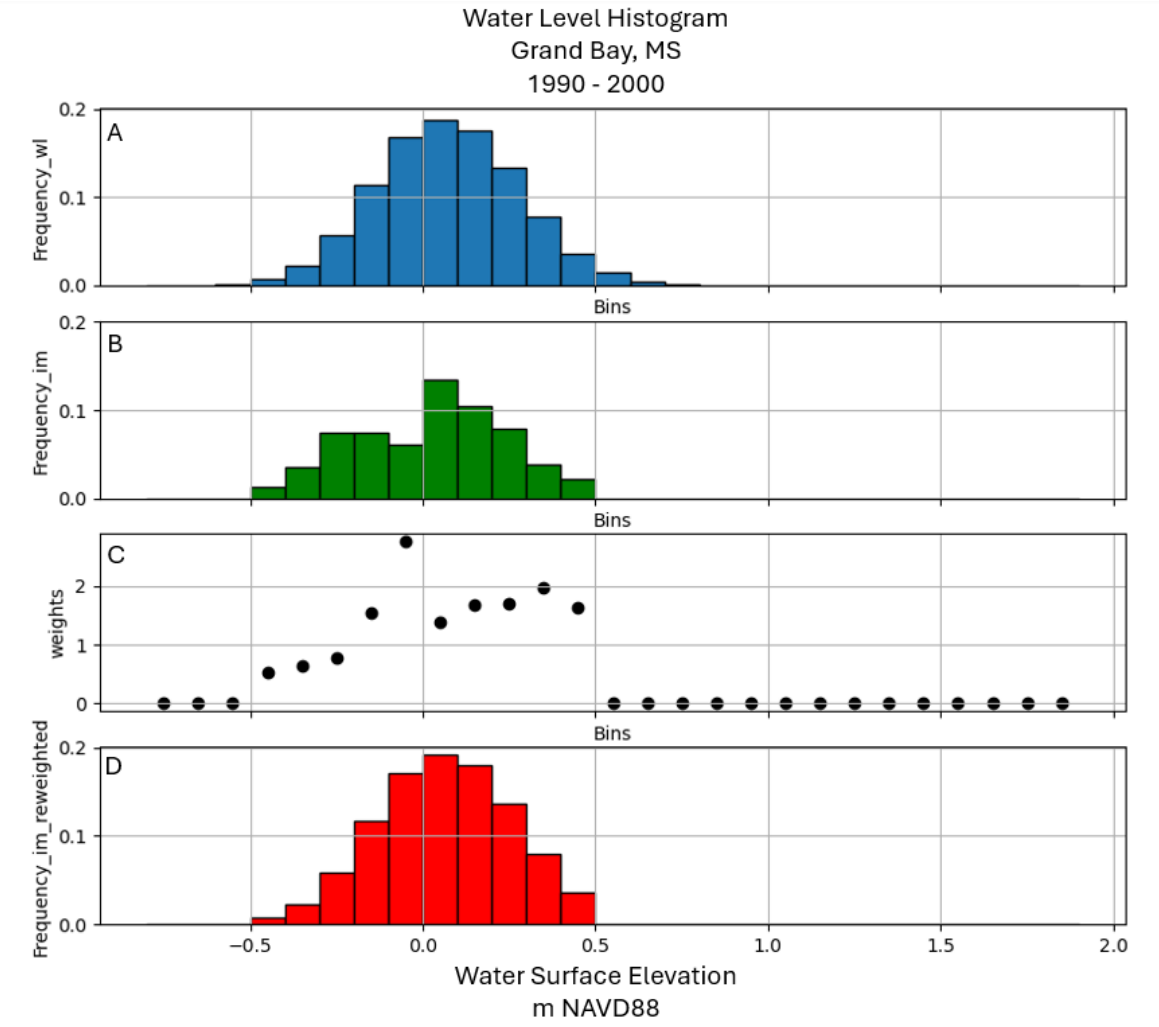

Figure 4. Process to compute image weights showing (A) histogram of water levels occurring at the Dauphin Island tide gauge, used at the Grand Isle site, (B) histogram of water levels occurring at the gauge that correspond with a satellite overpass, (C) weights used to reweight the satellite passes, (D) reweighted histogram of water levels that correspond to satellite overpasses.

Once the weights were computed, they were used to complete the image frequency computation (see Figure *5* for the results for Apalachicola, FL as an example). Note that no adjustment was made to the image frequency map to account for changes in sea level during the time of averaging. The maps represent the best estimate of inundation frequency by Partial Surface Water during the selected time period.

The water levels at Grand Bay and Apalachicola were obtained from NOAA gauges at Dauphin Island[1] and Apalachicola,[2] respectively. The water level record for Breton was obtained through NOAA's Coastal Ocean Reanalysis product (Center for Operational Oceanographic Products and Services, 2026) and corrected to NAVD88 using VDatum.

A section of an inundation frequency map at Apalachicola, FL is shown in Figure *5*. Some of the features were straightforward to interpret, such as wetland areas that were (A) flooded relatively frequently, when compared to (B) more upland areas, or (C) flow paths and small channels that appeared as very high partial surface water frequencies. But other features were more challenging to interpret visually. Areas of persistent open water show as very low frequencies in the Partial Surface Water map. This was true of permanent ponds (shown in D) and also of wider channels (E) where the channel margins showed as high values, but the interior of the channel neared zero. For similar reasons, mudflats that are only occasionally exposed (F) showed as low frequencies of partial surface water because those pixels more frequently appeared in the open water bands.

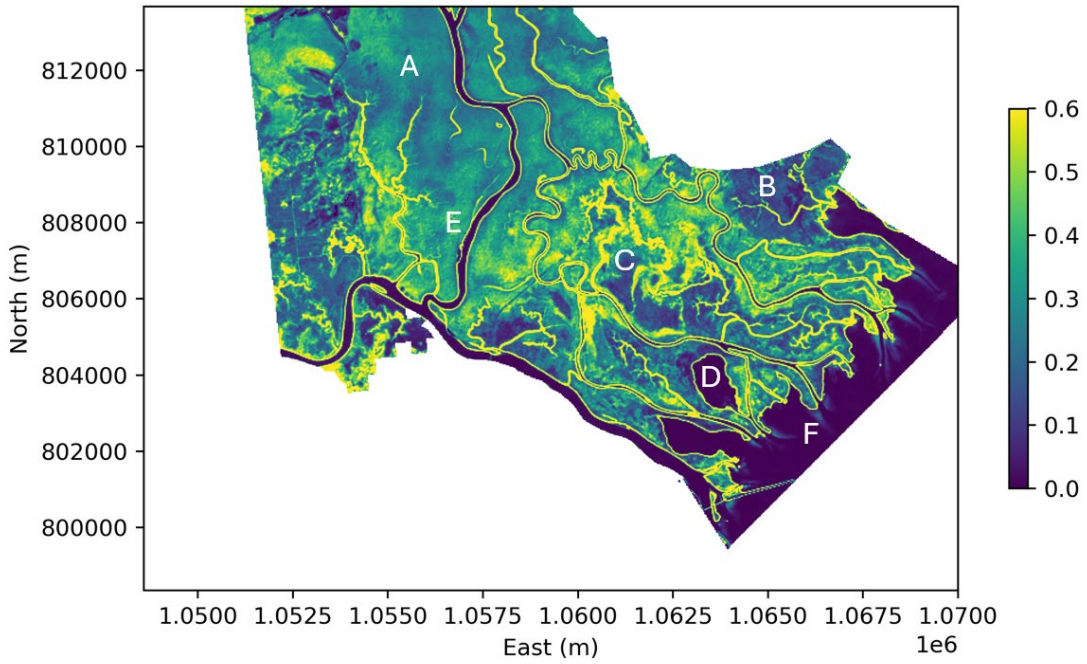

Figure 5. Frequency of Partial Surface Water at Apalachicola during the decade from 2010 to 2020.

[1] https://tidesandcurrents.noaa.gov/map/index.html?id=8735180
[2] https://tidesandcurrents.noaa.gov/map/index.html?id=8728690

2.1.1 Masking

Once the inundation frequency maps were produced, masks were constructed to define the extent of the analysis area. A single mask was used for each site, constructed from data collected during the 2010s. This choice restricted the analysis to changes in marsh surface elevation rather than extent. The masks were constructed so that locations that are outside of the tide range, or areas that are too permanently inundated by any type of water in the inundation frequency maps, were not included in the analysis. The mask criteria were augmented with shapefile polygons to exclude other land areas, developed features, or any other location where inundation frequency was not expected to be predictive of wetland elevation on a site-specific basis. All shapefiles were included in the GitHub code repository (Appendix A). The specific criteria for creating the analysis mask at each site are given below.

Grand Bay, MS

- Cells with elevation higher than 0.6 m were masked.
- Cells that were previously masked in the DEM were masked.
- Cells that were inundated by any type of water more than 90% of the time were masked.

Apalachicola, FL

- Cells with elevation higher than 0.6 m were masked.
- Cells that were previously masked in the DEM were masked.
- Cells that were inundated by any type of water more than 90% of the time were masked.

Breton Sound, LA

- Cells with elevation higher than 0.6 m were masked.
- Cells with elevation lower than or equal to -0.6 m were masked. The Breton DEM applies a uniform value of -0.6 in all open water areas, so these areas were masked out.
- Cells that were inundated by any type of water more than 90% of the time were masked.

The masked, directly sampled DEM for each study site is shown Figure 6 through Figure 8.

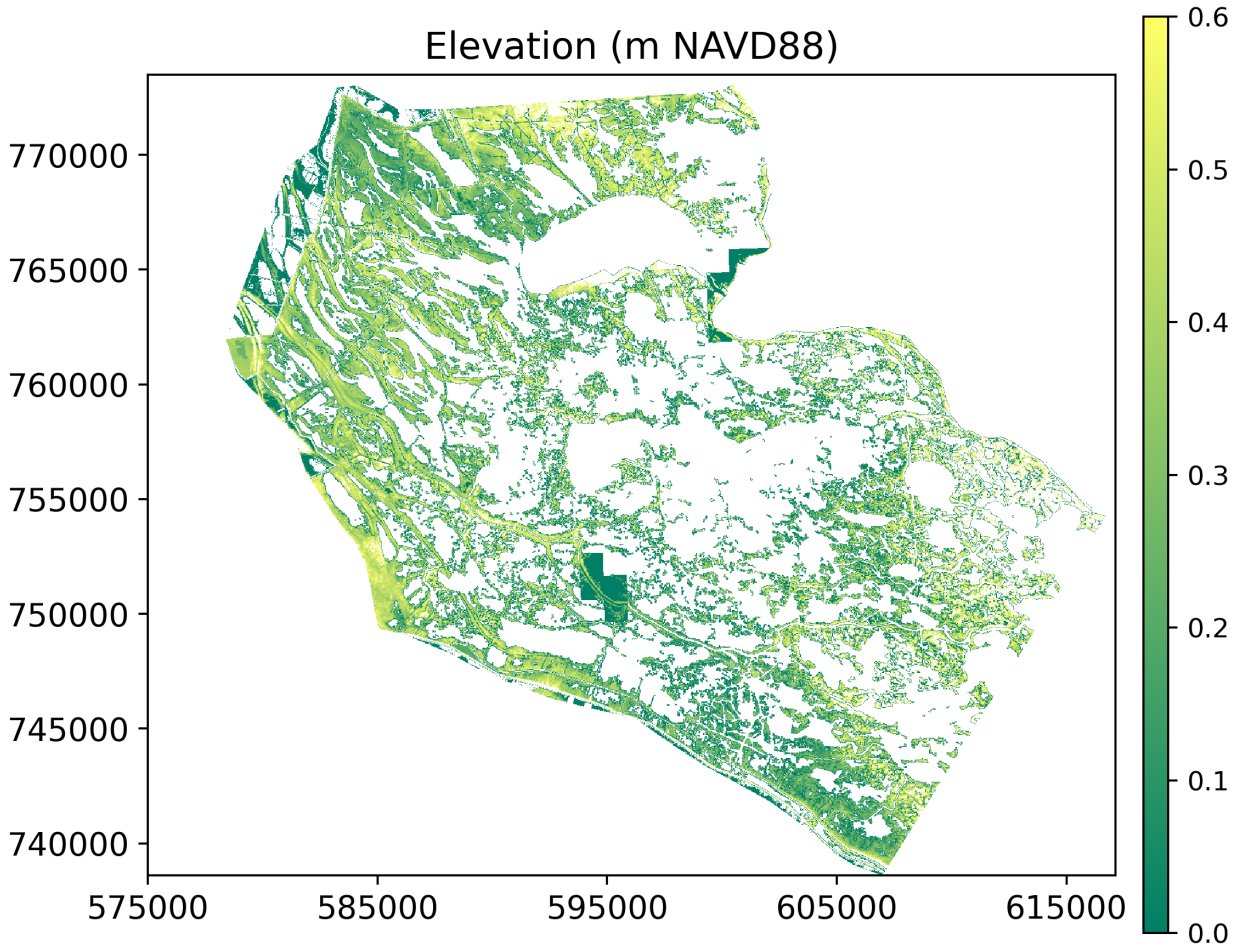

Figure 6. Breton Sound directly sampled DEM, resampled to 30 m, and masked to prepare for analysis.

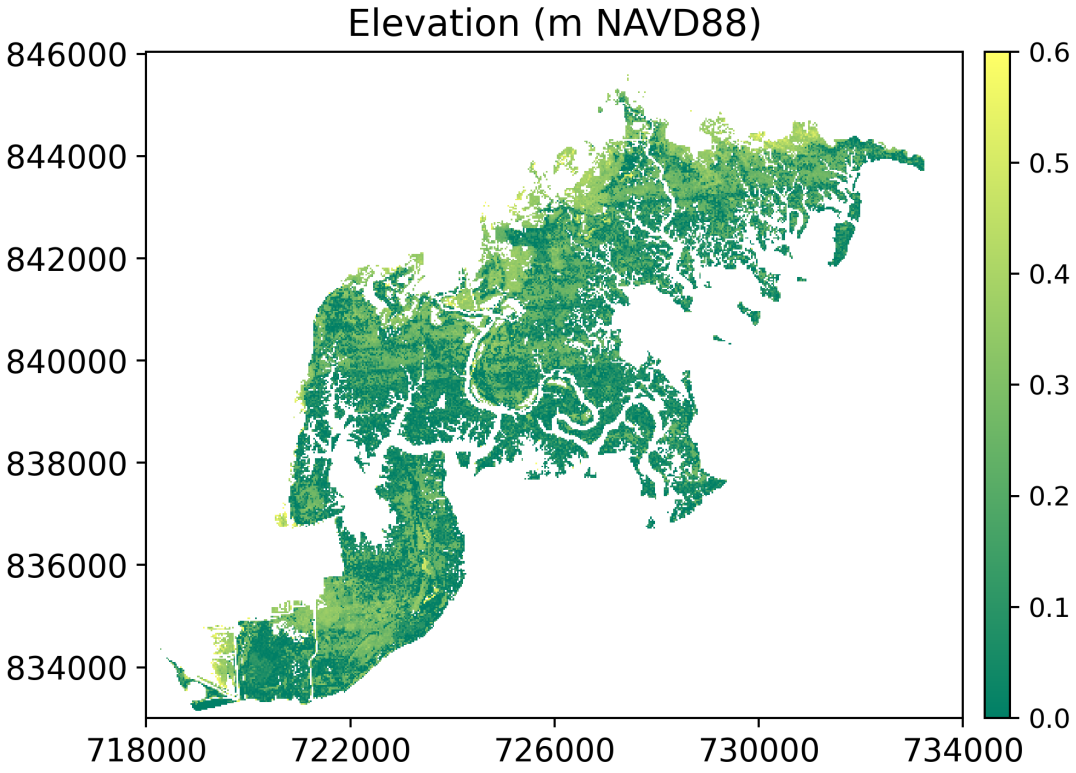

Figure 7. Grand Bay directly sampled DEM, resampled to 30 m, and masked to prepare for analysis.

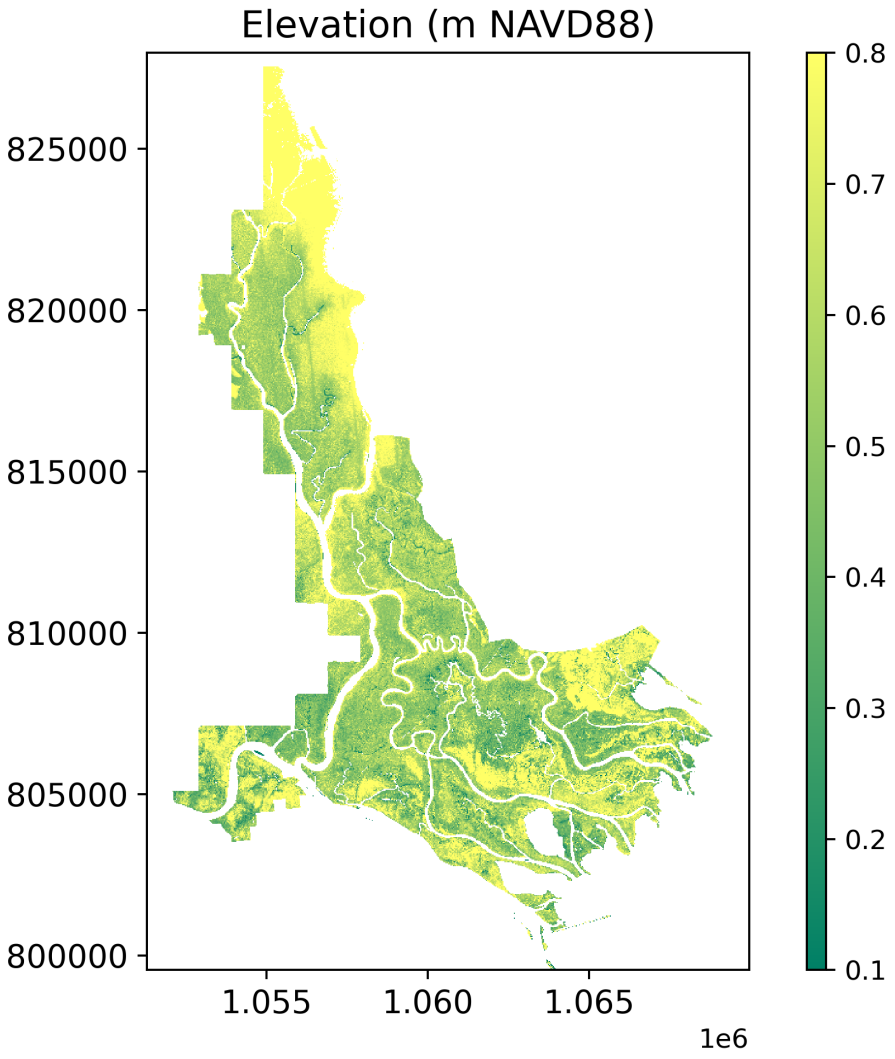

Figure 8. Apalachicola directly sampled DEM, resampled to 30 m, and masked to prepare for analysis.

2.2. RELATIVE ELEVATION AS A FUNCTION OF INUNDATION FREQUENCY

Once masked, the project domain could then be restricted to locations where inundation by tides is the primary driver of inundation frequency, and the maps of inundation frequency could be correlated with a pre-existing directly sampled DEM to provide a relationship that predicts elevation as a function of remotely sensed Partial Surface Water inundation frequency. Each directly sampled DEM used in this workflow was resampled to the 30-meter Landsat resolution.

At this stage, the relationship between elevation in the directly surveyed DEM and the remotely sensed frequency of partial surface water could be assessed visually. At the scale of the entire estuary (Figure 9) and at individual locations (Figure 10) the inverse relationship between elevation and inundation was evident. In some specific localized instances this relationship did appear to break down (e.g., Figure 11) often due to anthropogenic modification to surface water hydrology. The visual assessment is formalized as a correlation analysis later in this section.

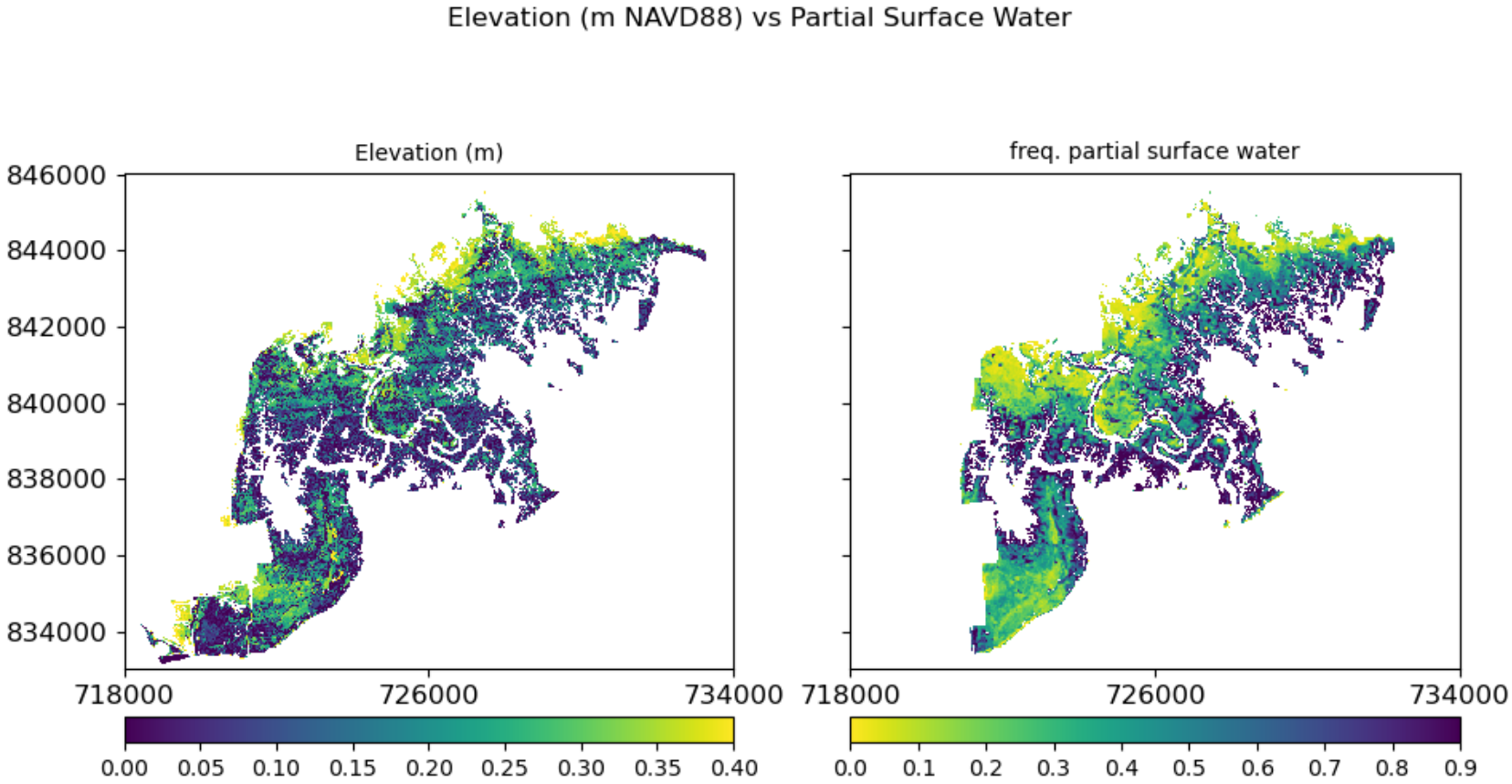

Figure 9. Full scale view of Elevation in the directly sampled DEM vs. frequency of Partial Surface Water at Grand Bay, from 2010–2020. Note that the color axis of the Elevation is restricted relative to Figure 7 in order to make gradients more visible, and that the color ramps on the left and right panels are reversed from one another.

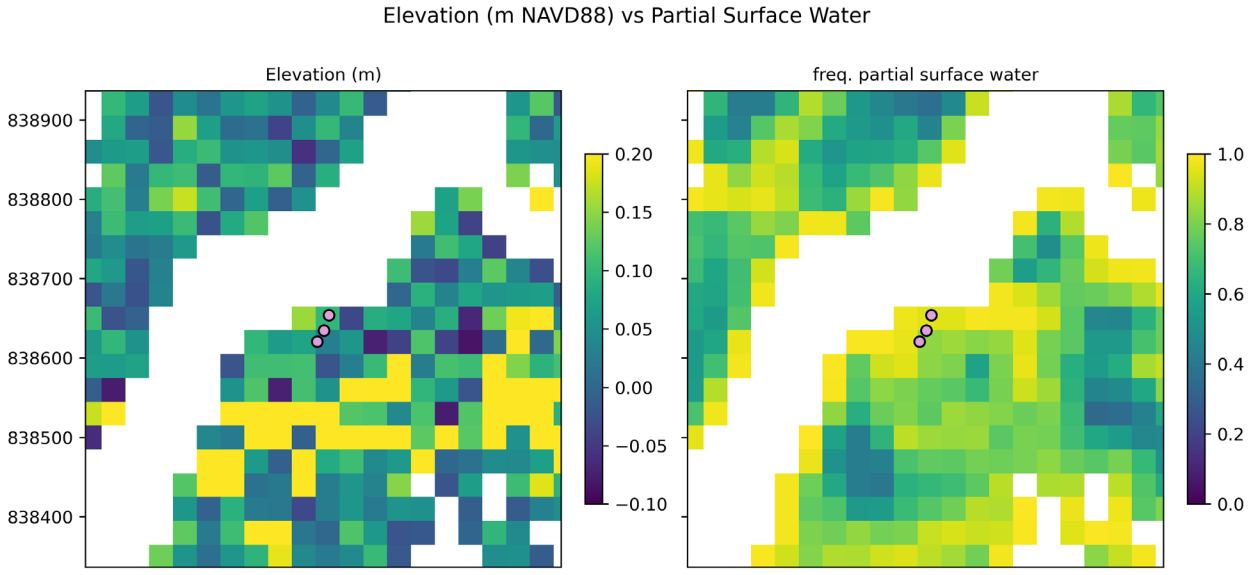

Figure 10. Zoomed in view of Elevation vs. frequency of partial surface water at Grand Bay, from 2010–2020. At the SPALT location. Lavendar dots with black outlines represent the locations of SETs at this location.

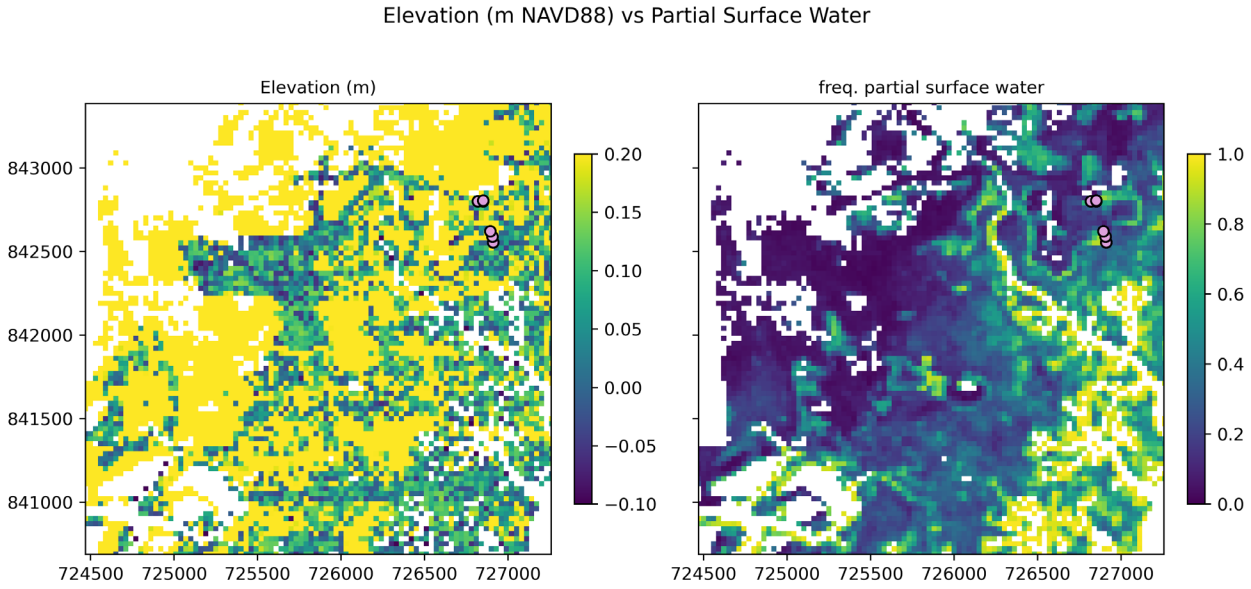

Figure 11. Zoomed in view of Elevation vs. frequency of partial surface water at Grand Bay at the CLMAJ sub-geography from 2010–2020. In this instance, there is a section where persistently low frequency of partial surface water inundation appears to be correlated with low elevation. Investigation is needed in every such instance, but this is likely to be due to localized poldering of the wetland at this location. Lavendar dots with black outlines represent the locations of SETs at this location.

Once the inundation frequency maps and the DEMs were masked appropriately, a correlation between inundation frequency and elevation was established at each study site using data from the most recent decade (2010–2020). In this project, simple linear regression was used, which had the benefit of broad applicability and ease of interpretation. But it should be noted that the specific relationship used at this stage of the synthetic DEM methodology is ripe for further exploration using more complicated functional relationships, machine learning, or spatially aware approaches.

An example correlation from the Grand Bay site is shown in Figure 12. Because landscapes and coastal hydrology are both very complex, the relationship between elevation and inundation is a noisy one, with points typically scattered widely across the parameter space. To filter through that noise, the correlation figures were colored by data density and a contour was drawn around the 50% of the points that are closest to the core of the data mass. These 50% of points were considered to be the core of the relationship between the two quantities, and a simple linear regression was fit to those points. In the example figure, the regression line connects a mass of points in the upper left quadrant (high elevation and low inundation) with a mass of points in the lower right (low elevation, high inundation), and the fit accounts for approximately half of the variation experienced among the filtered points. The filtering technique that was applied is related to kernel density estimation, and was implemented using the Seaborn statistical data visualization package in Python.[3]

[3] https://seaborn.pydata.org/generated/seaborn.kdeplot.html

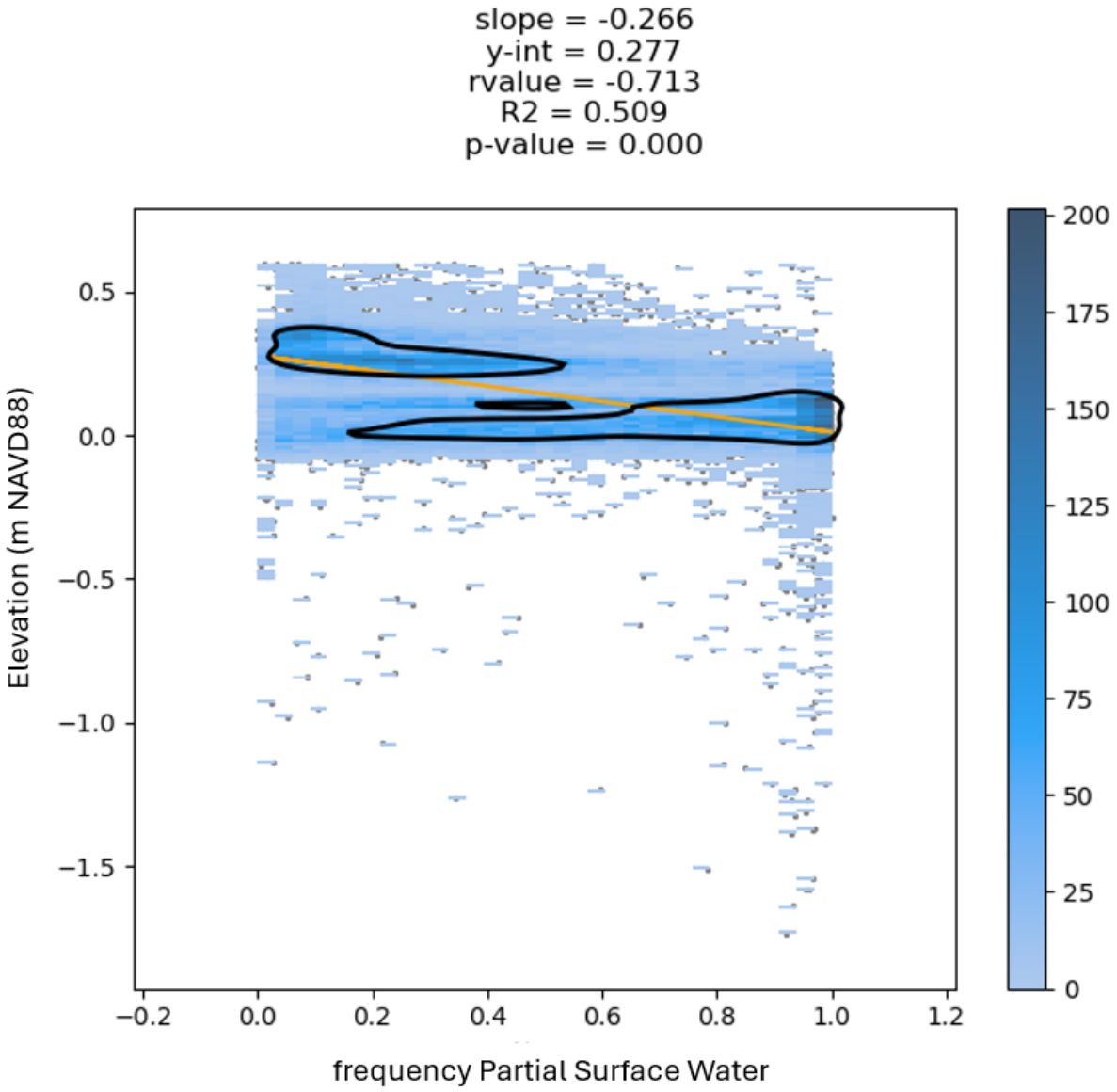

Figure 12. Linear regression between elevation (y-axis) and frequency of partial surface water (x-axis) at Grand Bay. The blue shading represents data density, as shown in the color bar. Individual data points are shown as gray dots that are only visible in locations where data coverage is sparse. The set of black contours surround the data kernel, as computed with the Seaborn statistical visualization package. The orange line is a simple linear regression function fit to the data within the black contours. Fit statistics are shown in the figure title.

2.3. APPLYING THE ELEVATION FUNCTION TO PREVIOUS TIME PERIODS

The regression relationships between inundation frequency (frequency of Partial Surface Water) and elevation were applied to maps of inundation frequency from previous time periods at the same location to produce a "synthetic" DEM representing that time period. As a final step, the resulting synthetic DEM was adjusted for changes to the mean sea level as observed at the relevant water level gauge.

2.4. PROJECT CODE DATABASE AND DATA DELIVERABLE

A description of the code used in this project is given in Appendix A, and the data deliverables and extra image sets are described in Appendix B. The code is available in a GitHub repository. This code base is applicable to any coastal wetland that has a directly surveyed DEM of sufficient quality during the remote sensing era and has at least one continuous water level monitoring station during that same period.

3.0 RESULTS

Results for each study site are provided below and are organized in a similar fashion to one another. First, an assessment of the synthetic DEMs is made by comparing the most recent synthetic DEM with the directly surveyed LiDAR based DEM. This assessment is performed for each site at a map scale and a local scale and by statistically comparing the differences between the two. It provides an overall estimate of the performance of the methodology for each study site. Next, visualizations for the map timeseries of inundation frequency and synthetic elevation for all decades since 1980 are shown. Finally, elevations derived from synthetic DEMs are compared with surveyed elevation points as they are available.

3.1. GRAND BAY, MS

The Grand Bay study site is shown in Figure 13. Locations of SET clusters are shown on the map and referred to in subsequent figures.

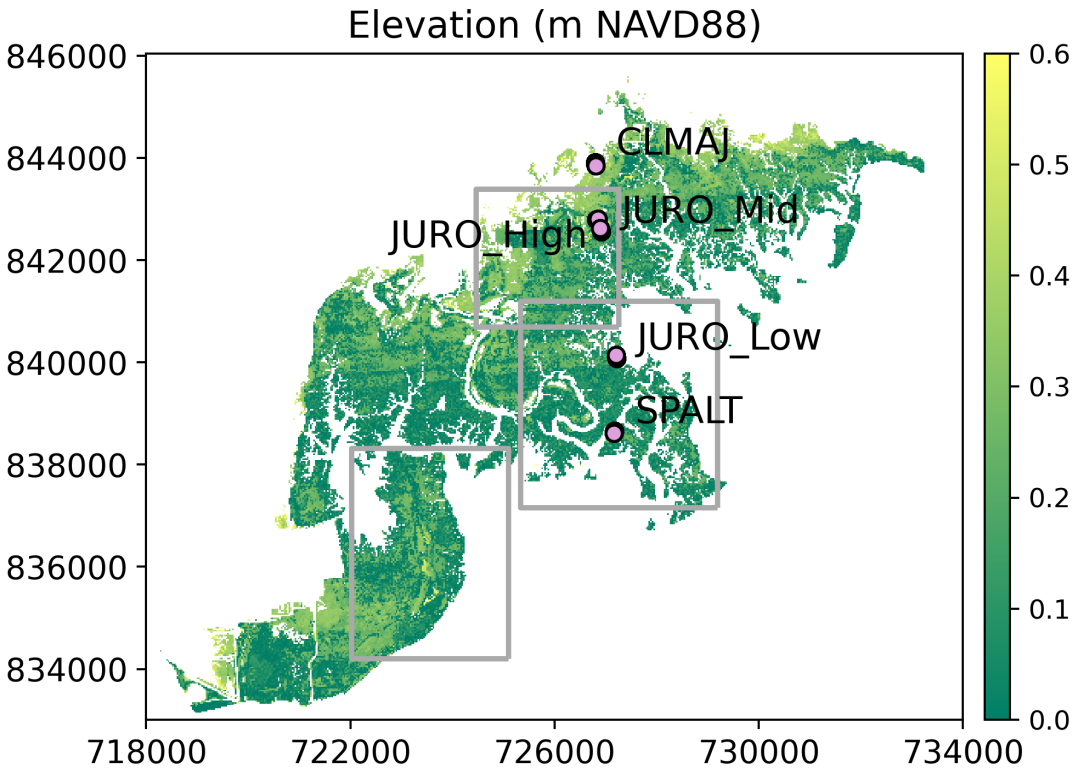

Figure 13. Grand Bay directly sampled DEM with the locations of SET clusters shown. Gray boxes indicate areas that are analyzed in detail. Lavender dots with black outlines represent the locations of SETs at this location.

3.1.1 Difference Assessment with recent DEM

Differencing the resampled LiDAR DEM and the synthetic DEM at Grand Bay during the 2010-2020 decade shows an error distribution with a mean difference of 1 cm and a standard deviation of 13 cm (Figure 14–15). The three selected sub-geographies perform similarly (Figures 16–25), though there are evident spatially coherent clusters of higher error visible in in the difference maps. Some of the spatial clusters are likely the result of a disconnect in the relationship between hydrology and elevation (e.g., Figure 16), while others result from high relief areas that are smoothed out by the simple linear regression approach (e.g., Figure 18).

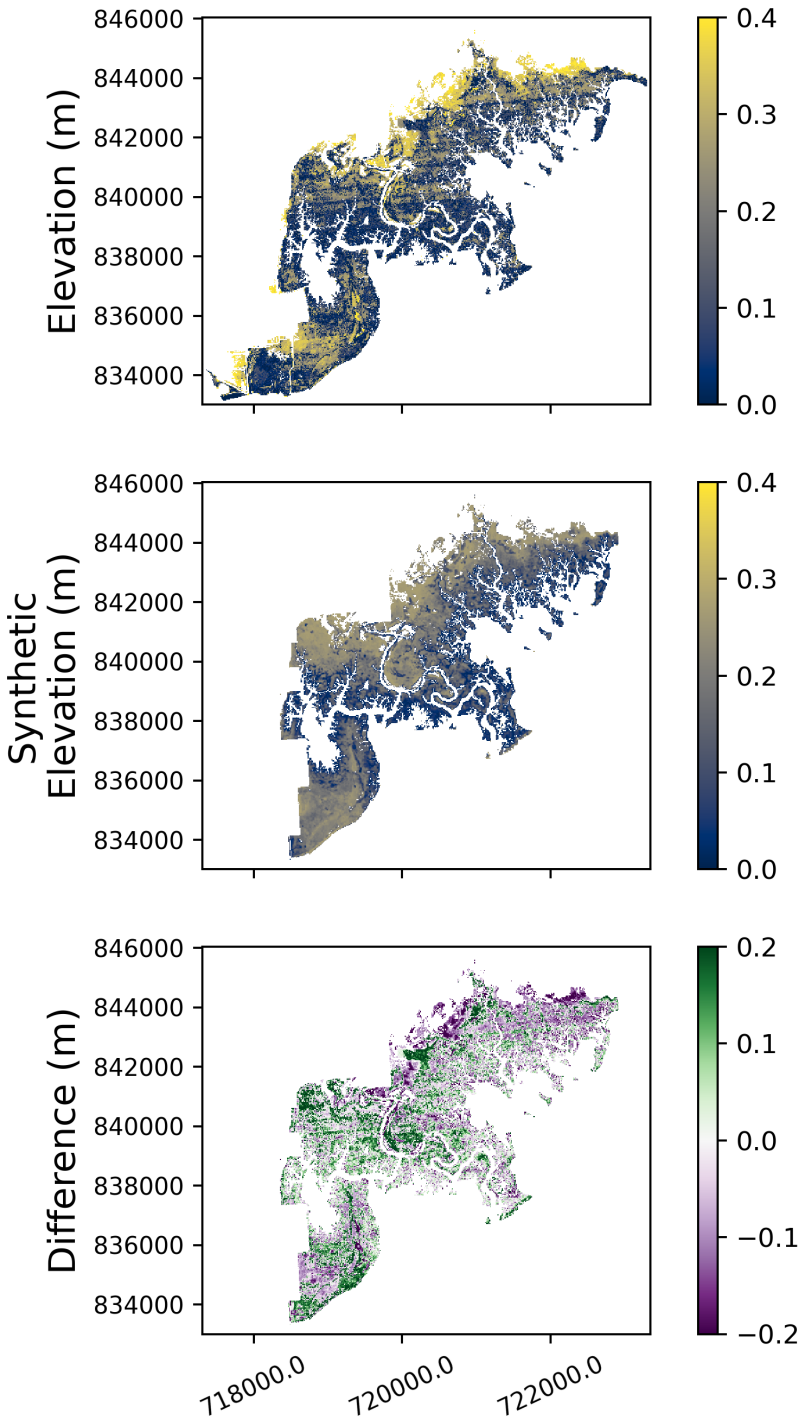

Figure 14. Difference map of previously existing DEM (left) and synthetic DEM for the 2010s (center)for the entire Grand Bay site. The difference between the two is shown in the right frame. A histogram of values in the difference map is shown in Figure 15.

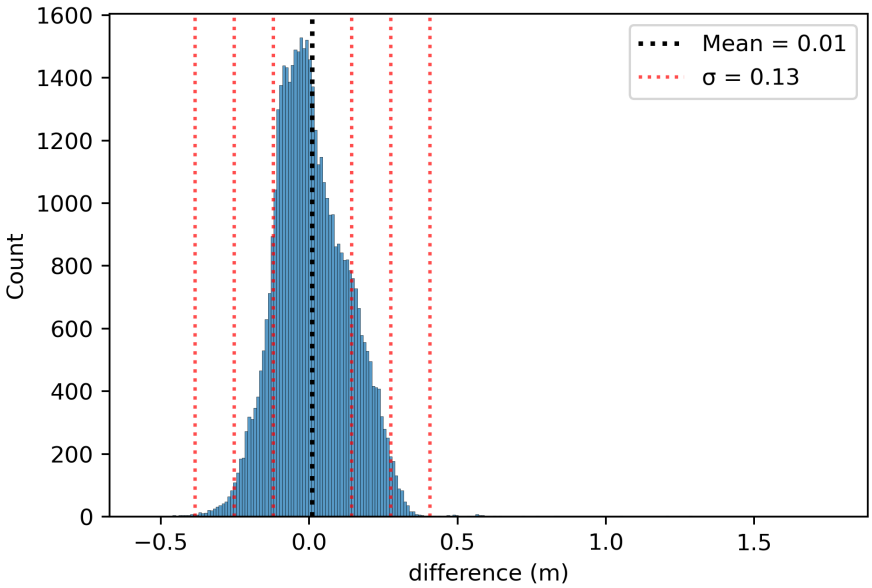

Figure 15. Histogram of difference values between previously existing DEM and the synthetic DEM for the 2010s for Grand Bay.

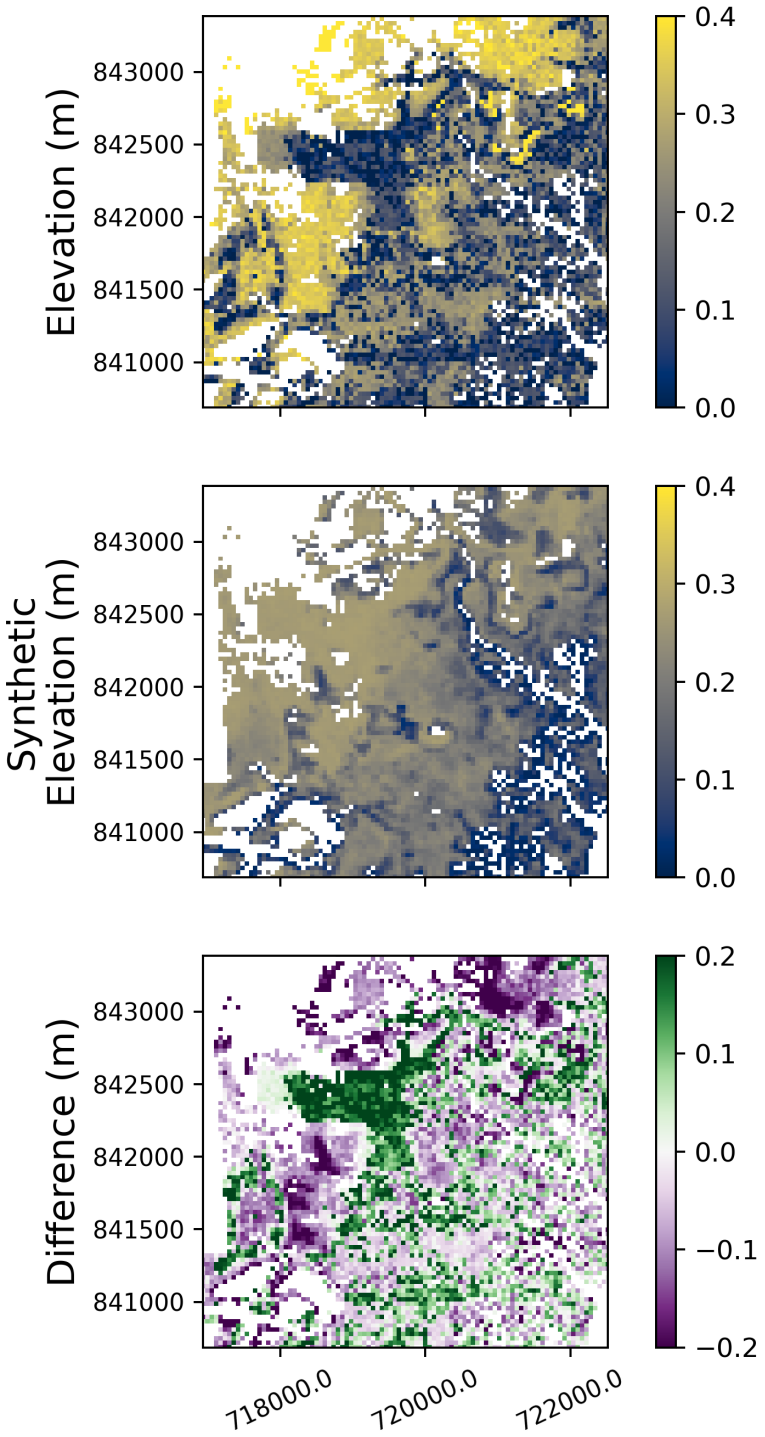

Figure 16. Difference map of previously existing DEM (left) and synthetic DEM for the 2010s (center), zoomed in to a subdomain of the Grand Bay site. The difference between the two is shown in the right frame. A histogram of values in the difference map is shown in Figure 37.

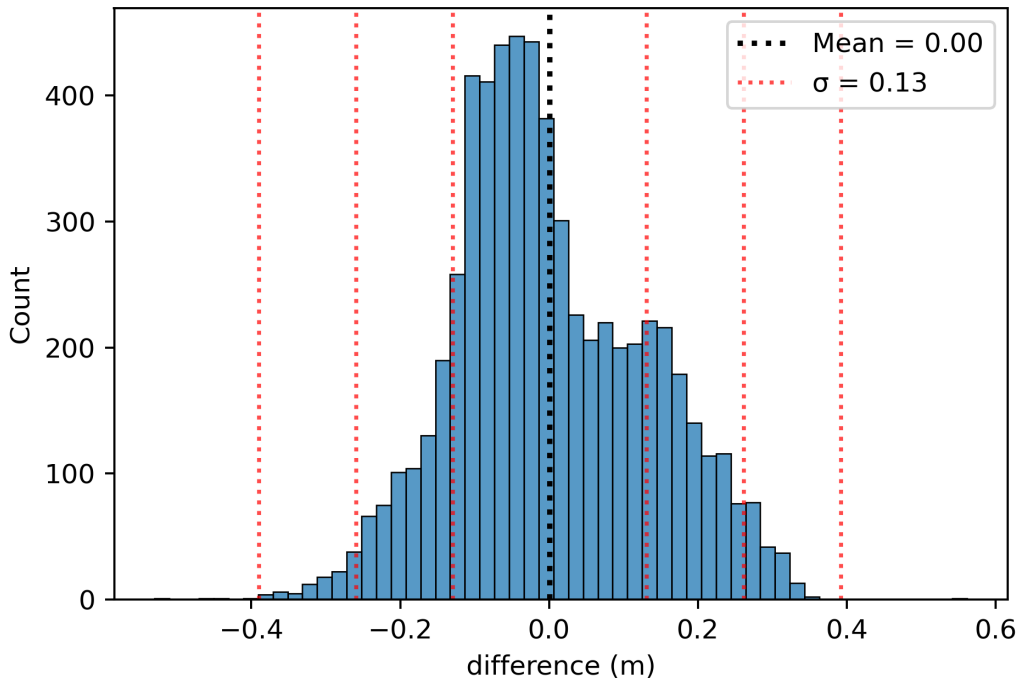

Figure 17. Histogram of difference values between previously existing DEM and the synthetic DEM for the 2010s for a subdomain of the Apalachicola site.

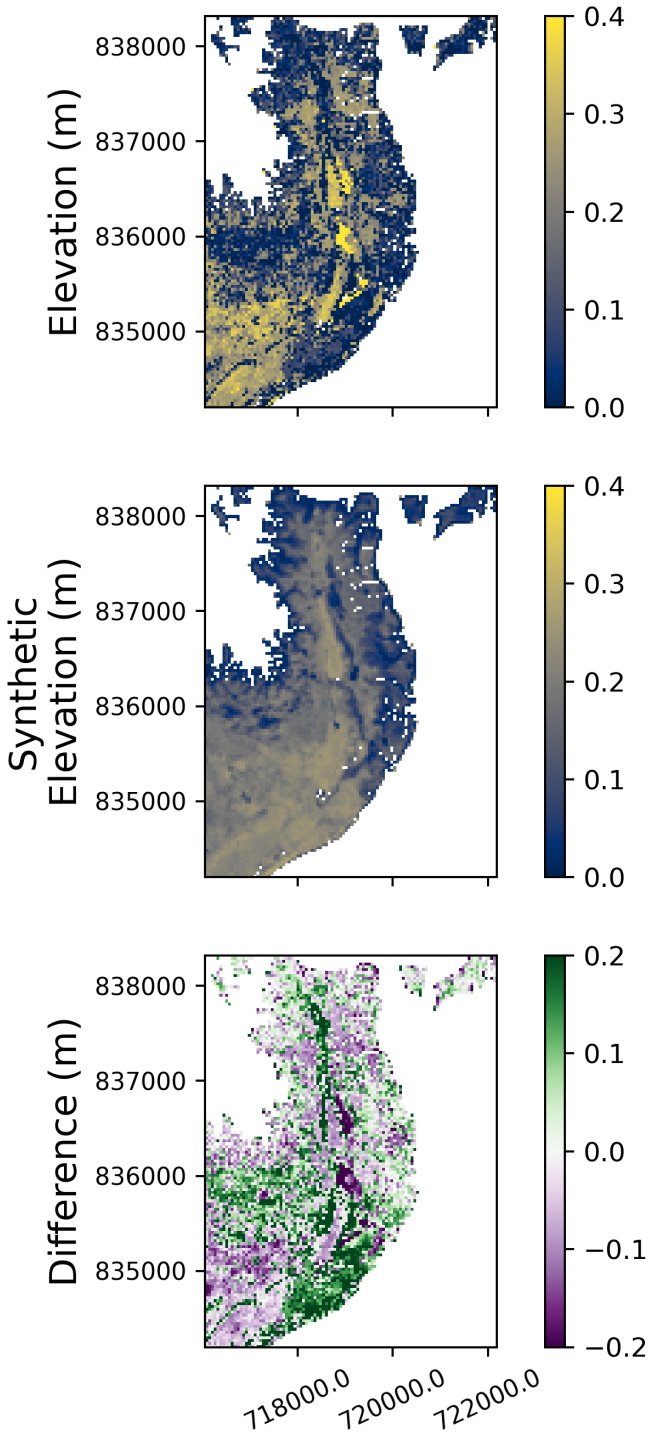

Figure 18. Difference map of previously existing DEM (left) and synthetic DEM for the 2010s (center), zoomed in to a subdomain of the Grand Bay site. The difference between the two is shown in the right frame. A histogram of values in the difference map is shown in Figure 37.

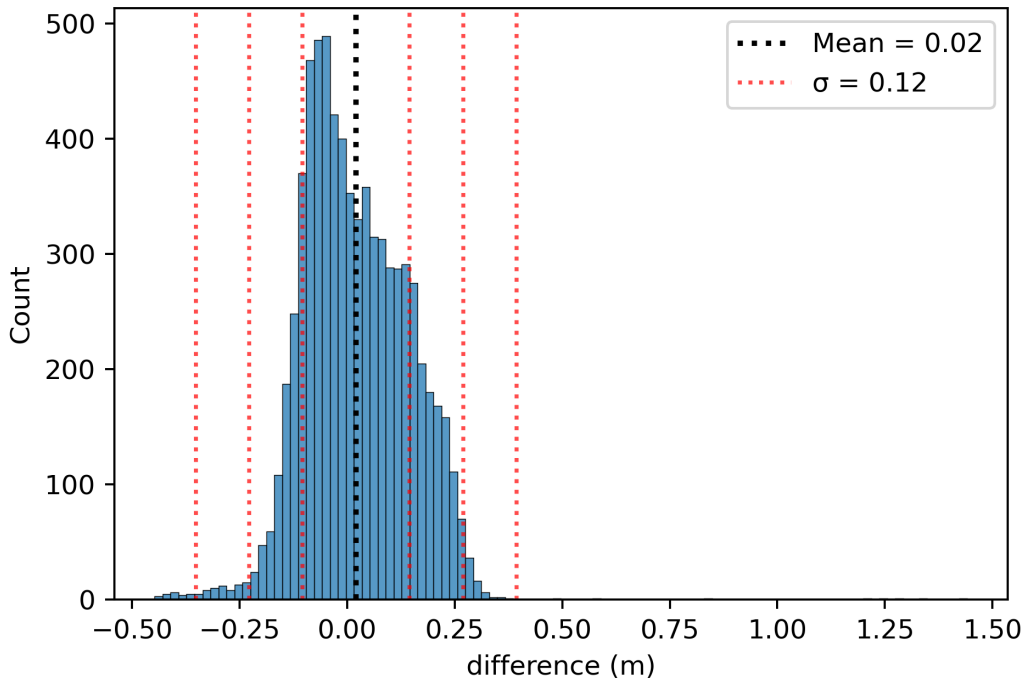

Figure 19. Histogram of difference values between previously existing DEM and the synthetic DEM for the 2010s for a subdomain of the Grand Bay site.

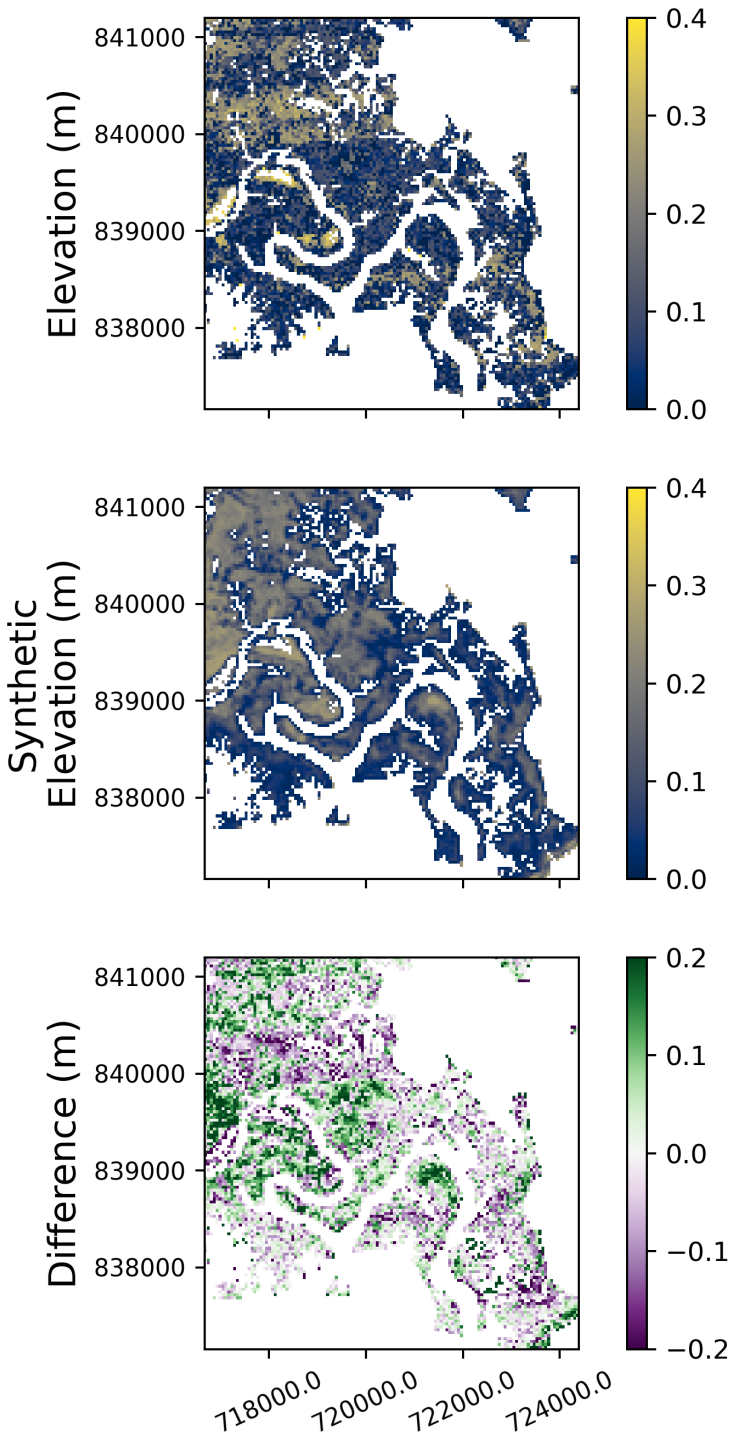

Figure 20. Difference map of previously existing DEM (left) and synthetic DEM for the 2010s (center), zoomed in to a subdomain of the Grand Bay site. The difference between the two is shown in the right frame. A histogram of values in the difference map is shown in Figure 37.

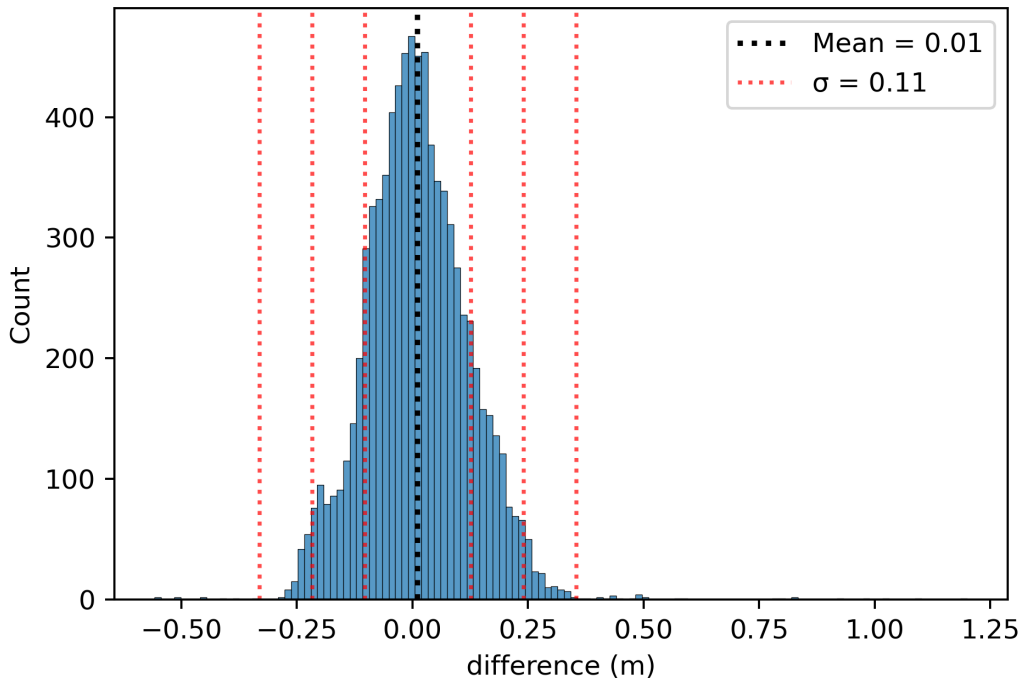

Figure 21. Histogram of difference values between previously existing DEM and the synthetic DEM for the 2010s for a subdomain of the Grand Bay site.

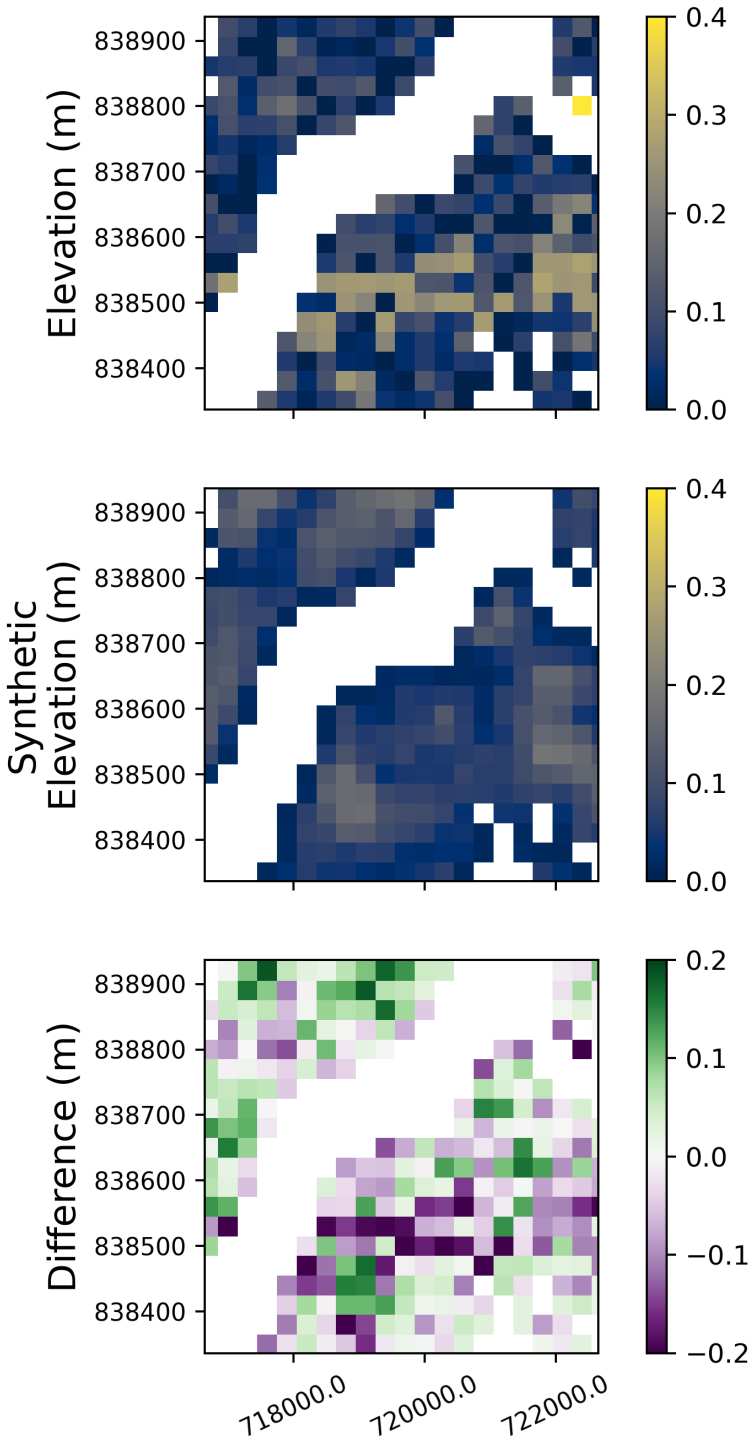

Figure 22. Digital elevation map from Medeiros et al. (2018; left), the synthetic DEM from this project for the 2010s (center), and the difference between the two (right); all zoomed in to the SPALT location. A histogram of values in the difference map is shown in Figure 23.

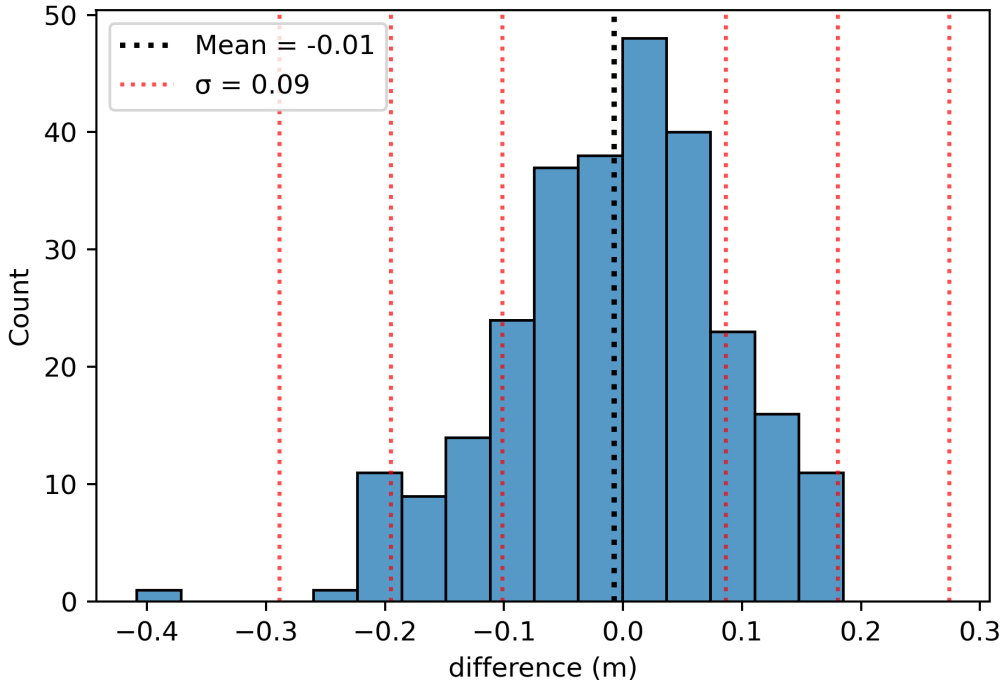

Figure 23. Histogram of difference values between previously existing DEM and the synthetic DEM for the 2010s for the SPALT location at Grand Bay.

3.1.2 Map Timeseries

This section shows decadal changes to the frequency of Partial Surface Water and to synthetic elevation at Grand Bay. The frequency of Partial Surface Water inundation has declined with time, and the changing pattern of inundation is represented spatially in the synthetic elevation.

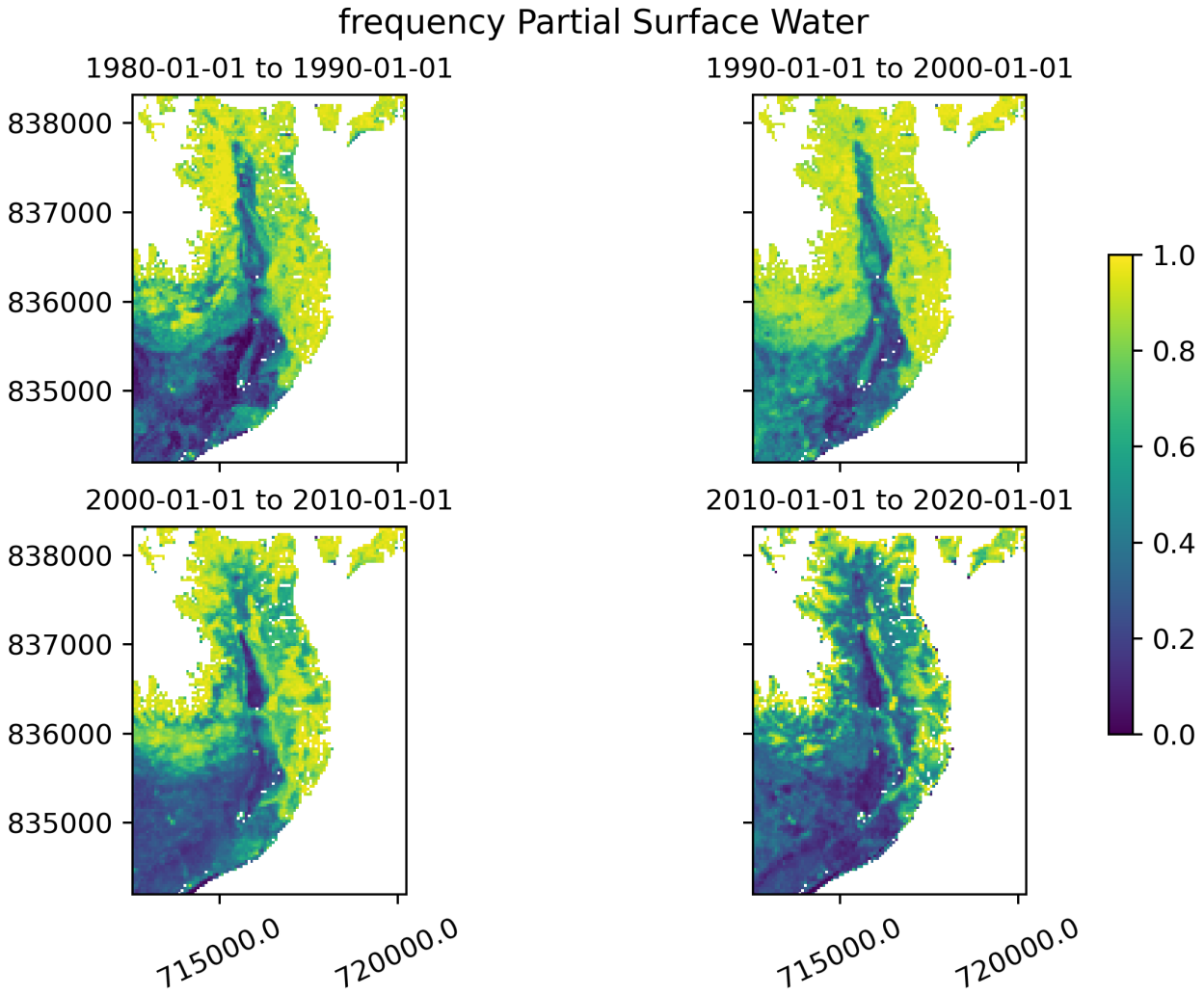

Figure 24. Partial surface water frequency at Grand Bay for each decade since the 1980s.

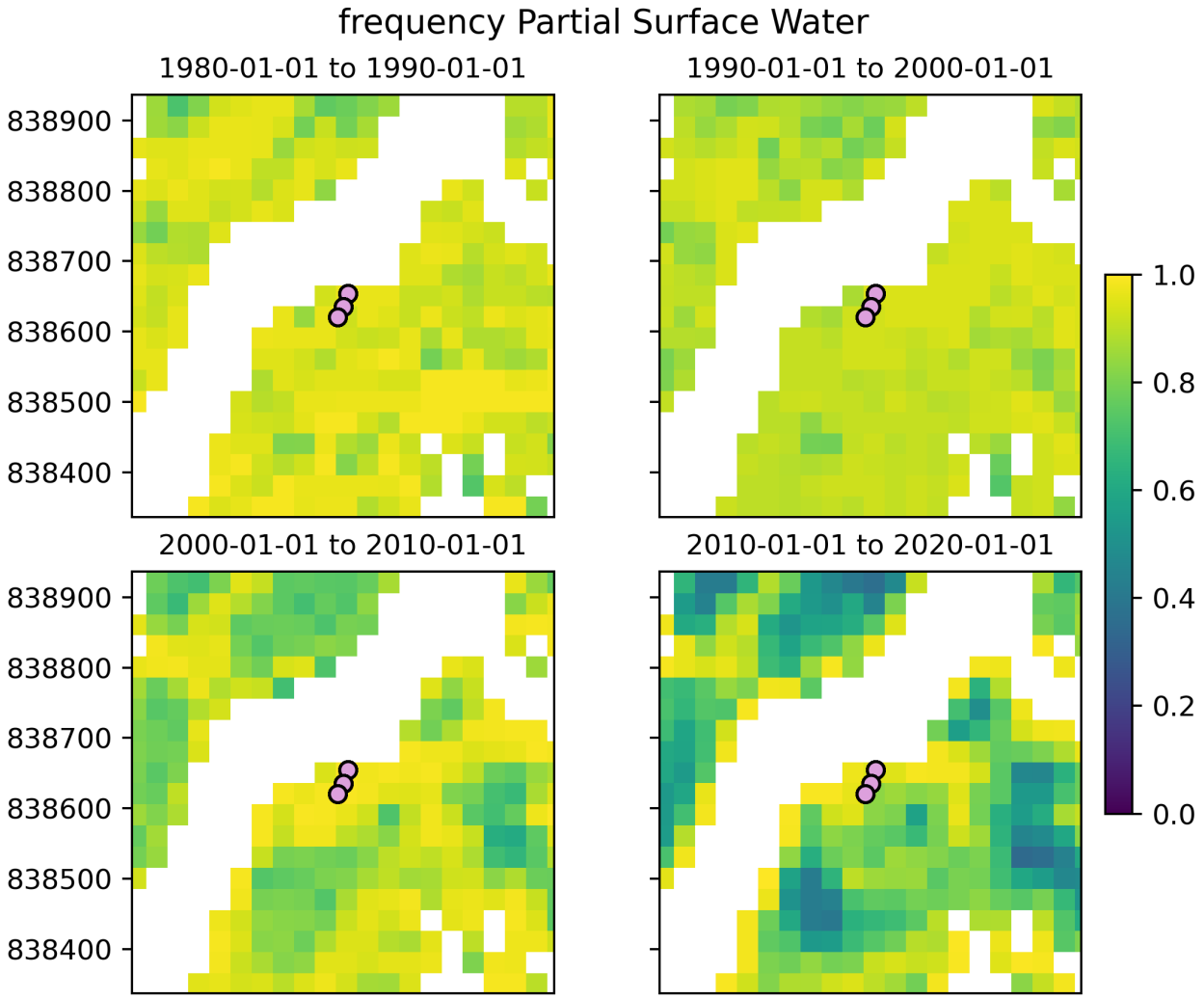

Figure 25. Partial surface water frequency at the SPALT site in Grand Bay for each decade since the 1980s. Lavender dots with black outlines represent the locations of SETs at this location.

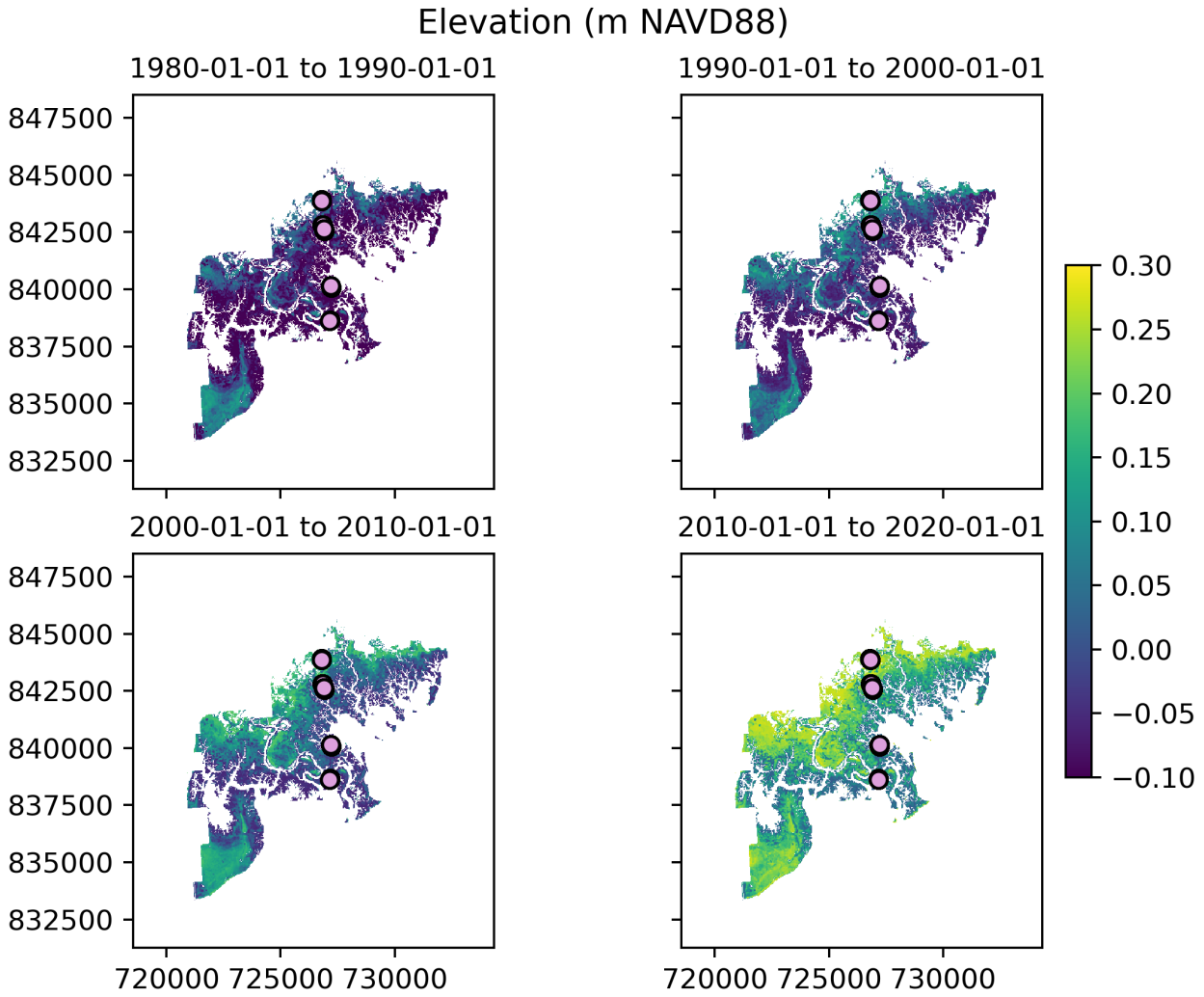

Figure 26. Synthetic elevation at Grand Bay for each decade since the 1980s. Lavender dots with black outlines represent the locations of SETs at this location.

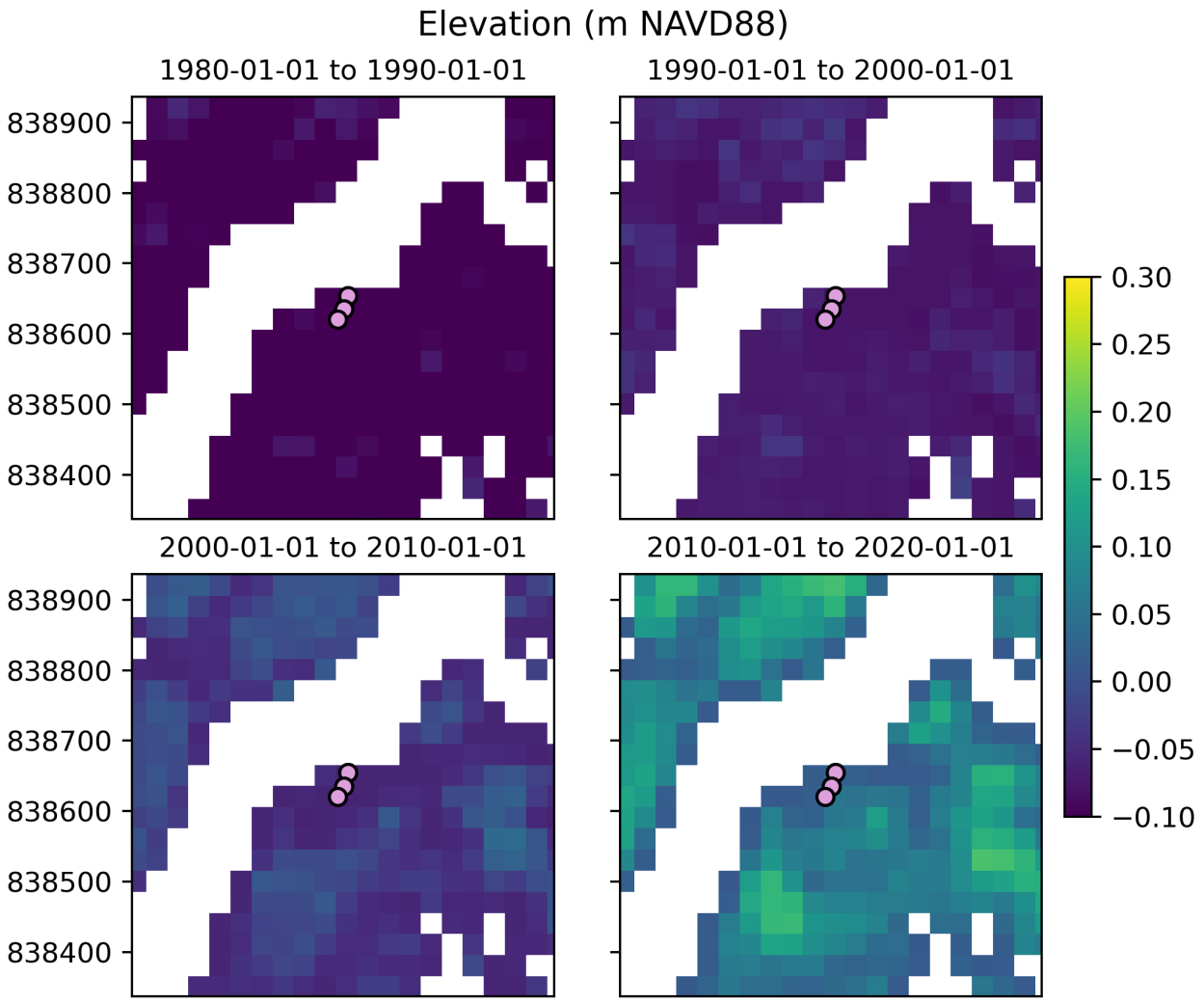

Figure 27. Synthetic elevation at the SPALT location in Grand Bay. Lavender dots with black outlines represent the locations of SETs at this location.

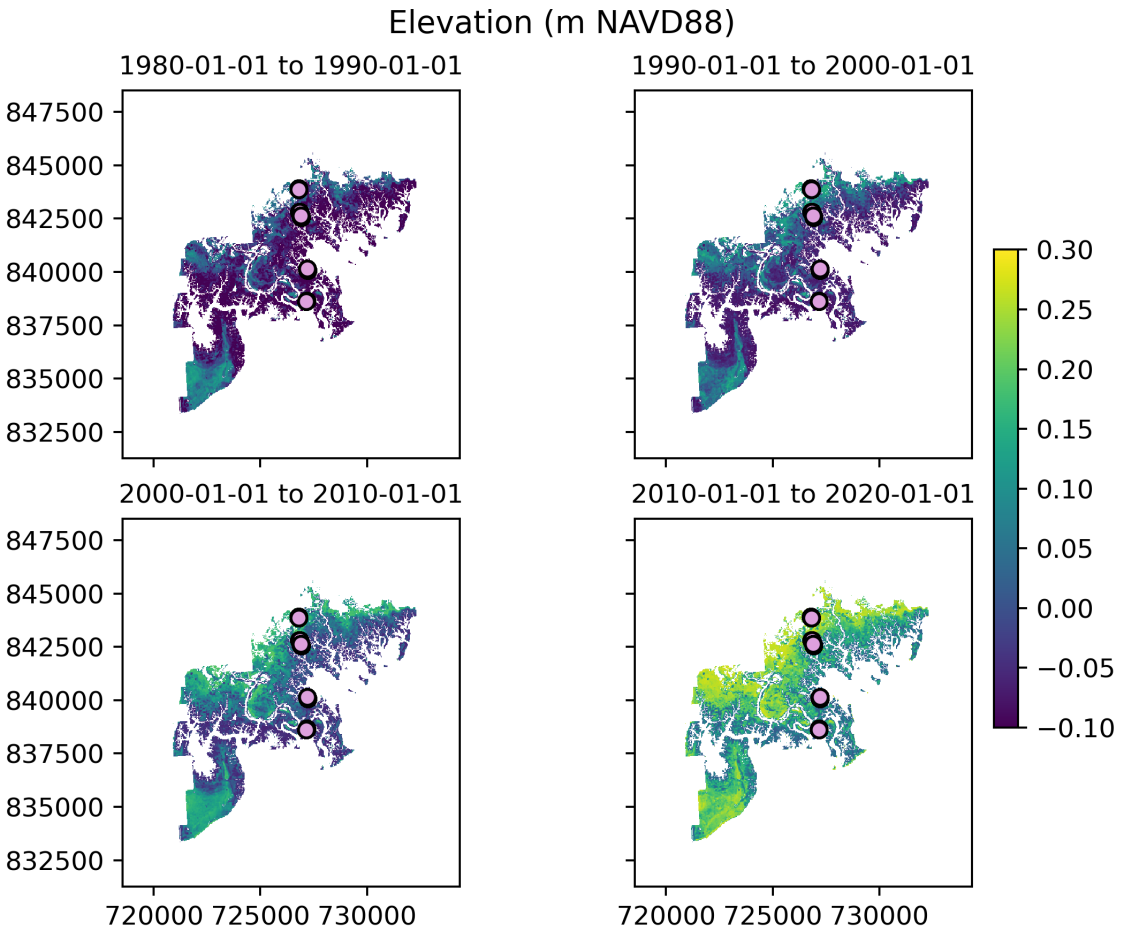

Figure 28. Synthetic Elevations at Grand Bay. 1980s–2020s, with SET locations shown. Lavender dots with black outlines represent the locations of SETs at this location.

3.1.3 Validation to Observational Data

The figures in this section show the elevations in the synthetic DEMs at the location of the SET control data. Dark colored circles indicate the synthetic elevation at the pixel of the SET monument shown in the same color. The time series of average SET-derived elevations at each site is shown as a solid line, and the measurements that were used to derive that average (mean elevation at each SET arm position) are shown in pale dots. Elevations from the directly observed DEM are shown as stars, colored respectively by site. The largest star shows the value of that DEM when resampled to Landsat resolution, while the smaller dots show the value of all of the pixels at full resolution that sit within the footprint of the Landsat pixel. Note here that a substantial component of the total uncertainty in the synthetic DEM process appears to arise from the resampling of the directly observed DEM to the 30m Landsat resolution. This is evident in Figure 31, where the resampled DEM condenses over 20 cm of relief into a single point.

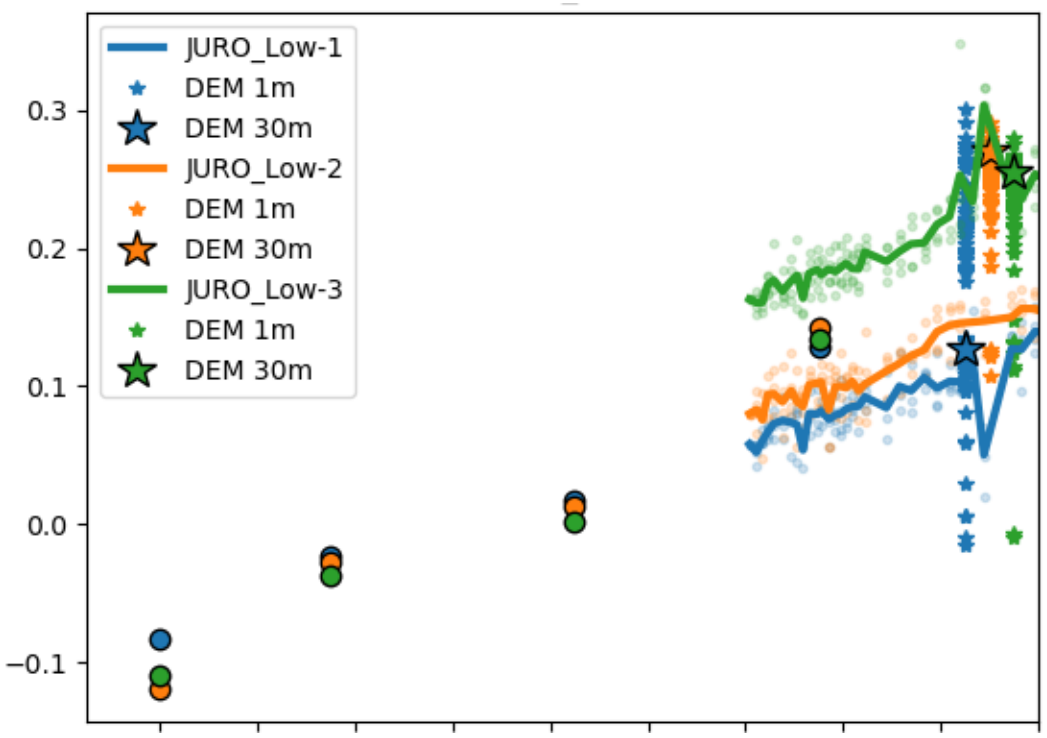

Figure 29. Validation to SET derived elevations at the JURO-Low cluster of sites in Grand Bay.

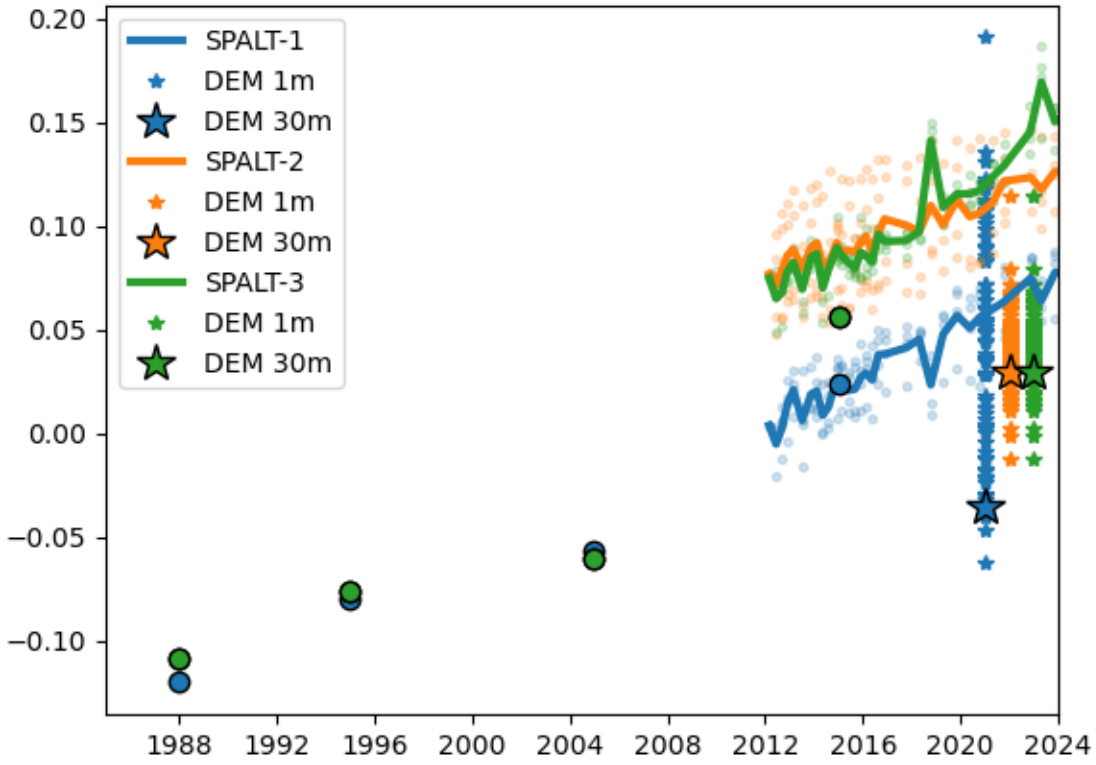

Figure 30. Validation to SET derived elevations at the SPALT cluster of sites in Grand Bay.

3.2. APALACHICOLA, FL

The Apalachicola study site is shown in Figure 33. Locations of SET clusters are shown on the map and referred to in subsequent figures.

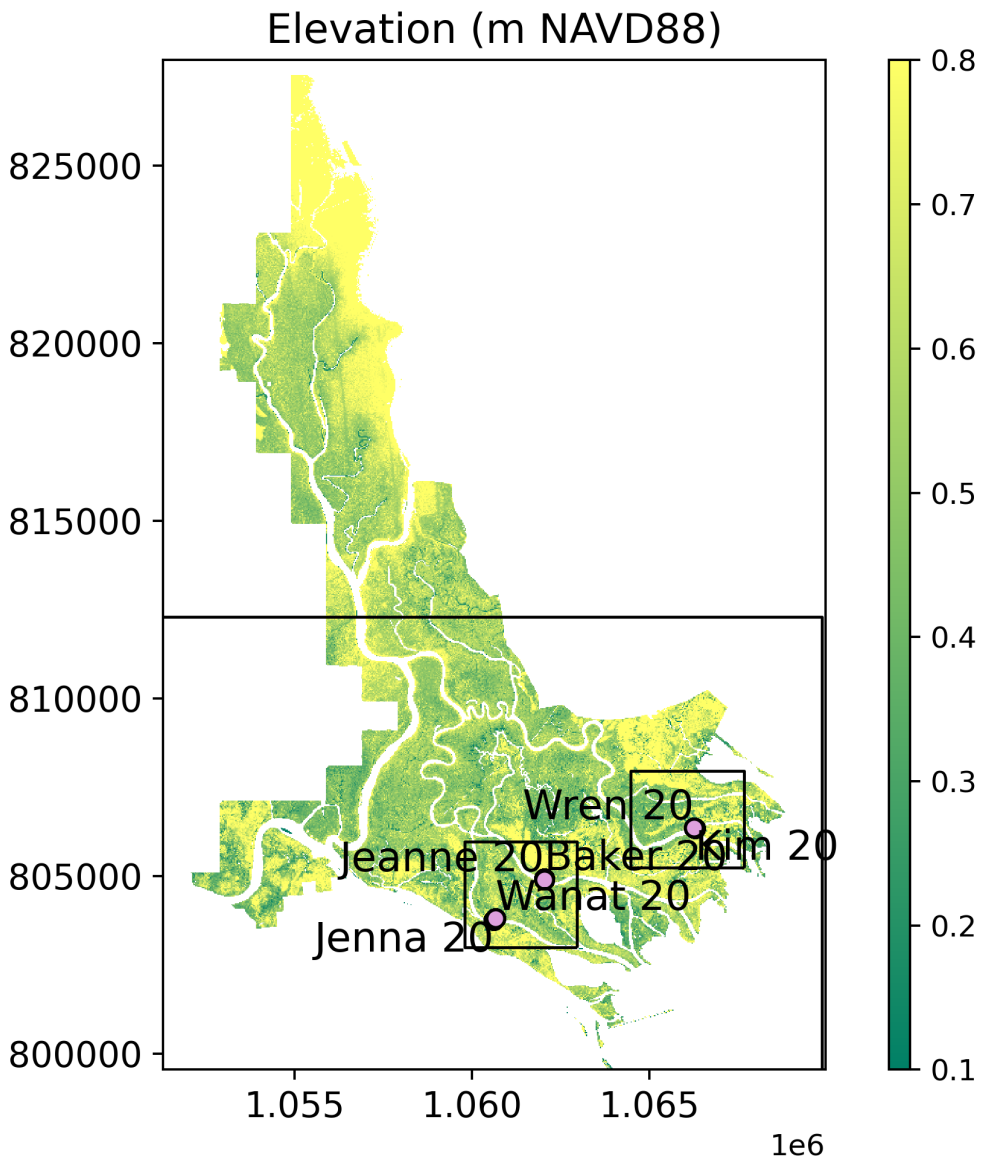

Figure 31. Apalachicola directly sampled DEM, resampled to 30 m, and masked to prepare for analysis. Lavender points show the locations of SET stations used in the validation efforts. Areas outlined in black show analysis areas that are treated individually in this report or the accompanying figure set.

3.2.1 Difference Assessment with Recent DEM

Differencing the resampled LiDAR DEM and the synthetic DEM at Apalachicola during the 2010-2020 decade shows an error distribution with a mean difference of 4 cm, and a standard deviation of 18 cm (Figures 34–35). The three selected sub-geographies perform less well (Figures 36–39), and as with Grand Bay, there are evident spatially coherent clusters of higher error visible in in the difference maps. This performance is less accurate than the synthetic DEMs at Grand Bay. One possible explanation for this is that the fluvial character of the wetlands at Apalachicola mean that inundation frequency is a less accurate predictor of elevation than in Grand Bay.

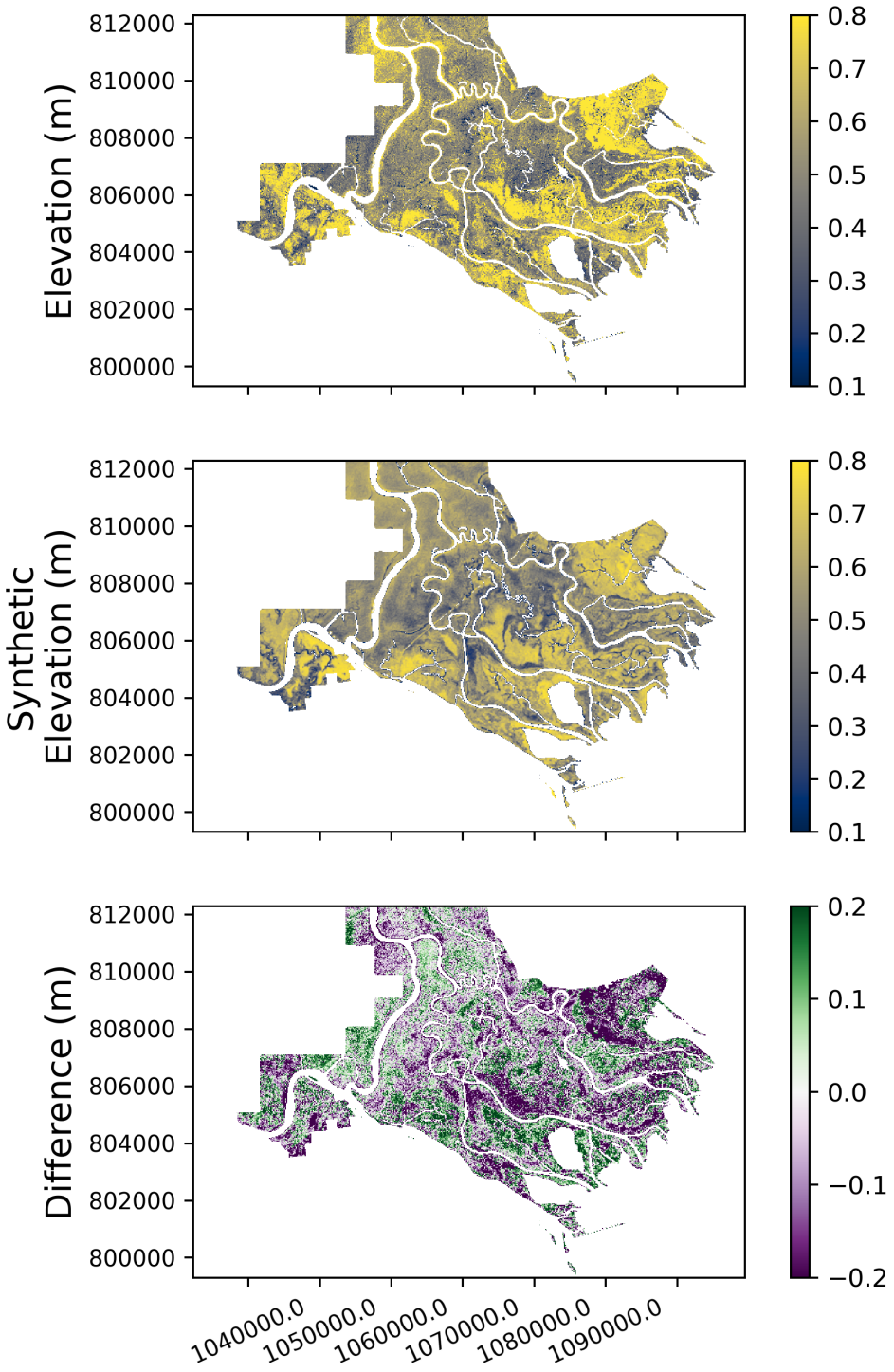

Figure 32. Difference map of previously existing DEM (left) and synthetic DEM for the 2010's (center). The difference between the two is shown in the right frame. A histogram of values in the difference map is shown in Figure 37.

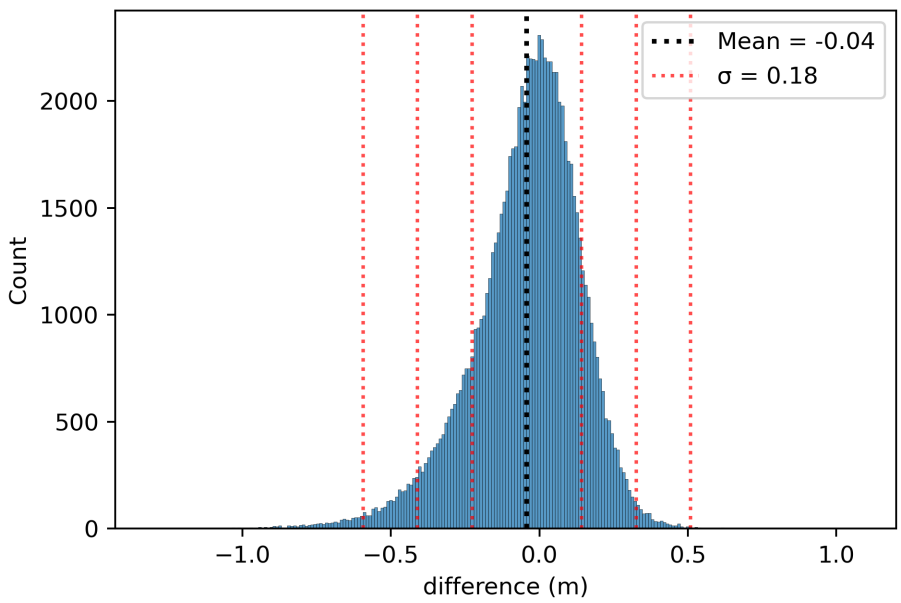

Figure 33. Histogram of difference values between previously existing DEM and the synthetic DEM for the 2010's for a subdomain of the Apalachicola site.

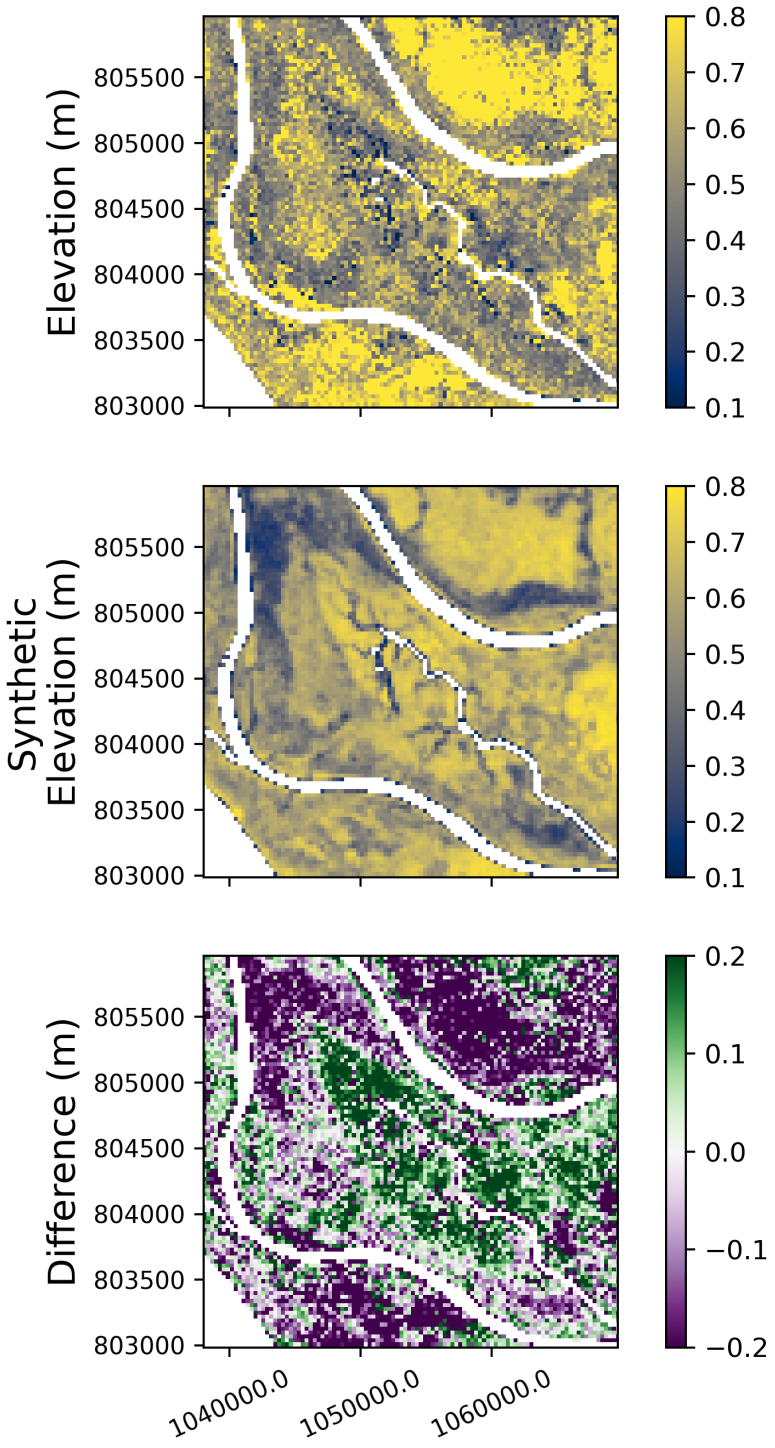

Figure 34. Difference map of previously existing DEM (left) and synthetic DEM for the 2010s (center), zoomed in to a subdomain of the Atchafalaya site. The difference between the two is shown in the right frame. A histogram of values in the difference map is shown in Figure 37.

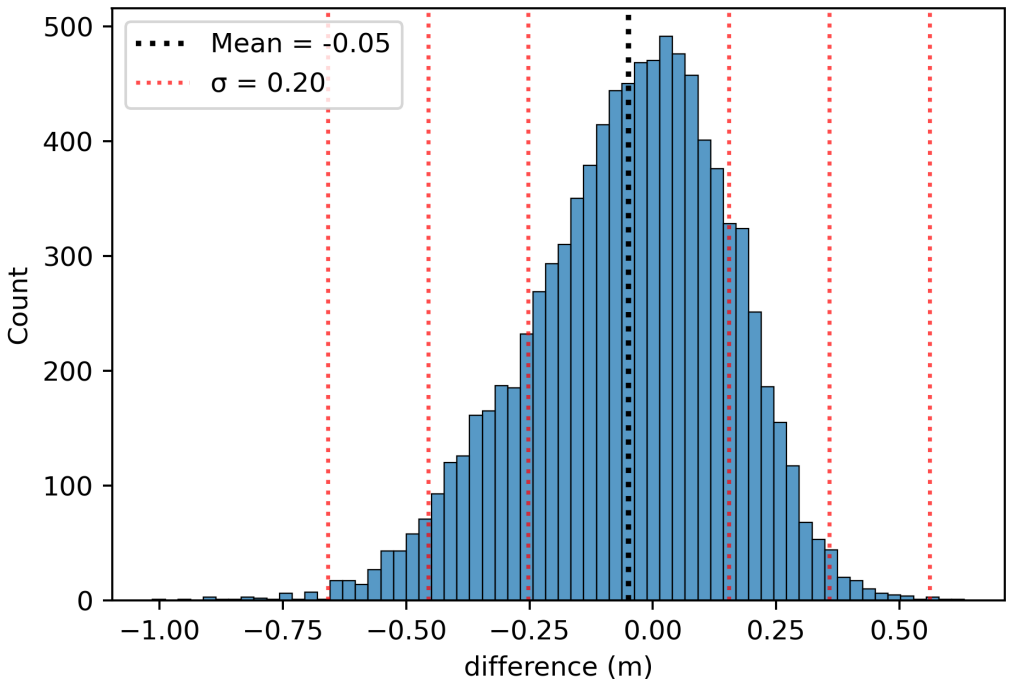

Figure 35. Histogram of difference values between previously existing DEM and the synthetic DEM for the 2010s for a subdomain of the Apalachicola site.

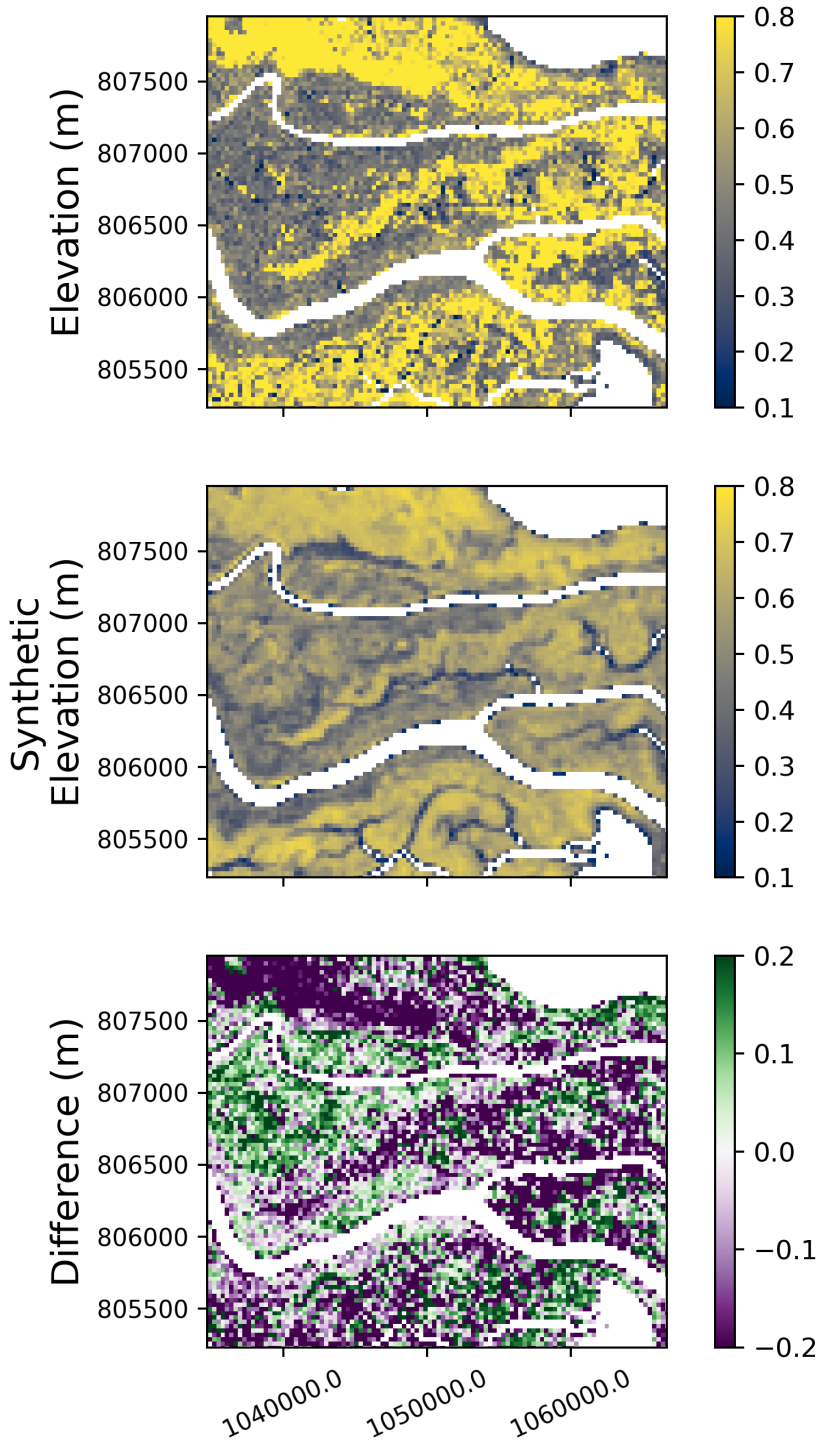

Figure 36. Difference map of previously existing DEM (left) and synthetic DEM for the 2010s (center), zoomed in to a subdomain of the Atchafalaya site. The difference between the two is shown in the right frame. A histogram of values in the difference map is shown in Figure 37.

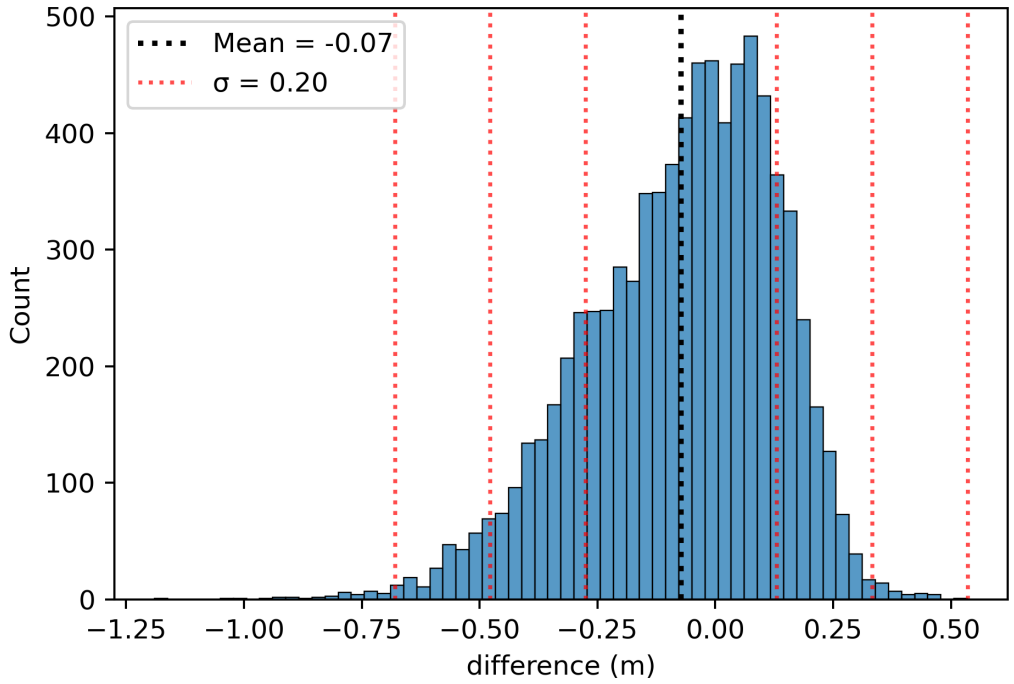

Figure 37. Histogram of difference values between previously existing DEM and the synthetic DEM for the 2010s for a subdomain of the Apalachicola site.

3.2.2 Map Timeseries

This section shows decadal changes to the frequency of Partial Surface Water and to synthetic elevation at Apalachicola. The frequency of Partial Surface Water inundation has not consistently changed over time as was observed in Grand Bay. Rather, the spatial pattern has changed, with some areas increasing in coverage and some decreasing. This site has more influence from the river than Grand Bay does, and it is possible that the tidal inundation signal is obscured by the hydrology of the river, which is not accounted for in this analysis.

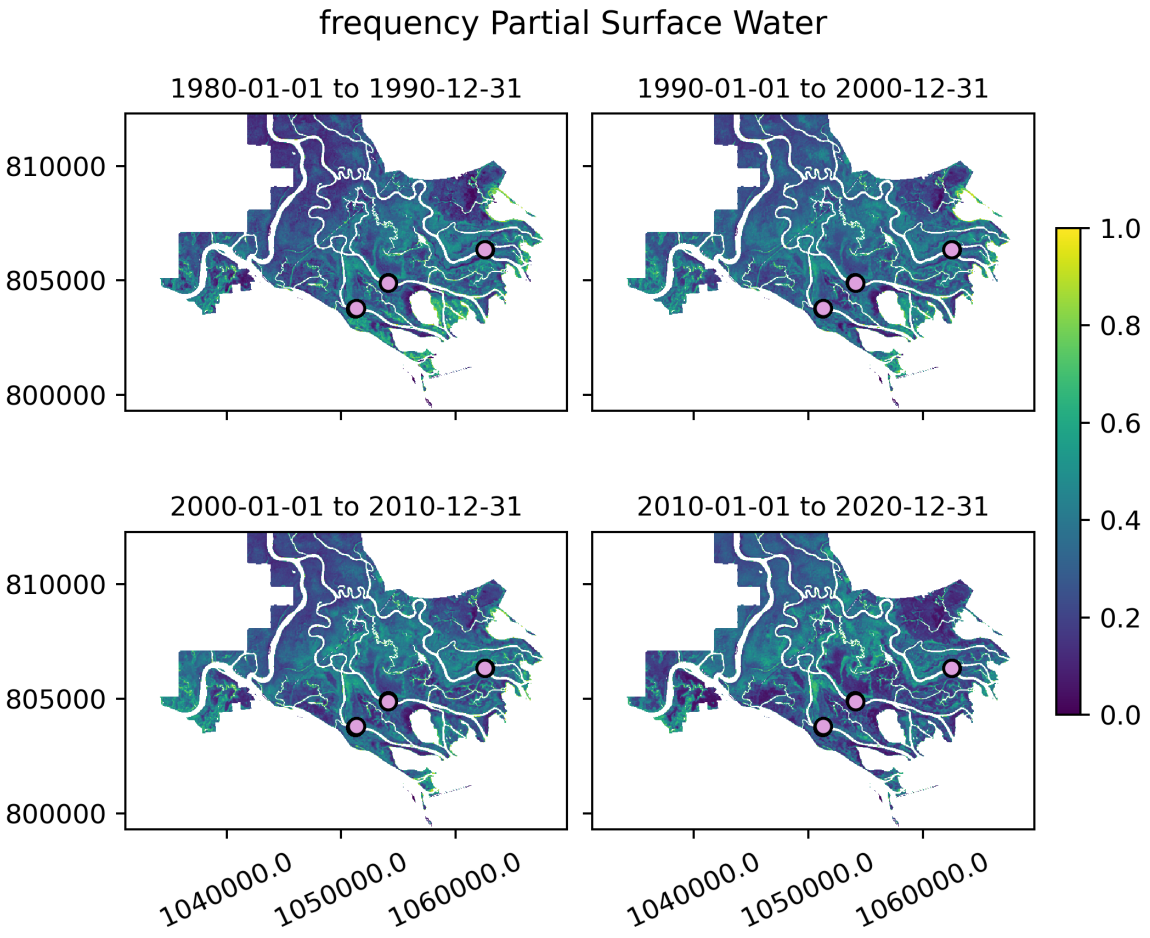

Figure 38. Partial surface water frequency at Apalachicola for each decade since the 1980s. Lavender dots with black outlines represent the locations of SETs at this location.

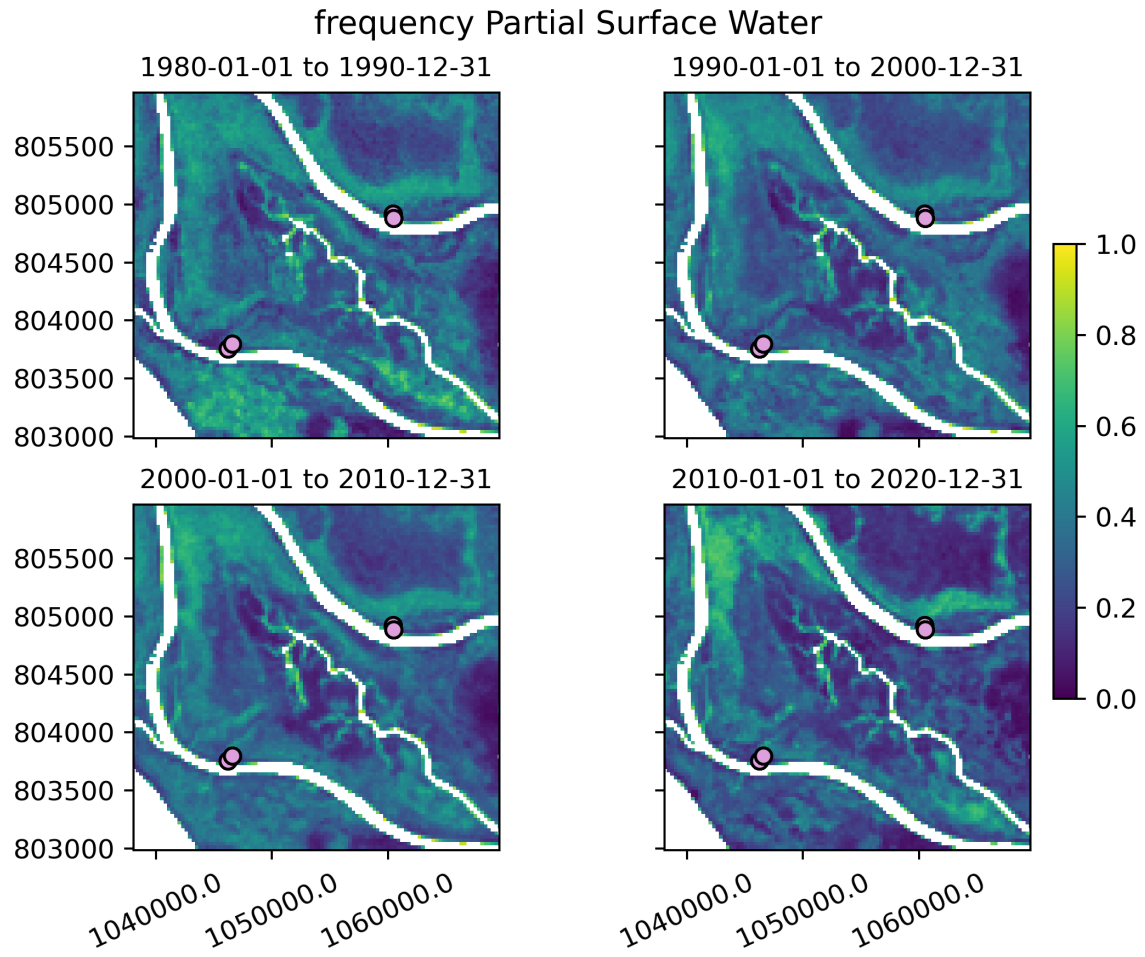

Figure 39. Partial Surface Water frequency at a subdomain of Apalachicola for each decade since the 1980s. Lavender dots with black outlines represent the locations of SETs at this location.

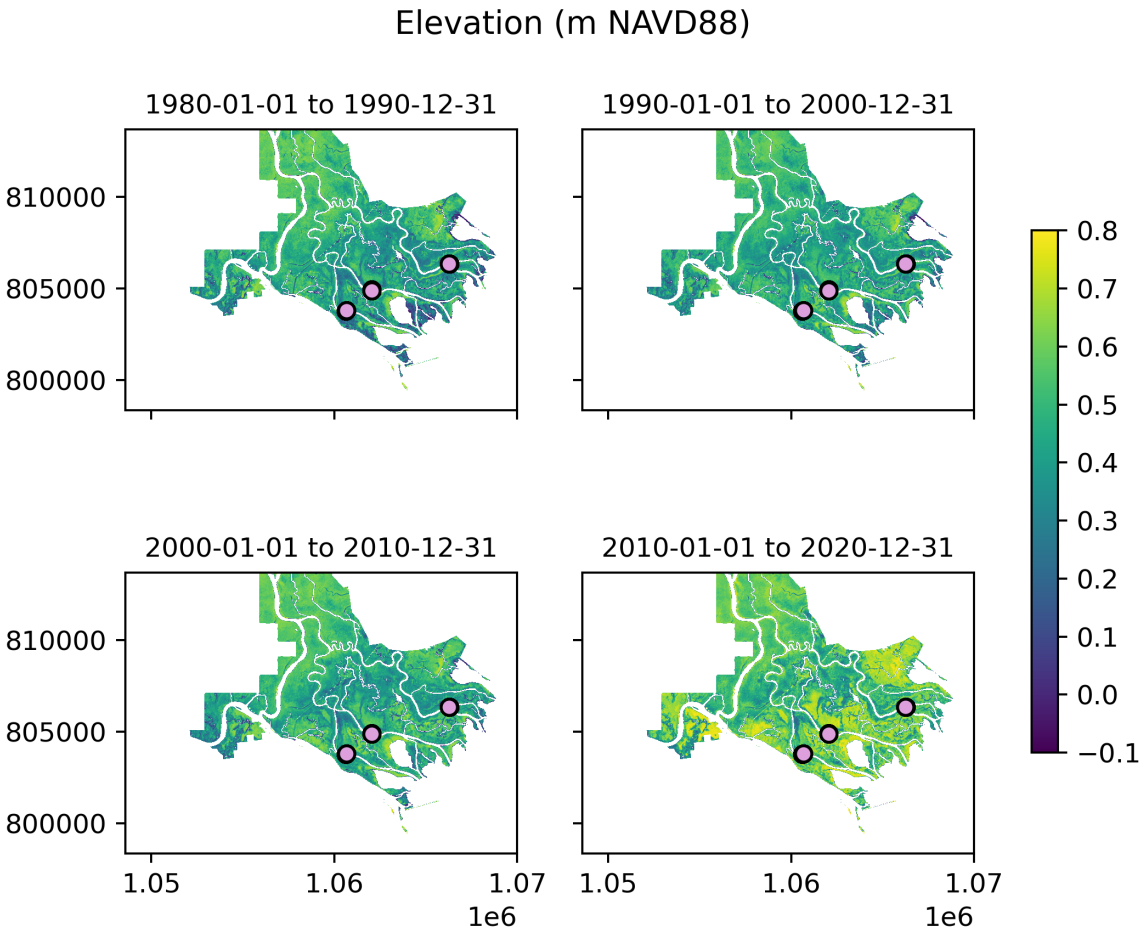

Figure 40. Synthetic elevation at Apalachicola for each decade since the 1980s. Lavender dots with black outlines represent the locations of SETs at this location.

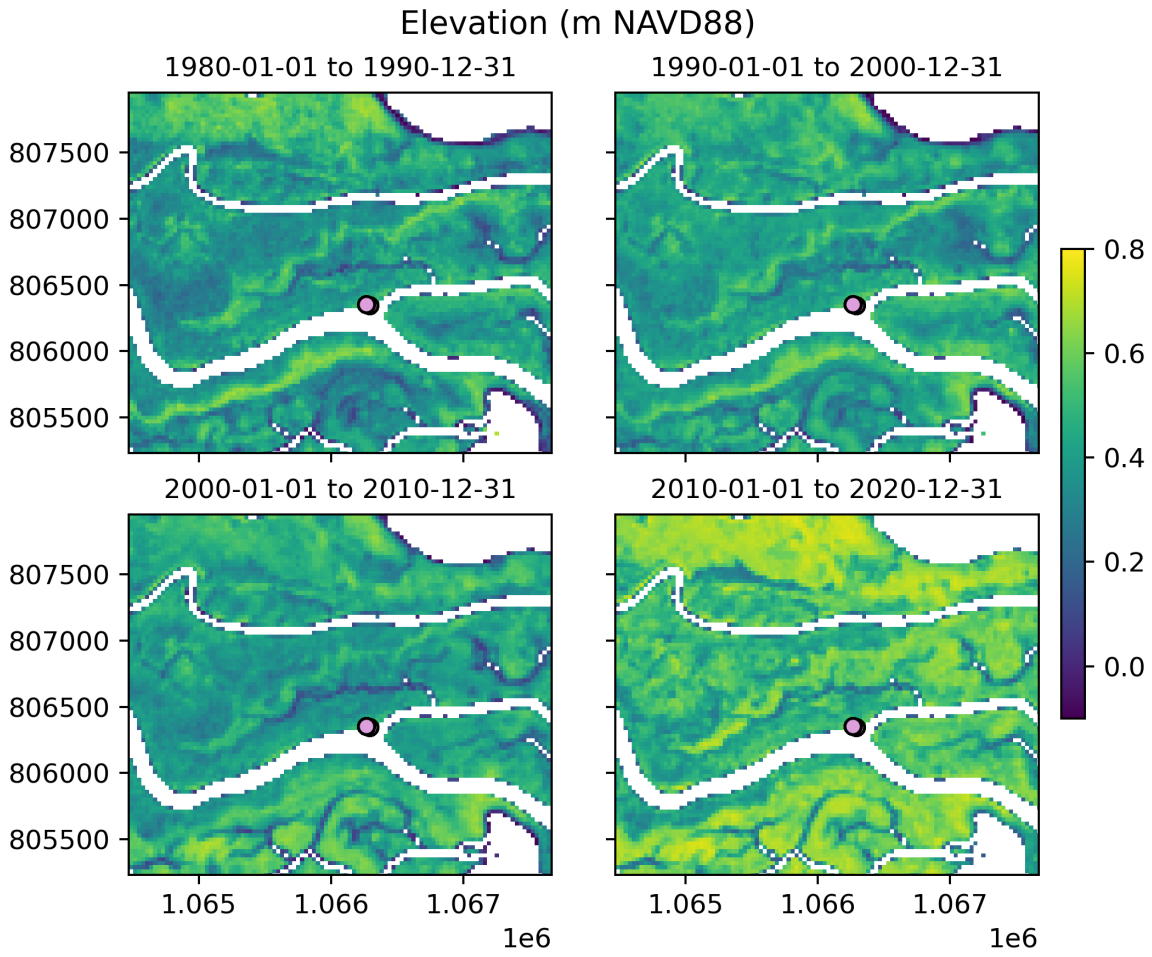

Figure 41. Synthetic elevation at a subdomain of Apalachicola for each decade. Lavender dots with black outlines represent the locations of SETs at this location.

3.2.3 Validation to Observational Data

The figures in this section show the elevations in the synthetic DEMs at the location of the SET control data. Solid colored circles indicate the synthetic elevation at the pixel of the indicated SET monument. The time series of average SET-derived elevations at each site is shown as a solid line, and the measurements that were used to derive that average (mean elevation at each SET arm position) are shown in pale dots. Elevations from the directly observed DEM are shown as stars. The largest star shows the value of that DEM when resampled to Landsat resolution, while the smaller dots show the value of all of the pixels at full resolution that sit within the footprint of the Landsat pixel. Note here that a substantial component of the total uncertainty in the synthetic DEM process seems to arise from the resampling of the directly observed DEM to the 30m Landsat resolution. Only a selection of the SET data is shown in this report. Remaining data can be found in the data archive described in Appendix B.

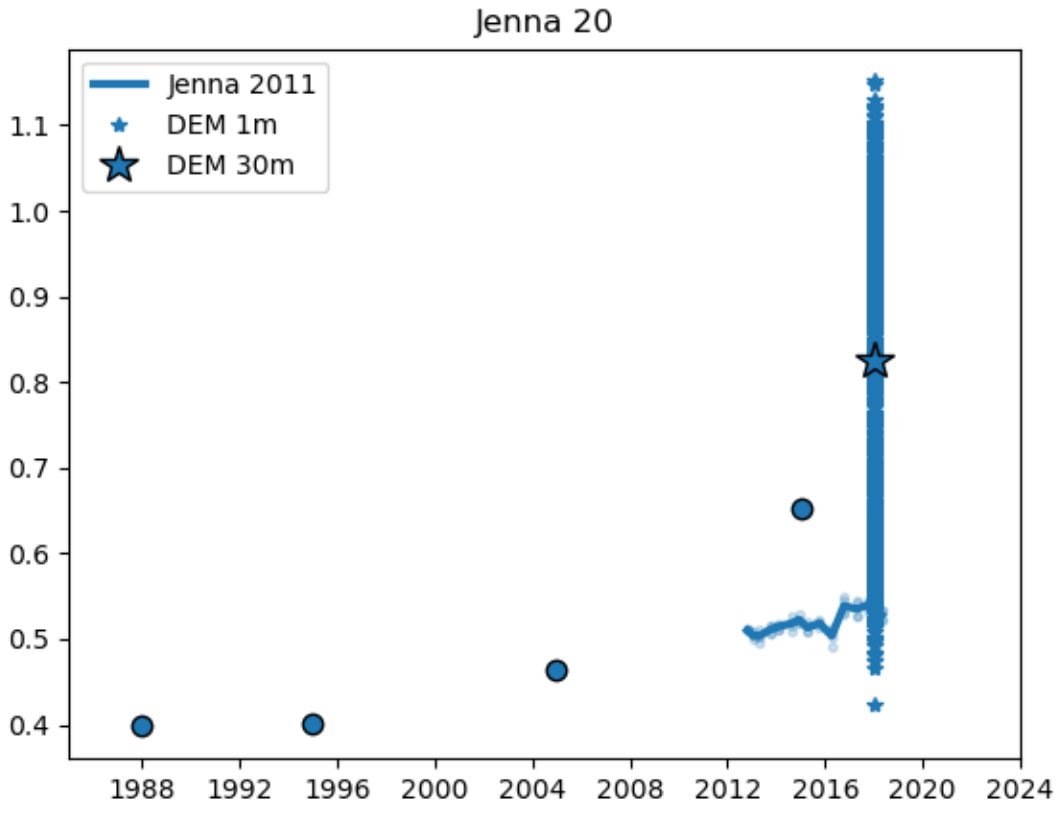

Figure 42. Validation to SET derived elevations at the Baker SET site in Apalachicola.

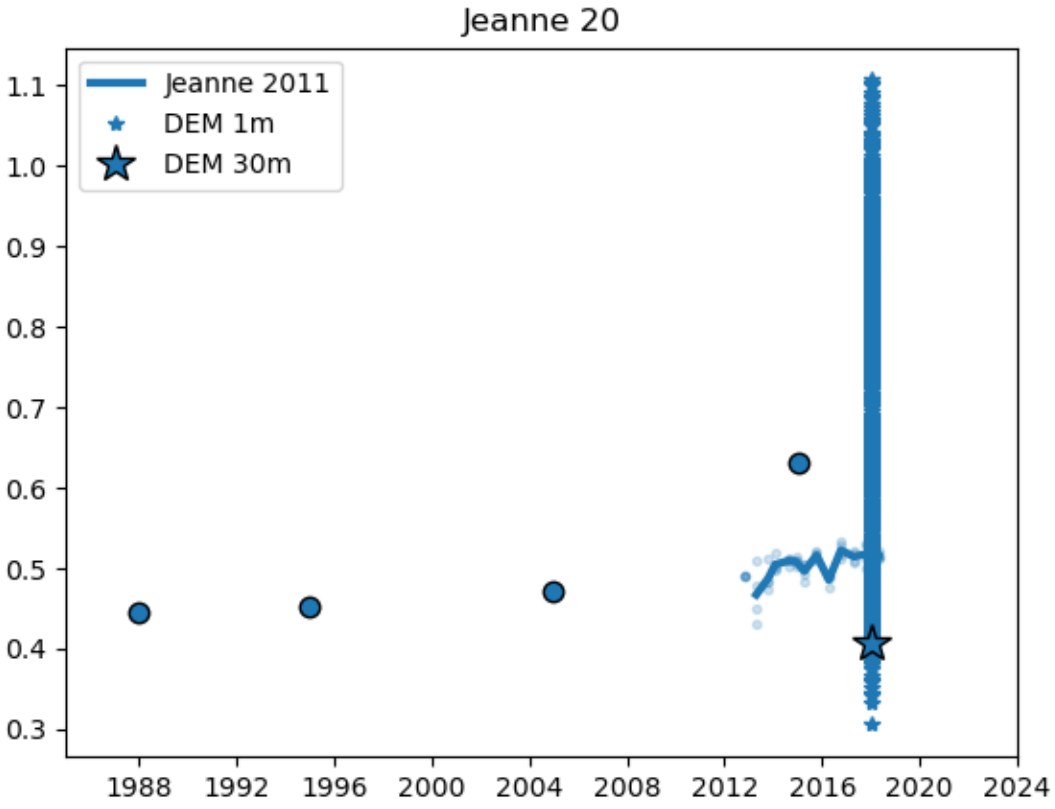

Figure 43. Validation to SET derived elevations at the Jeanne SET site in Apalachicola.

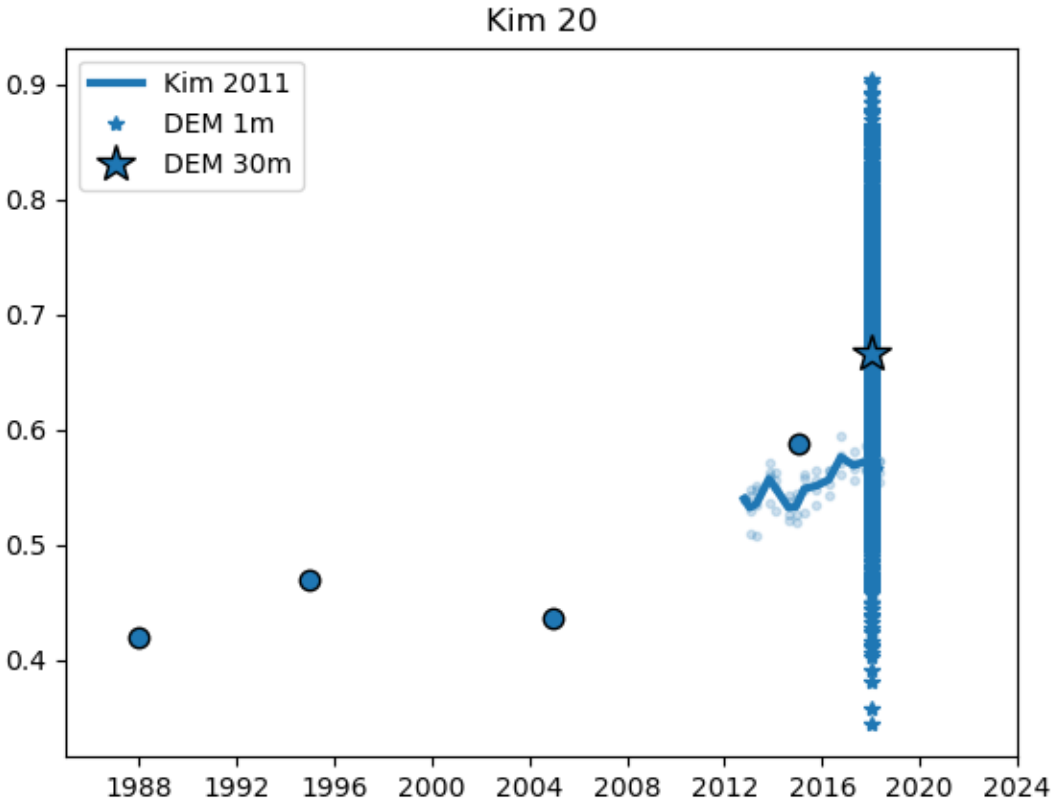

Figure 44. Validation to SET derived elevations at the Kim SET site in Apalachicola.

3.3. BRETON SOUND, LA

The Breton Sound study site is shown in Figure 47. Locations of CRMS SET stations are shown on the map and referred to in subsequent figures.

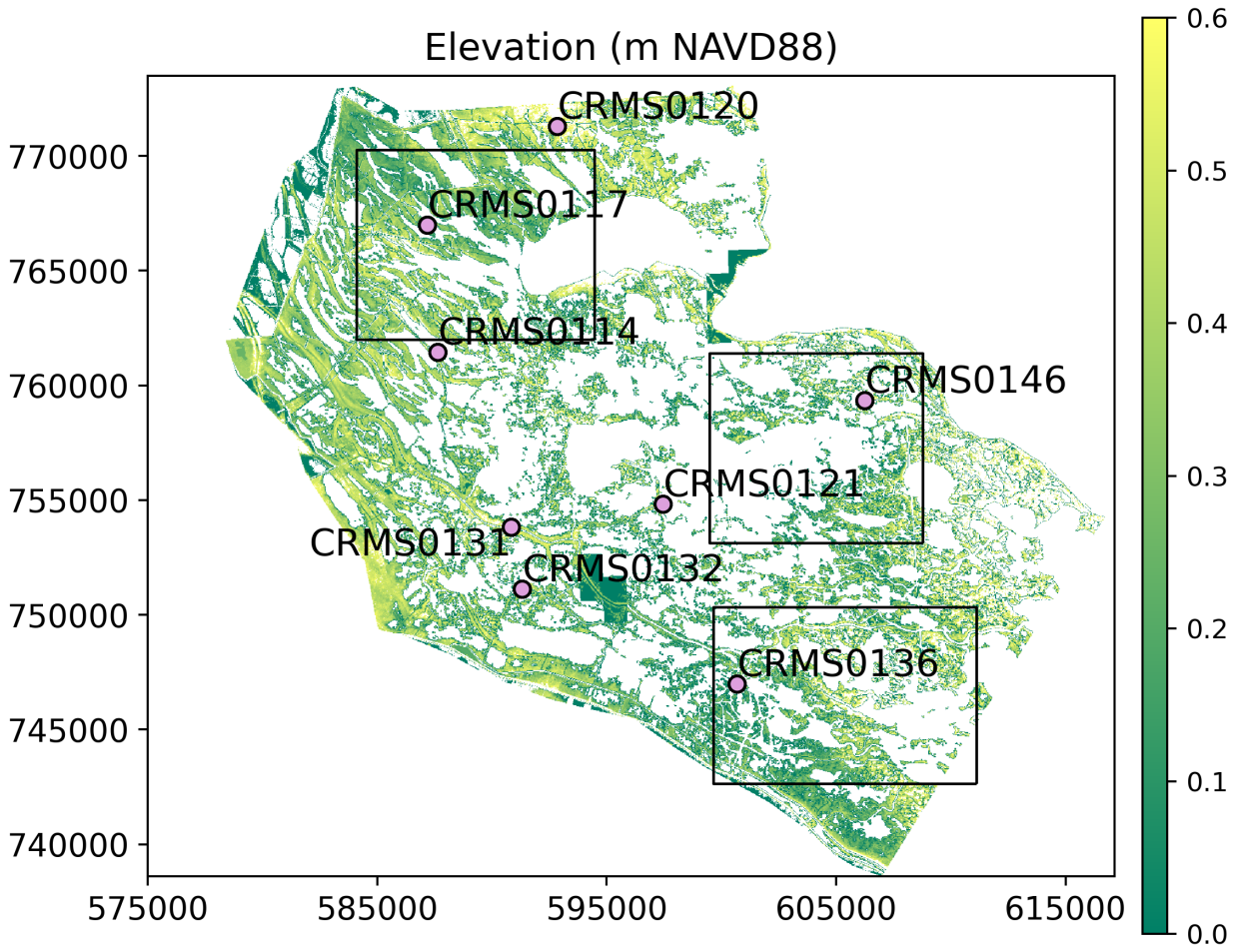

Figure 45. Breton Study site, modern masked DEM, with analysis locations shown in black boxes. SET stations are shown as lavendar colored points with black outlines.

3.3.1 Difference Assessment with Recent DEM

Differencing the resampled LiDAR DEM and the synthetic DEM at Breton Sound during the 2010-2020 decade shows an error distribution with a mean difference of 4 cm, and a standard deviation of 40 cm (Figures 46–47). The three selected sub-geographies perform even less well (Figure 48–53), with standard deviations as high as 50 cm. This performance is less accurate than the synthetic DEMs at either Grand Bay or Apalachicola.

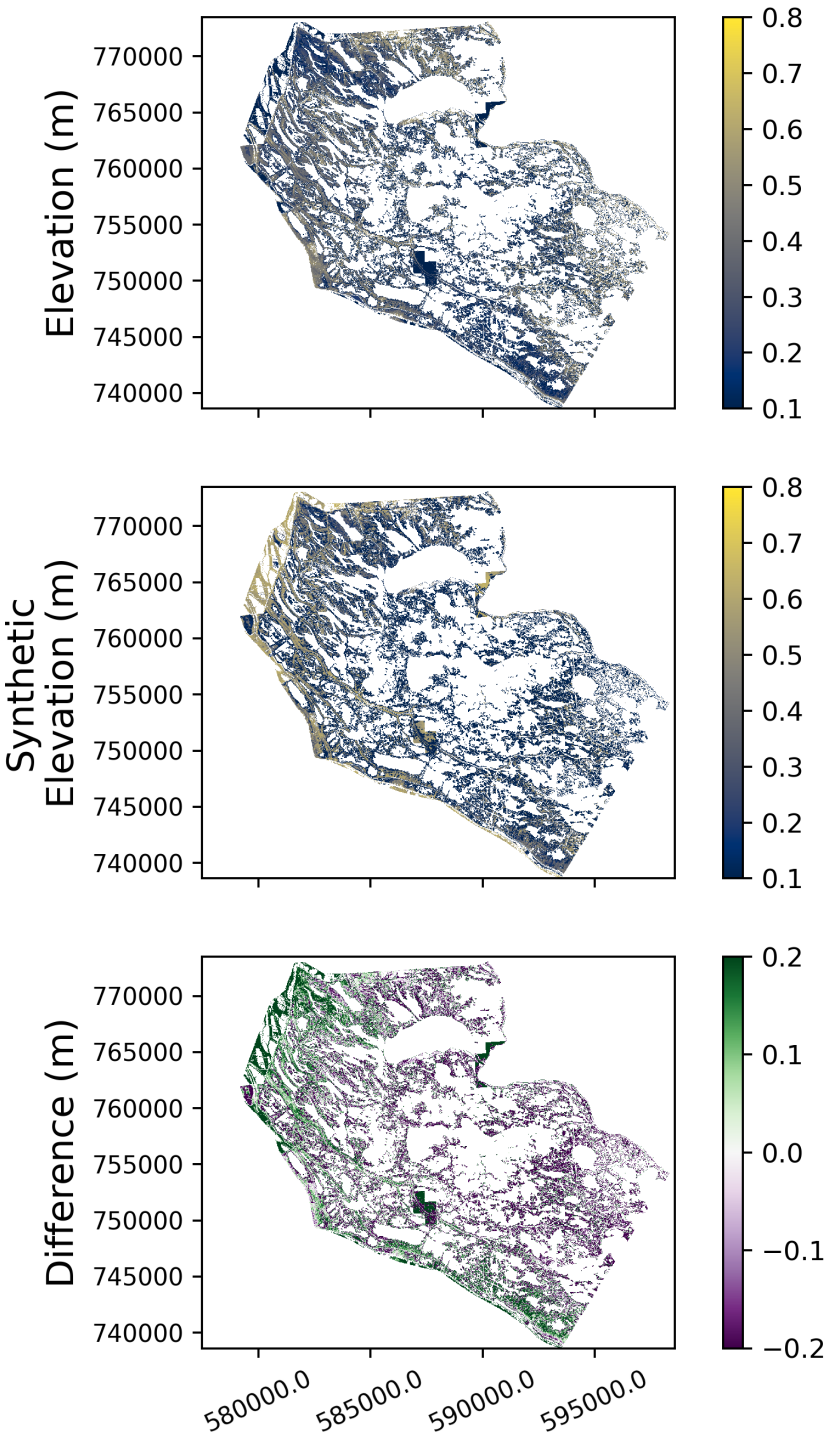

Figure 46. Difference map of previously existing DEM (left) and synthetic DEM for the 2010's (center) at Breton Sound.

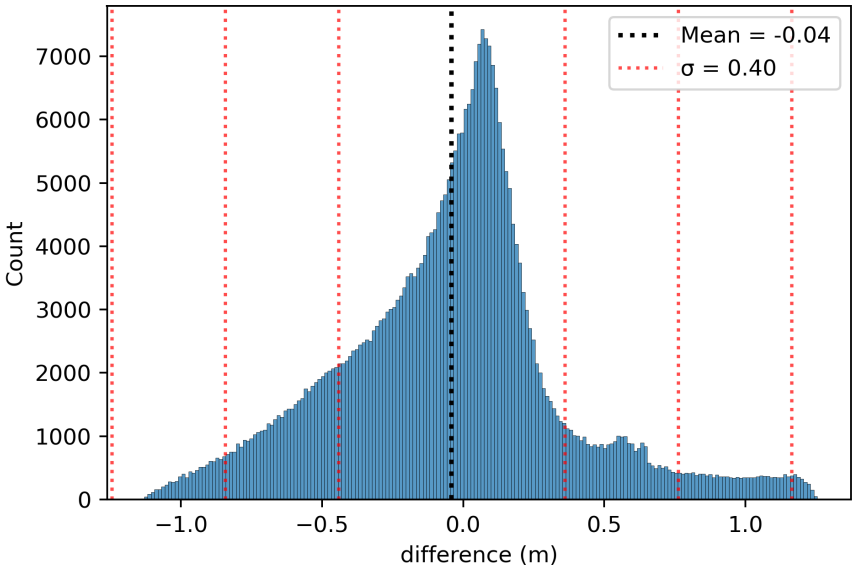

Figure 47. Histogram of difference values between previously existing DEM and the synthetic DEM for the 2010's for a subdomain of the Breton Sound site.

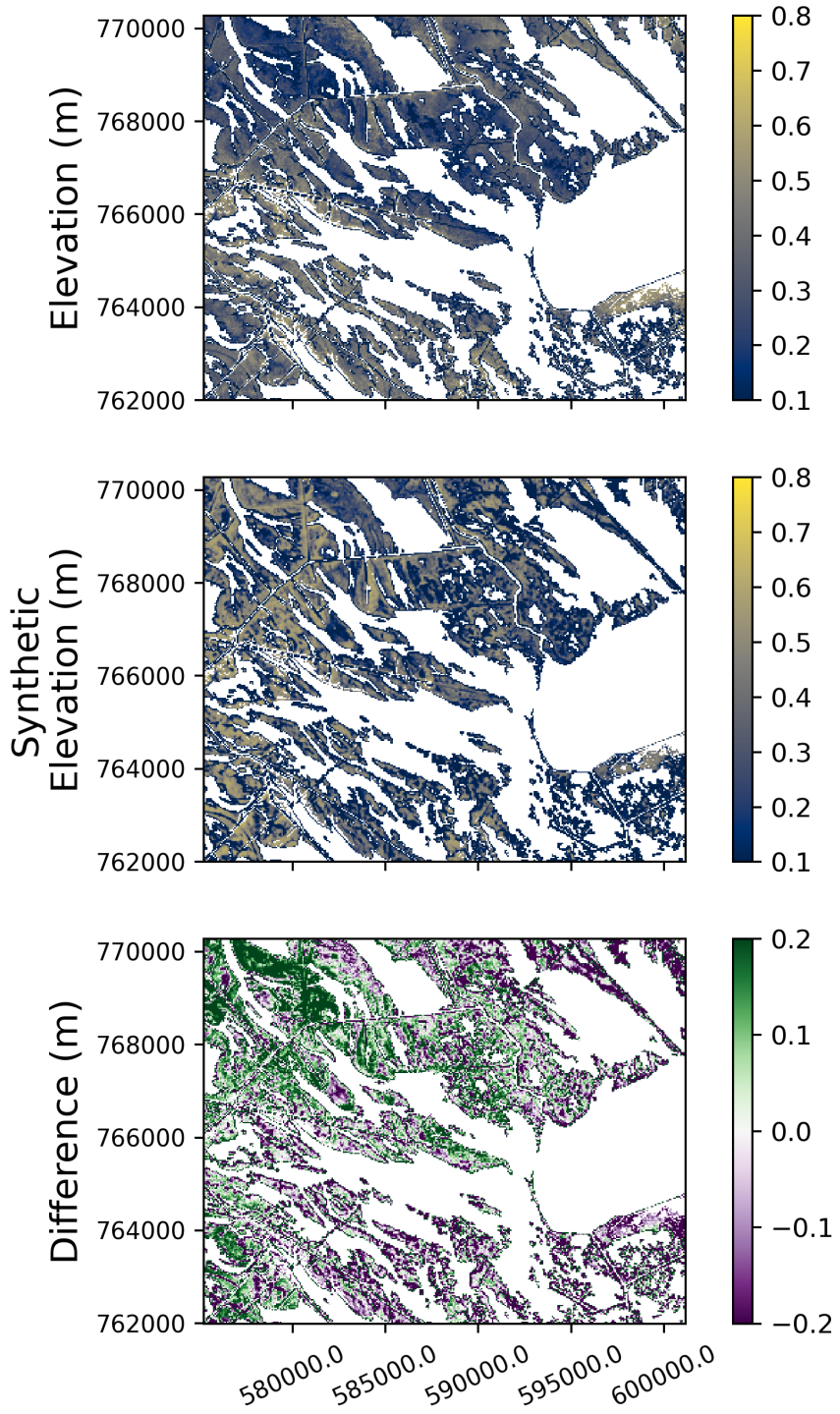

Figure 48. Difference map of previously existing DEM (left) and synthetic DEM for the 2010s (center), zoomed in to a subdomain of the Breton site. The difference between the two is shown in the right frame. A histogram of values in the difference map is shown in Figure 49.

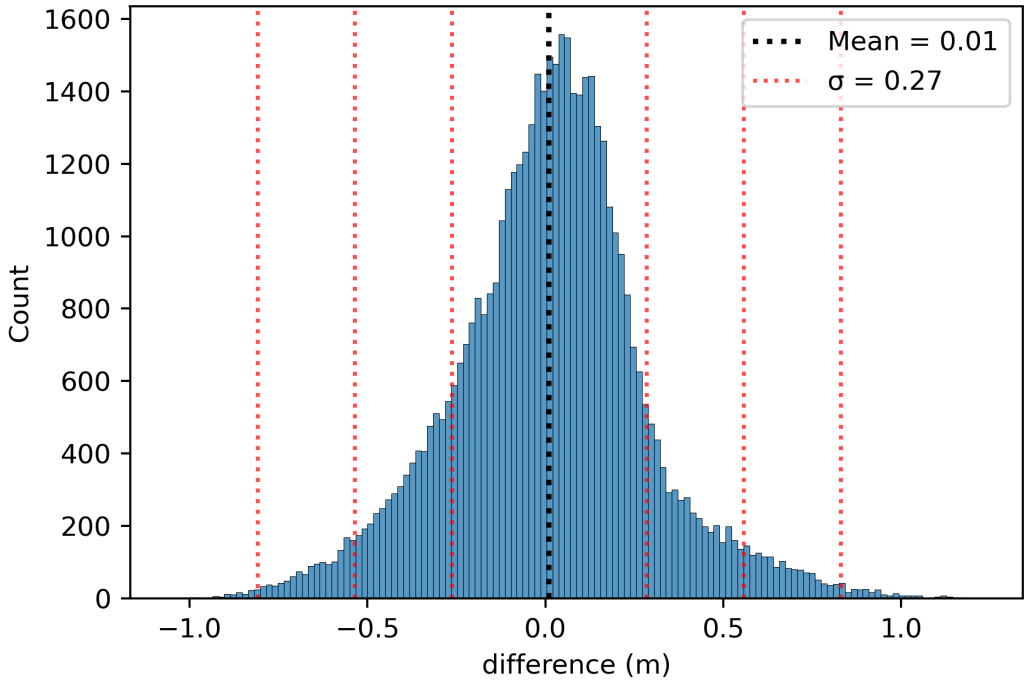

Figure 49. Histogram of difference values between previously existing DEM and the synthetic DEM for the 2010s for a subdomain of the Breton site.

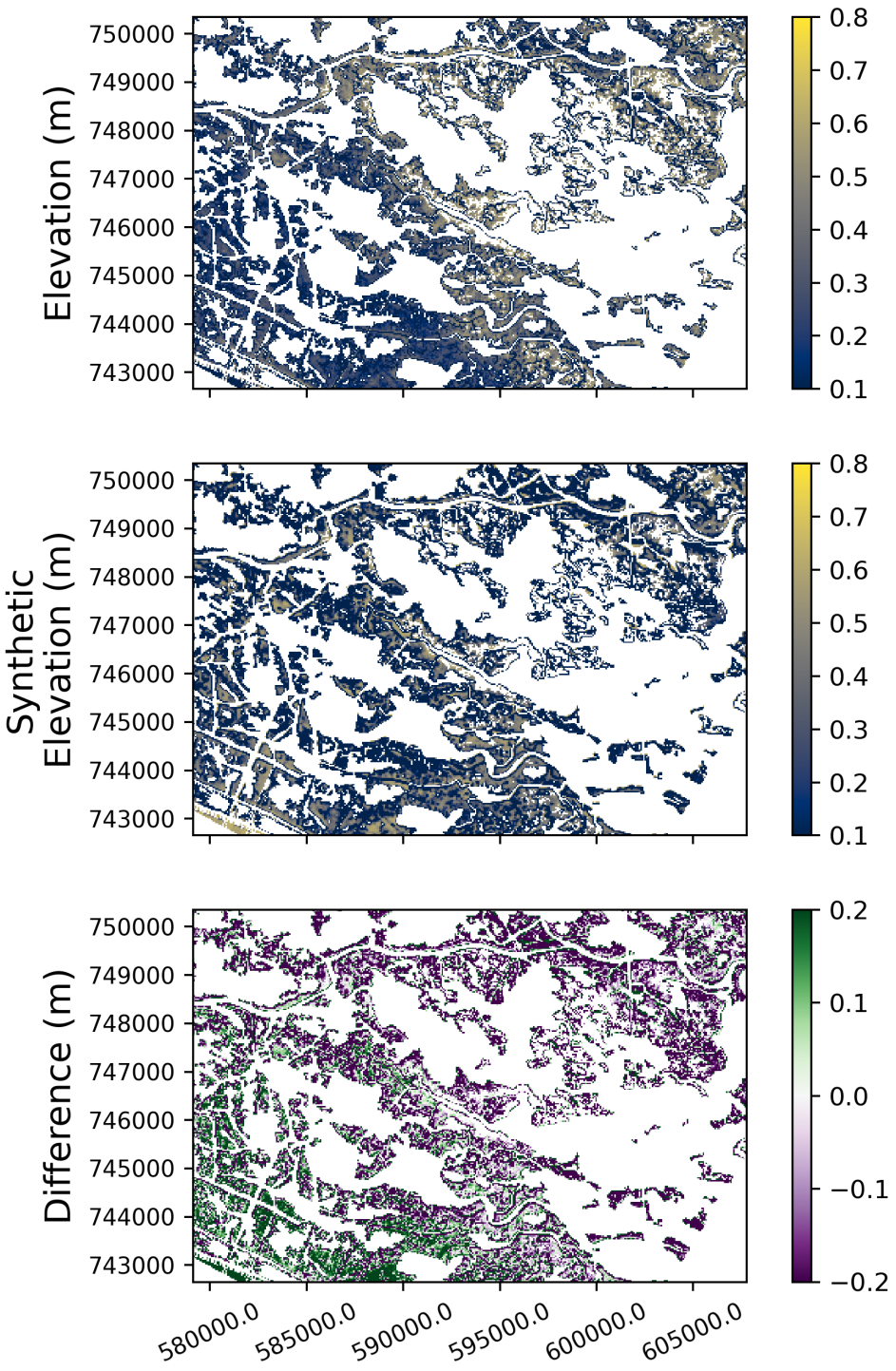

Figure 50. Difference map of previously existing DEM (left) and synthetic DEM for the 2010s (center), zoomed in to a subdomain of the Breton site. The difference between the two is shown in the right frame. A histogram of values in the difference map is shown in Figure 51.

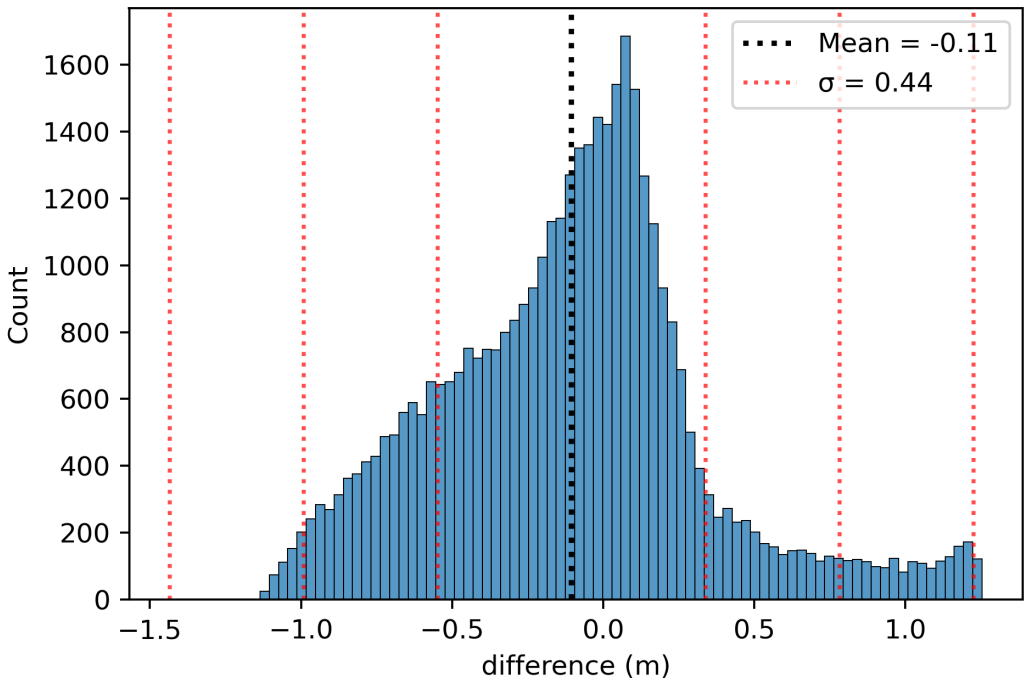

Figure 51. Histogram of difference values between previously existing DEM and the synthetic DEM for the 2010s for a subdomain of the Breton site.

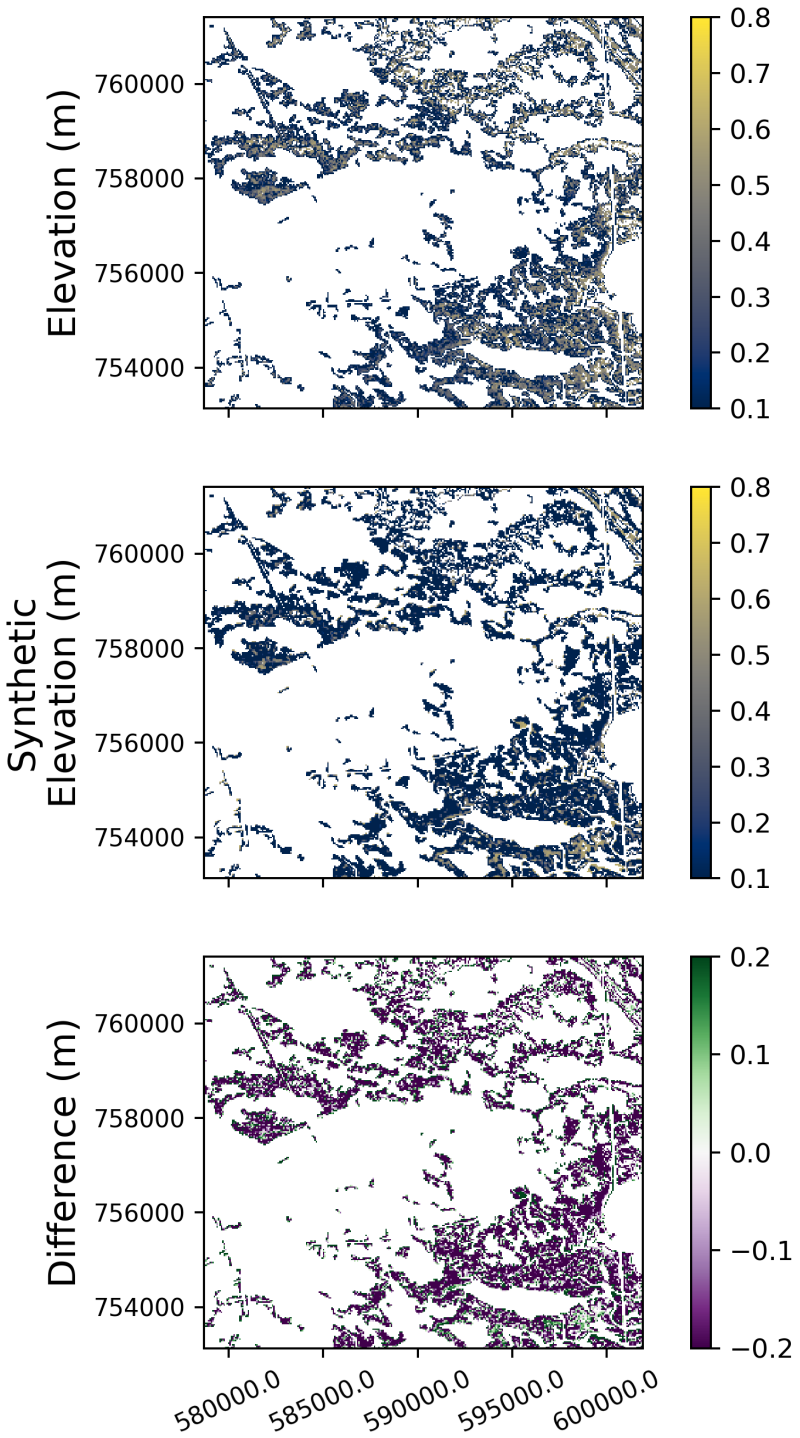

Figure 52. Difference map of previously existing DEM (left) and synthetic DEM for the 2010s (center), zoomed in to the subdomain of the Breton site. The difference between the two is shown in the right frame. A histogram of values in the difference map is shown in Figure 53.

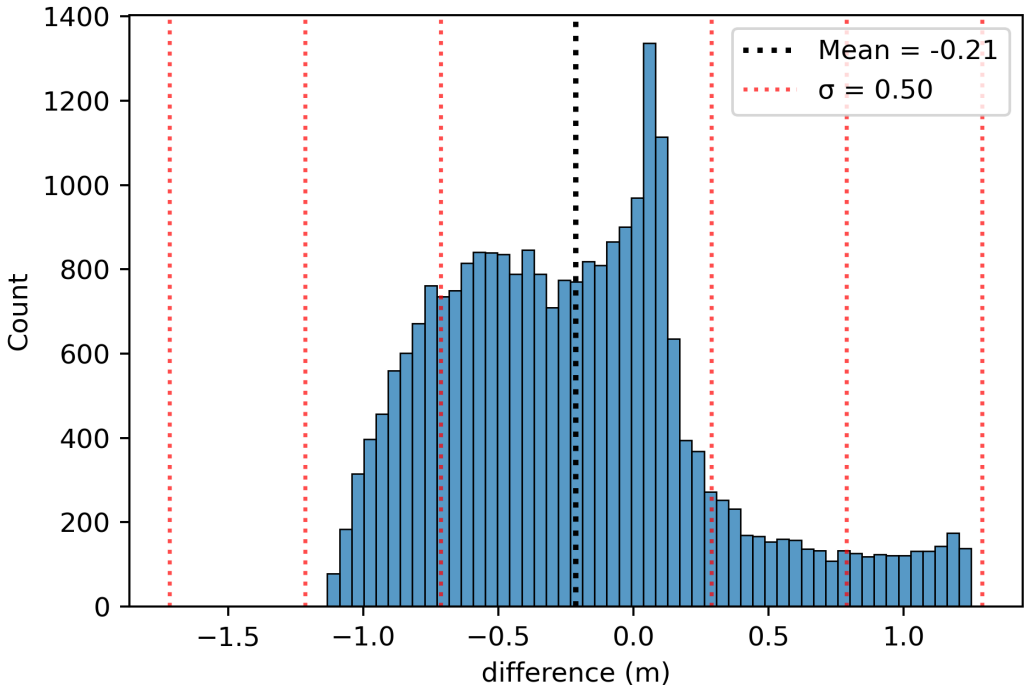

Figure 53. Histogram of difference values between previously existing DEM and the synthetic DEM for the 2010s for a subdomain of the Breton site.

3.3.2 Map Timeseries

Map timeseries of partial surface water in Breton Basin show a complicated picture. It appears that inundation frequency was higher in the past, but does not increase towards the coast as can be seen in Grand Bay and Apalachicola. To make matters more complicated, Breton has lost a substantial portion of its wetland area since 1980, so changes to wetland hydrology are likely more significant than at either Grand Bay or Apalachicola. The relationship between inundation and relative elevation does not seem to be strong here, so the synthetic DEM production process does not perform well at Breton Sound.

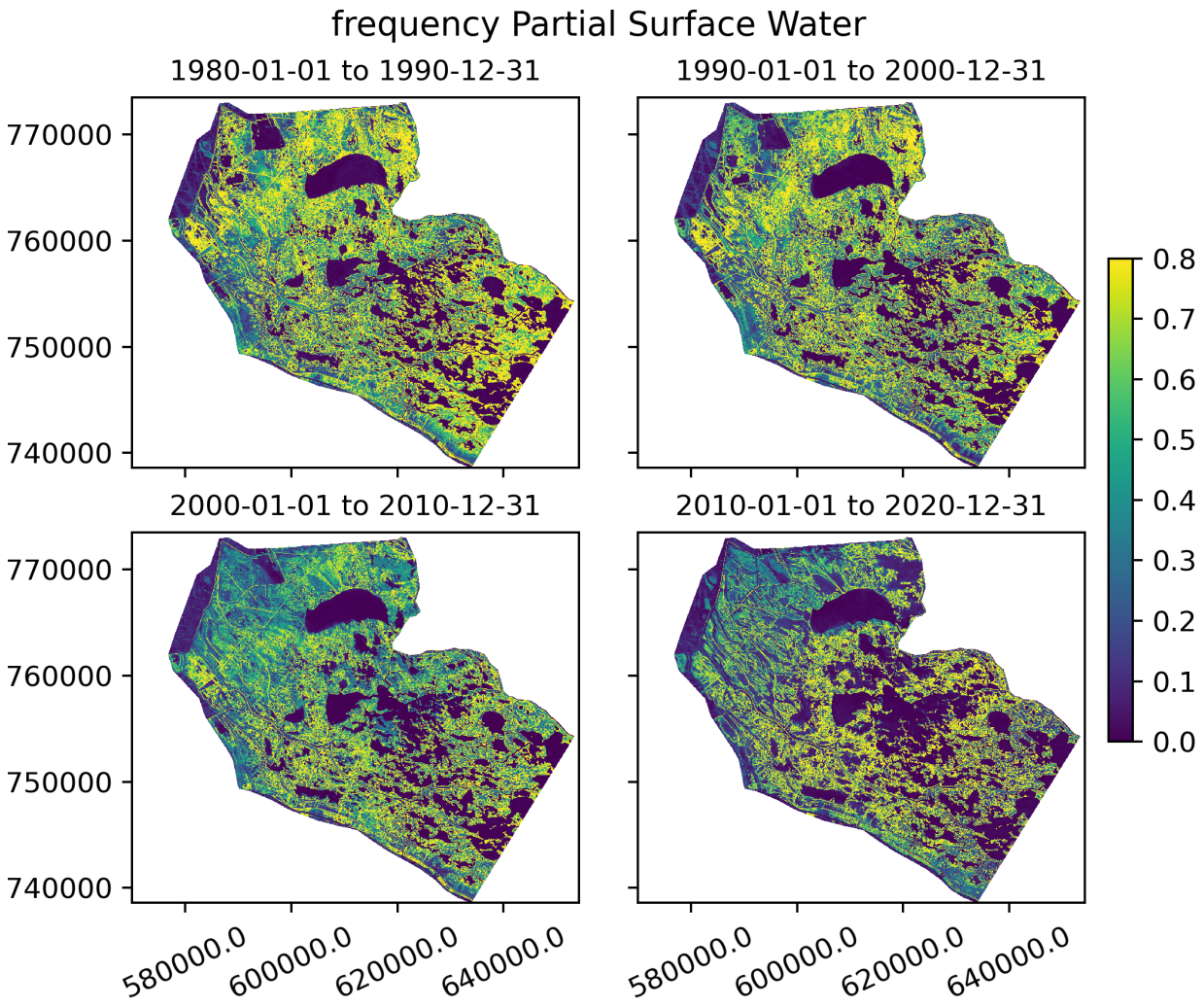

Figure 54. Breton Basin, frequency of partial surface water.

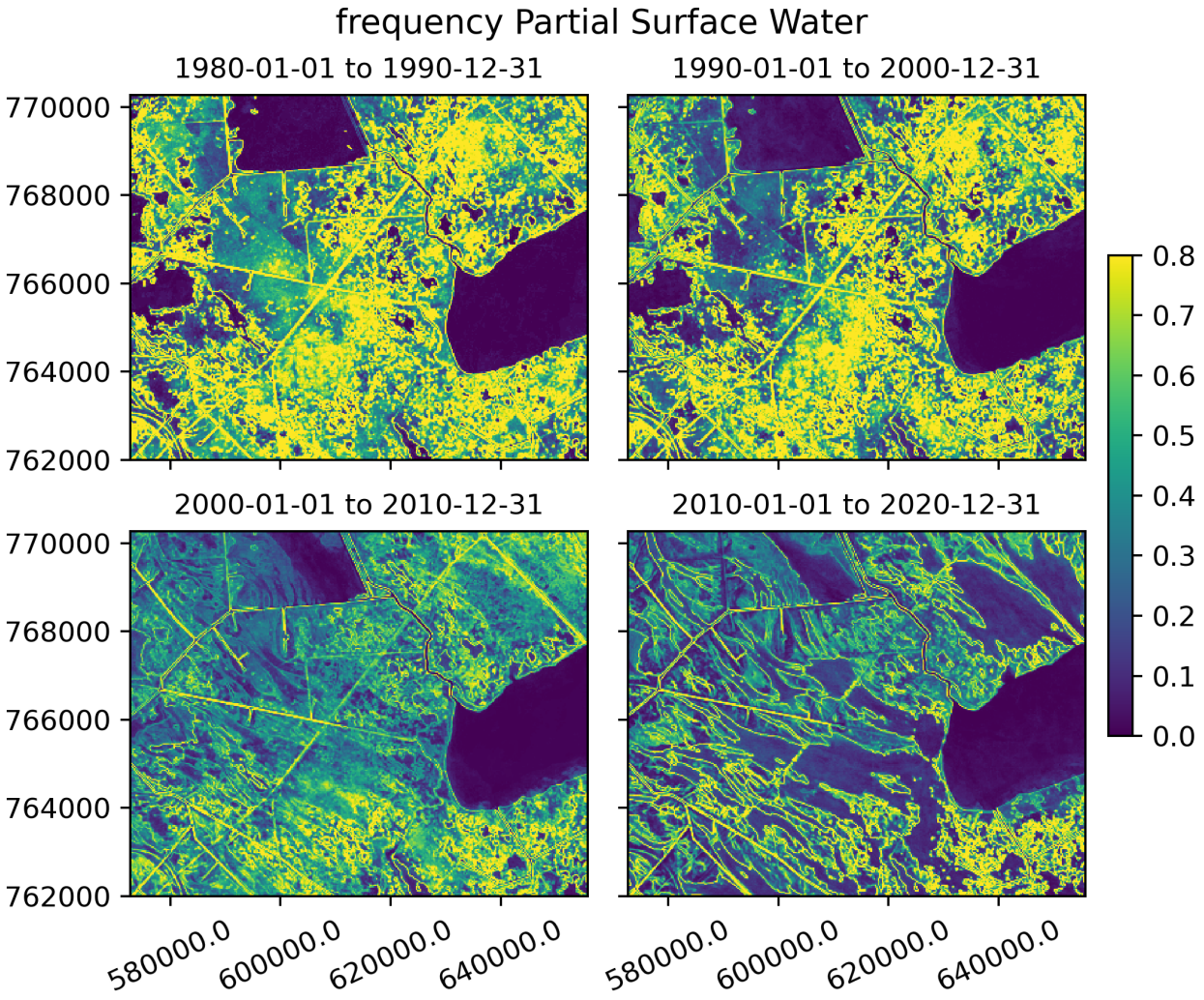

Figure 55. Breton Basin, frequency pf partial surface water in the upper basin. Note that significant changes to this region occurred during Hurricane Katrina in 2005. These changes are fully evident in the 2010 –2020 map and are averaged with pre-Katrina landscape in the 2000 – 2010 map.

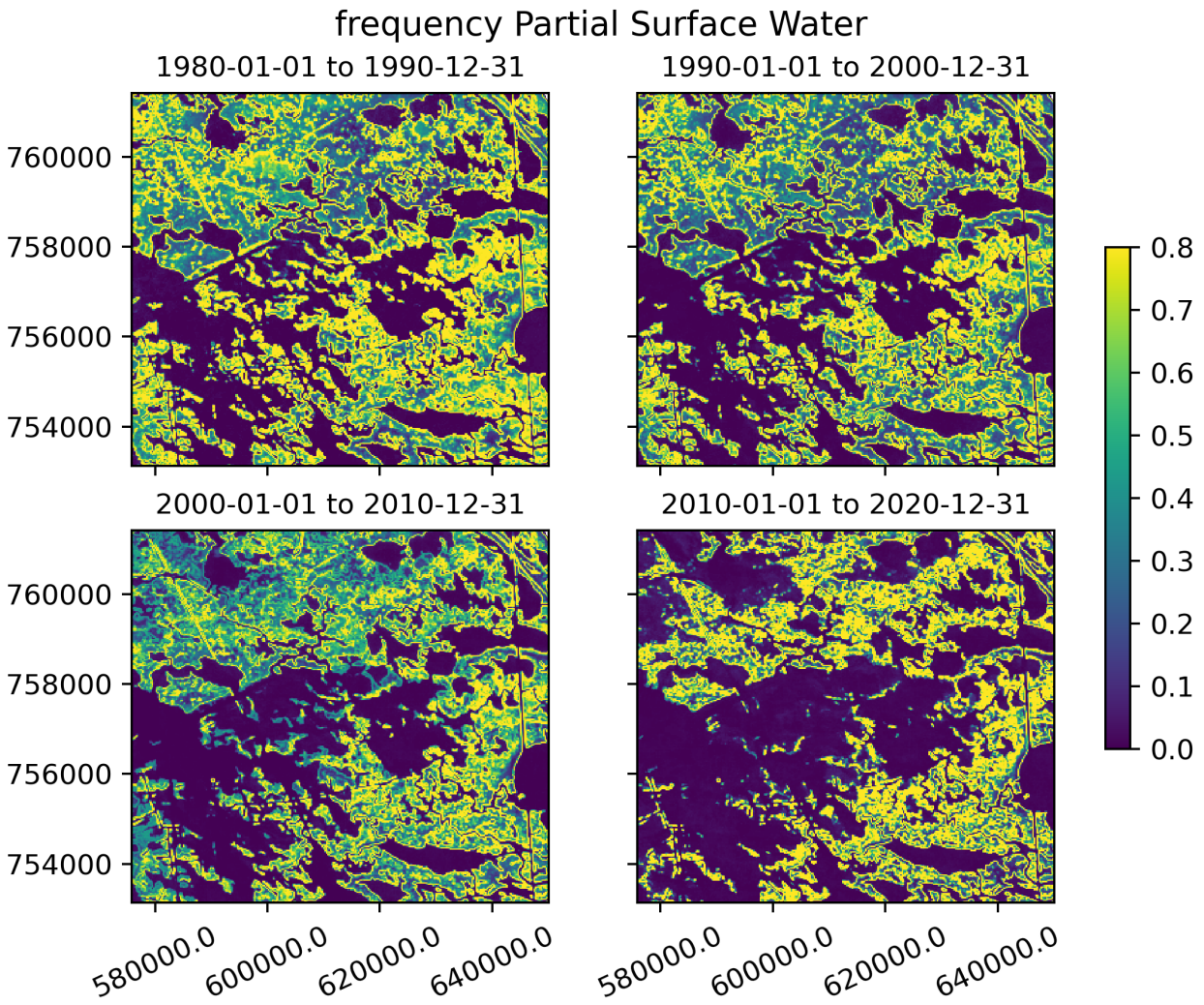

Figure 56. Breton basin, frequency pf partial surface water in the mid-basin.

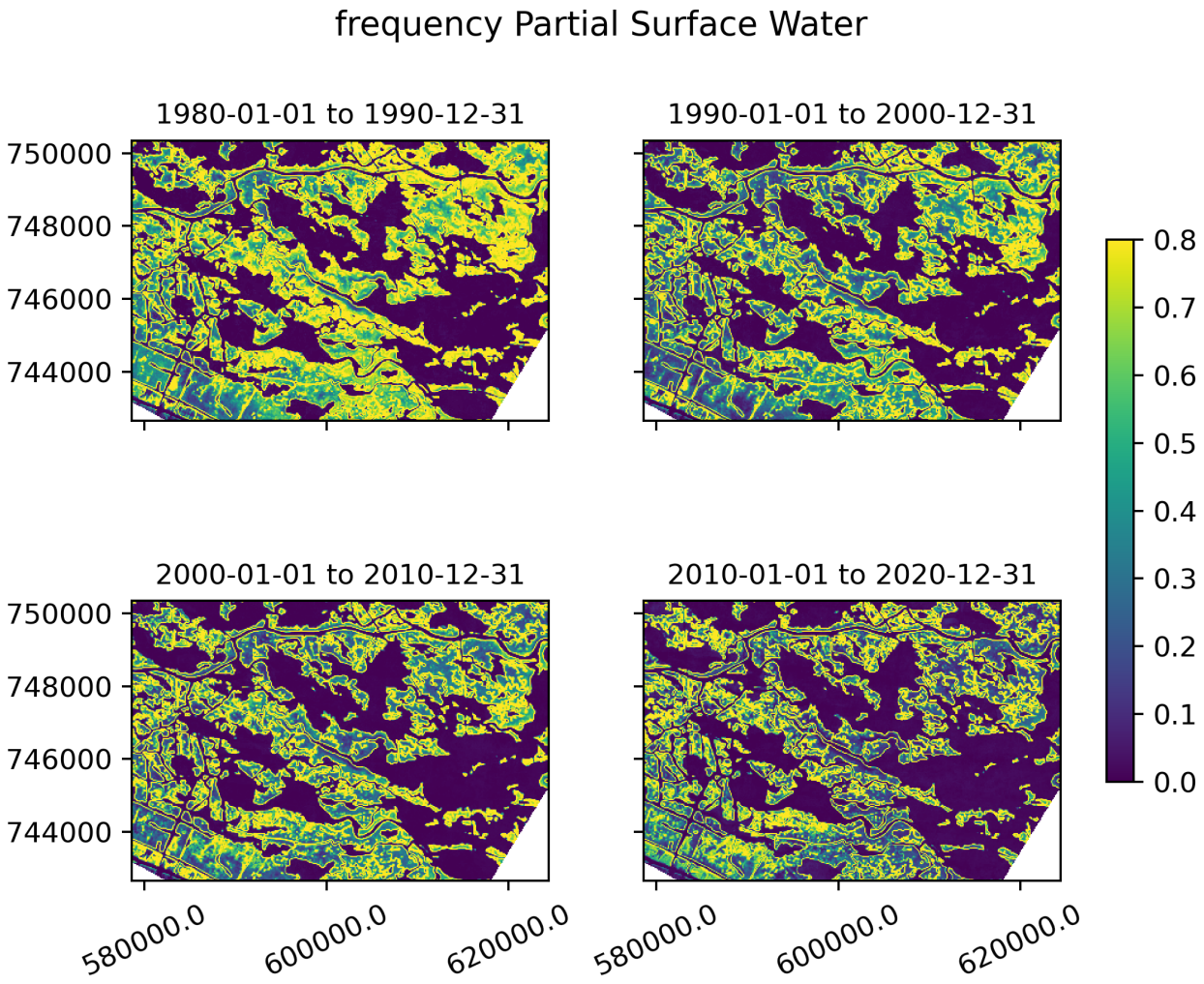

Figure 57. Breton basin, frequency pf partial surface water in the lower basin.

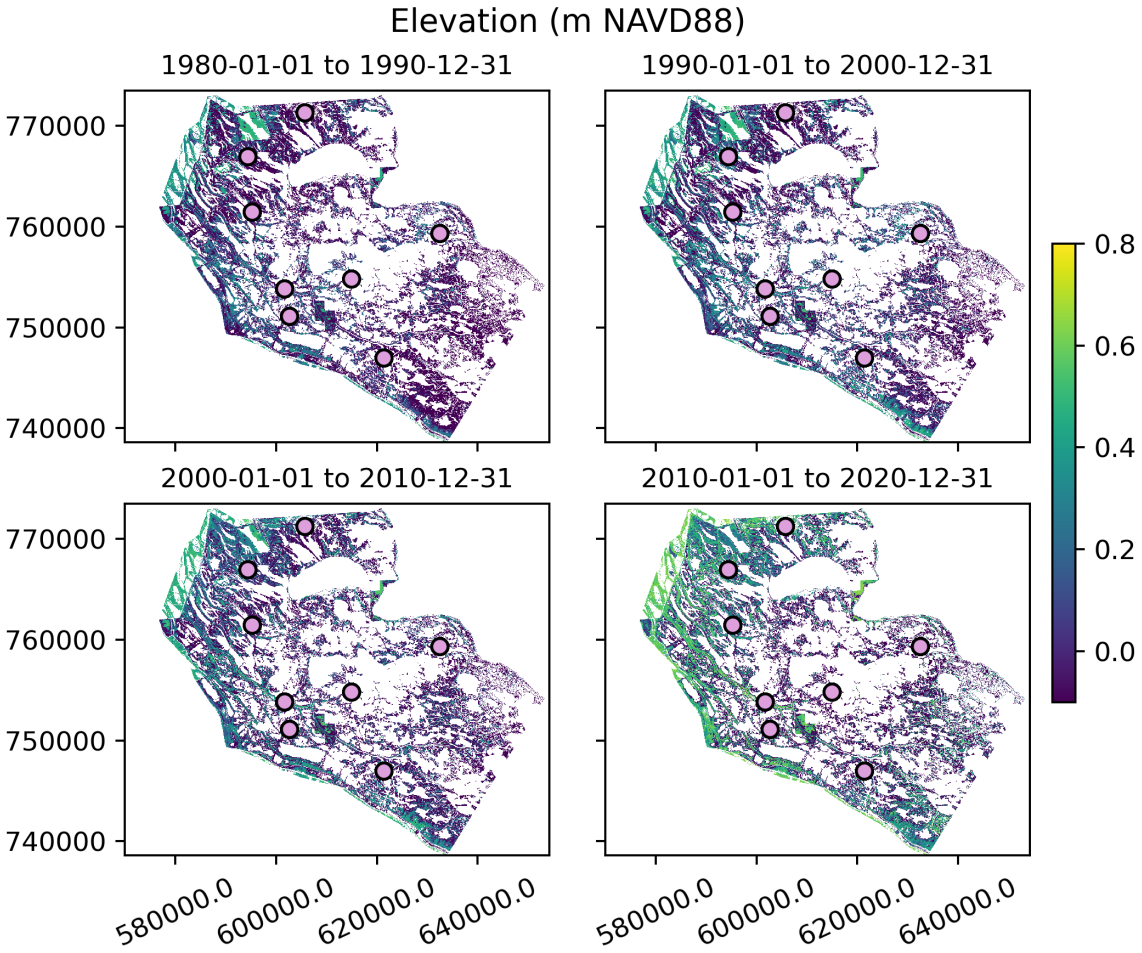

Figure 58. Breton elevation timeseries. Lavender dots with black outlines represent the locations of SETs at this location.

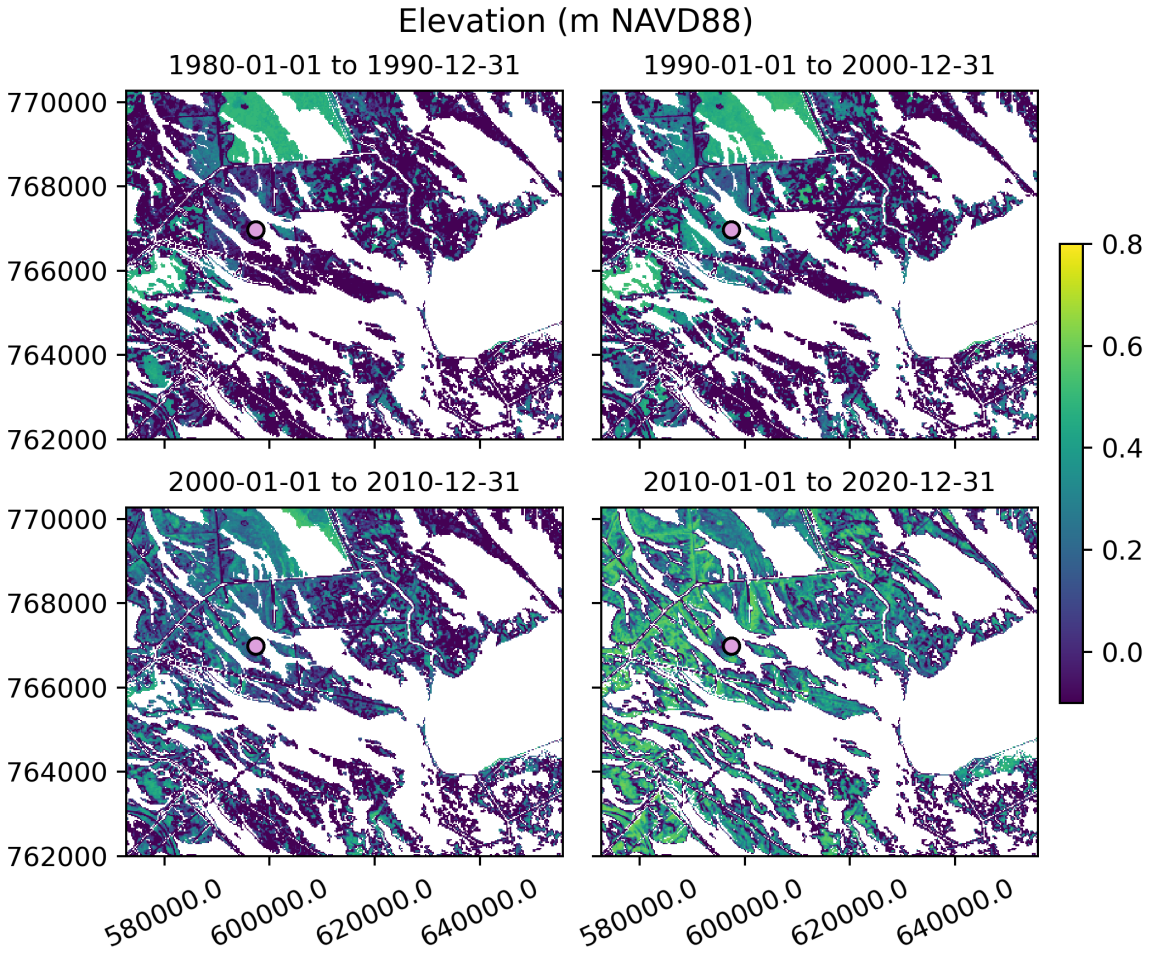

Figure 59. Breton elevation timeseries maps, upper basin. Lavender dots with black outlines represent the locations of SETs at this location.

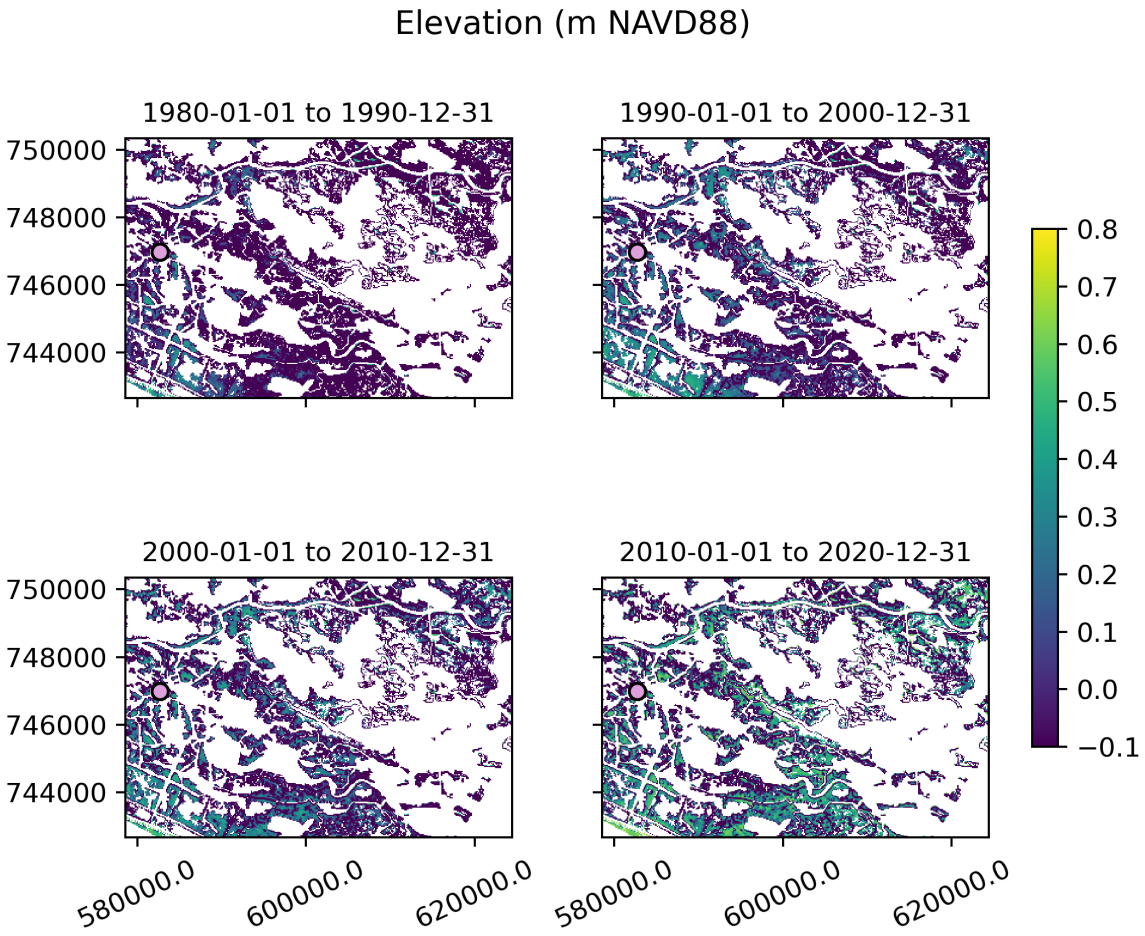

Figure 60. Breton elevation timeseries maps, mid-basin. Lavender dots with black outlines represent the locations of SETs at this location.

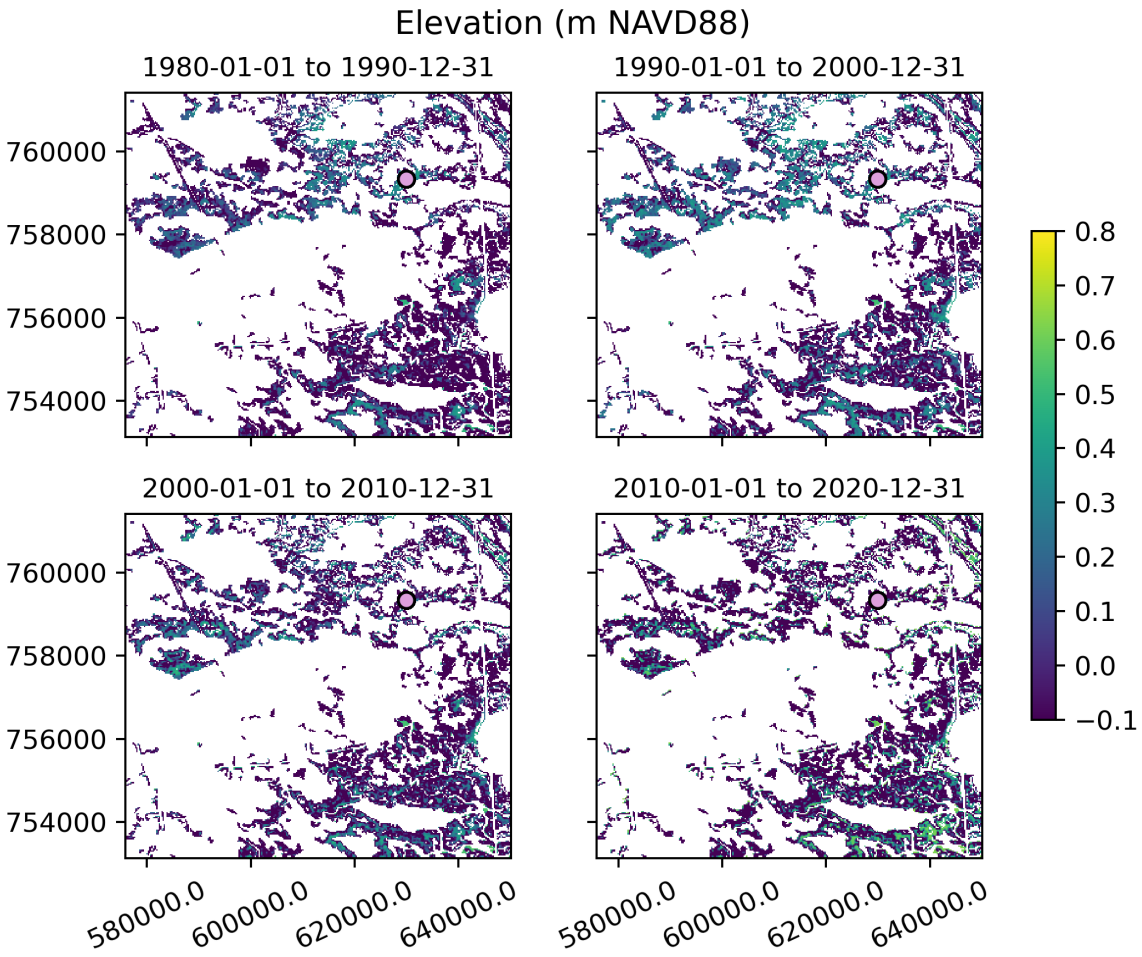

Figure 61. Breton elevation timeseries maps, lower basin. Lavender dots with black outlines represent the locations of SETs at this location.

3.3.3 Validation to Observational Data

The figures in this section show the elevations in the synthetic DEMs at the location of the SET control data. Solid colored circles indicate the synthetic elevation at the pixel of the indicated SET monument. The time series of average SET-derived elevations at each site is shown as a solid line, and the measurements that were used to derive that average (mean elevation at each SET arm position) are shown in pale dots. Elevations from the directly observed DEM are shown as stars. The largest star shows the value of that DEM when resampled to Landsat resolution, while the smaller dots show the value of all of the pixels at full resolution that sit within the footprint of the Landsat pixel. Note here that a substantial component of the total uncertainty in the synthetic DEM process seems to arise from the resampling of the directly observed DEM to the 30m Landsat resolution. Only a selection of the SET data is shown in this report. Remaining data can be found in the supplemental figure archive described in Appendix B.

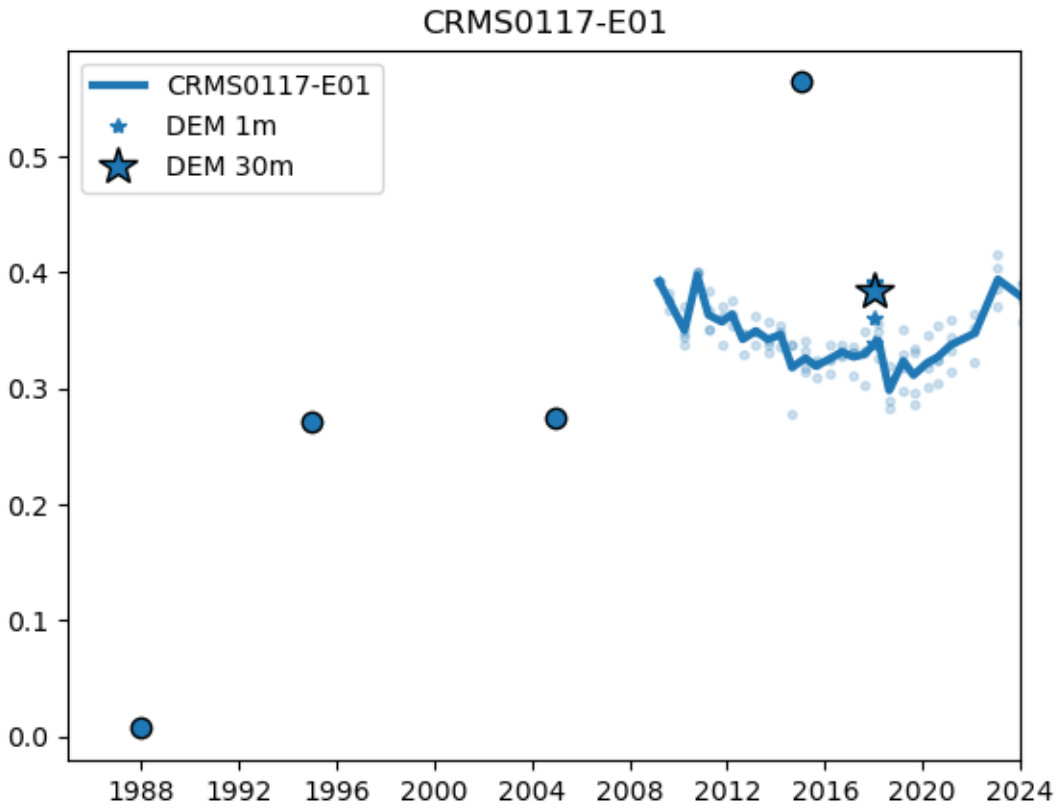

Figure 62. Synthetic DEM validation to CRMS station 01117.

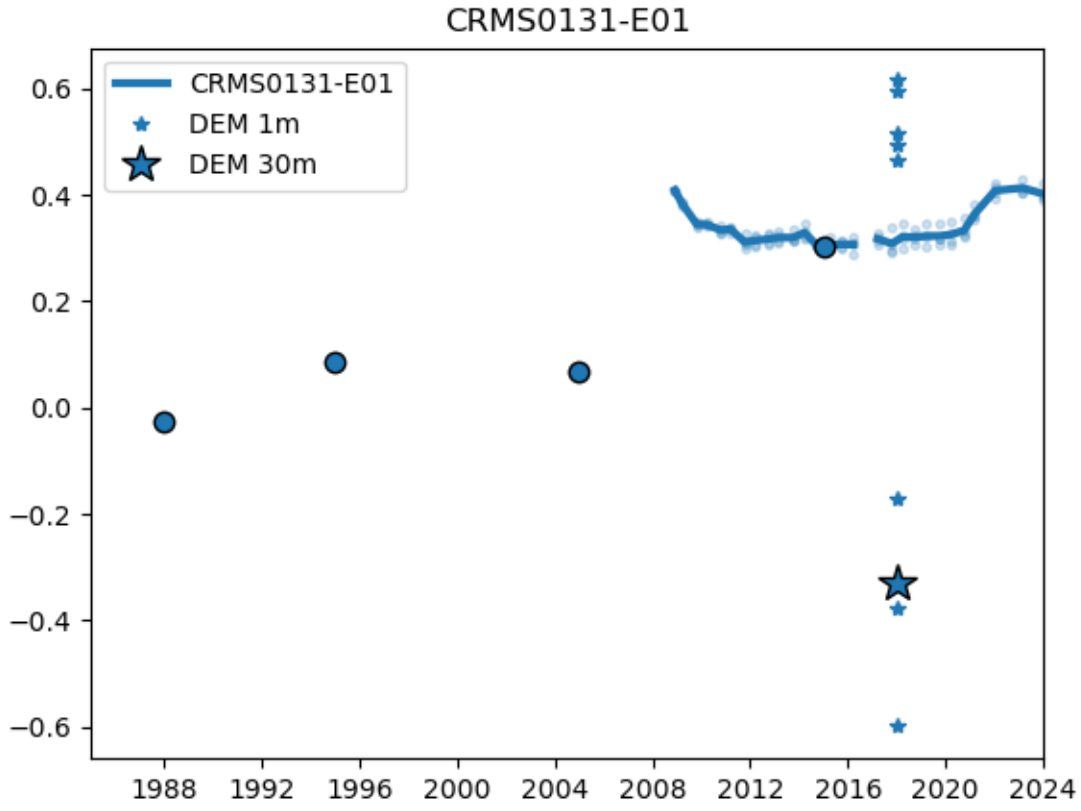

Figure 63. Synthetic DEM validation to CRMS station 01131.

4.0 DISCUSSION AND CONCLUSIONS

The workflow demonstrated in this report is sufficient to produce synthetic DEMs for any tidally influenced location provided that 1) a sufficient water level record exists, 2) an existing DEM or other spatially continuous elevation map exists during the period of 1982 to the present, and 3) there is a robust relationship between elevation and inundation.

The best performance observed among the three study sites was at Grand Bay, where the mean difference between synthetic DEM from the 2010 – 2020 time period and the LiDAR derived DEM from the same time period was 1 cm, with a standard deviation of 13 cm. Performance at Apalachicola was less accurate, with a mean biased by 4 cm and a standard deviation of 18 cm. And the performance at Breton was less accurate still, with a bias of 4 cm and a standard deviation of 40 cm.

One possible explanation for the lower performance at Apalachicola is that the fluvial influence from the river disrupts the relationship between elevation and inundation that the synthetic DEM workflow depends on. However, despite that, the results at Grand Bay and Apalachicola are likely to be sufficient starting points for coastal marsh modeling efforts. In both cases a range of +/- 1 standard deviation in the errors would place most of the error within the range of a typical LiDAR survey (Alizad et al., 2020). And a +/- 2 standard deviation range would still be within the typical tidal range of a wetland on the northern Gulf coast. It is unlikely, though, that this synthetic DEM production workflow would be a functional way to produce elevation maps in Breton Sound. The Breton estuary is too hydraulically complex to provide the meaningful relationship between inundation and elevation that the workflow depends on, resulting in the large observed errors.

While the focus of this effort is to produce synthetic DEMs, the inundation maps that were produced as intermediate data products are likely to be highly useful to retrospective marsh model calibration efforts. The inundation maps have the benefit of being relatively straightforward to produce and are derived through a simple weighted average of an established and widely applied remote sensing product. They are therefore subject to less interpretation than the synthetic DEMs, and with some specific validation can be regarded as an authoritative estimate of coastal wetland inundation. Further, many coastal marsh models first produce estimates of inundation that become inputs for ecosystem dynamics models (e.g. Alizad et al., 2016; Clough, 2016), which allows for a direct conduit for the inundation maps to become incorporated into modeling workflows.

From this first effort using a novel workflow, four paths to improving this work are suggested.

1. A simple linear regression was used in this study as the functional relationship between wetland inundation and elevation. This choice was made for simplicity during this initial workflow development, and to facilitate clearer conversation with the marsh modelers who would be using the synthetic DEMs. But further efforts with spatially aware techniques and modern machine learning workflows are likely to ameliorate some of the errors that were seen to cluster around high topographical gradients in the three study sites.

2. The synthetic DEMs as well as the inundation maps will form the basis of a recently initiated comparative wetland modeling effort. This effort also presents an opportunity to experiment with iteratively correcting the synthetic DEMs based on comparisons of numerical model outputs with the wetland inundation maps. This could be a productive way of indirectly improving the performance of the synthetic DEMs.

3. The synthetic DEM workflow necessitates resampling an existing DEM to the Landsat spatial scale of 30 m pixels. This adds substantial uncertainty to the process, as is evident in the observational data validation figures. The resampling is necessary because the input DEM data needs to be gridded to Landsat resolution of 30m. Most of the available DEMs come at a 1m resolution, however, so this requires resampling ~900 points into a single grid cell, losing that variability in the averaging process. It was necessary to use Landsat in this effort because the objective was to produce synthetic DEMs for as far back as the 1980s. But there are other satellite remote sensing platforms available for more recent decades that also provide DSWE equivalent data outputs. An examination of these could provide insight into improvements that can be made to the workflow's treatment of Landsat data.

4. Finally, the wetland inundation frequency calculation described in Section 2.1 relies on a single point of water surface elevation, thereby making an implicit assumption that there is no spatial variability in water surface elevation. This is not correct in most coastal wetland applications, and an immediate improvement to this methodology could be made by incorporating spatial variability into the water level weighting calculation.

5.0 REFERENCES

Alizad, K., Hagen, S. C., Morris, J. T., Bacopoulos, P., Bilskie, M. V., Weishampel, J. F., & Medeiros, S. C. (2016). A coupled, two-dimensional hydrodynamic-marsh model with biological feedback. *Ecological Modelling*, *327*, 29–43. https://doi.org/10.1016/j.ecolmodel.2016.01.013

Alizad, K., Medeiros, S. C., Foster-Martinez, M. R., & Hagen, S. C. (2020). Model Sensitivity to Topographic Uncertainty in Meso- and Microtidal Marshes. *IEEE Journal of Selected Topics in Applied Earth Observations and Remote Sensing*, *13*, 807–814. https://doi.org/10.1109/JSTARS.2020.2973490

Center for Operational Oceanographic Products and Services. (2026). Coastal Ocean Reanalysis (CORA) [Data set]. Retrieved from https://www.fisheries.noaa.gov/inport/item/75048

Clough, J. S. (2016). SLAMM Technical Documentation, 100.

CRMS. (2023). Coastwide Reference Monitoring System. Retrieved June 20, 2023, from https://www.lacoast.gov/crms/Home.aspx

Earth Resources Observation and Science (EROS) Center. (2022a). *Landsat Level-3 Dynamic Surface Water Extent, Collection 2 [dataset]. U.S. Geological Survey*. U.S. Geological Survey. Retrieved from https://doi.org/10.5066/P9DPWBUS

Earth Resources Observation and Science (EROS) Center. (2022b). *Landsat Level-3 Dynamic Surface Water Extent, Collection 2 [dataset]. U.S. Geological Survey*. U.S. Geological Survey. Retrieved from https://doi.org/10.5066/P9DPWBUS

Hossain, M. S., Bujang, J. S., Zakaria, M. H., & Hashim, M. (2015). Assessment of the impact of Landsat 7 Scan Line Corrector data gaps on Sungai Pulai Estuary seagrass mapping. *Applied Geomatics*, *7*(3), 189–202. https://doi.org/10.1007/s12518-015-0162-3

Jones, J. W. (2015). Efficient Wetland Surface Water Detection and Monitoring via Landsat: Comparison with in situ Data from the Everglades Depth Estimation Network. *Remote Sensing*, *7*(9), 12503–12538. https://doi.org/10.3390/rs70912503

Jones, J. W. (2019). Improved Automated Detection of Subpixel-Scale Inundation—Revised Dynamic Surface Water Extent (DSWE) Partial Surface Water Tests. *Remote Sensing*, *11*(4), 374. https://doi.org/10.3390/rs11040374

Martin, S., Cameron, C., Collini, R., Woodard, N., Buckel, C., Meckley, T., et al. (2022). *Marsh Model Retrospective Workshop* (p. 84). Beaufort, NC: Place: SLR. Retrieved from https://placeslr.org/wp-content/uploads/2022/08/Marsh-Model-Retrospective-Workshop-Final-1.pdf

Medeiros, S. C., Hagen, S., Weishampel, J., & Angelo, J. (2015). Adjusting Lidar-Derived Digital Terrain Models in Coastal Marshes Based on Estimated Aboveground Biomass Density. *Remote Sensing*, *7*(4), 3507–3525. https://doi.org/10.3390/rs70403507

Medeiros, S. C., Alizad, K., Abdelwahab, K., & Bobinsky, J. S. (2022a). Adjusted digital elevation models (DEMs) for the Apalachee Bay region of the Florida panhandle, representative of 2018-03-01 conditions (NCEI Accession 0256313) [Data set]. NOAA National Centers for Environmental Information. https://doi.org/10.25921/Z1EN-YX85

Medeiros, S. C. ., Alizad, K., Abdelwahab, K., & Bobinsky, J. S. (2022b). Adjusted digital elevation models (DEMs) for the lower Pascagoula River region in Mississippi representative of 2019-03-31 conditions (NCEI Accession 0256369) [Data set]. NOAA National Centers for Environmental Information. https://doi.org/10.25921/KCCA-FK49

NOAA, GOMA, NGOM, & Sea Grant MS-AL. (2018). *Northern Gulf of Mexico Sea Level Rise and Marshes Workshop*. Retrieved from https://placeslr.org/wp-content/uploads/2021/05/Sea-Level-Rise-and-Marshes-Workshop-2018.pdf

Snedden, G. A. (2019). Patterning emergent marsh vegetation assemblages in coastal Louisiana, USA , with unsupervised artificial neural networks. *Applied Vegetation Science*, *22*(2), 213–229. https://doi.org/10.1111/avsc.12425

USGS. (2020). USGS 1 Meter LA_CoastalLouisiana_2020_D20 [Data set]. Retrieved from https://www.sciencebase.gov/catalog/item/6572b1b6d34e952b22742a53

APPENDICES

APPENDIX A. CODE DOCUMENTATION

An extensive body of code was developed in python for this project and is available in a public repository on GitHub at https://github.com/waterinstitute/marsh_dem. The code base is broken into four primary modules, as well as documented scripts that employ the module functions. The four modules are:

1. image_pipeline.py
   Code to download, organize, and query the DSWE data.

2. imfreq.py
   Code to produce image frequency maps from the downloaded DSWE data.

3. synthmap.py
   Code to correlate image frequency maps with LiDAR DEMs to produce the synthetic DEMs.

4. synthmap_tools.py
   Code to display, QA, and adjust the synthetic DEMs.

The overall workflow is shown in Figure A-1. Full documentation of the code and its use is provided in the GitHub repository. This code is presently being maintained and used for a subsequent project to support coastal marsh modeling.

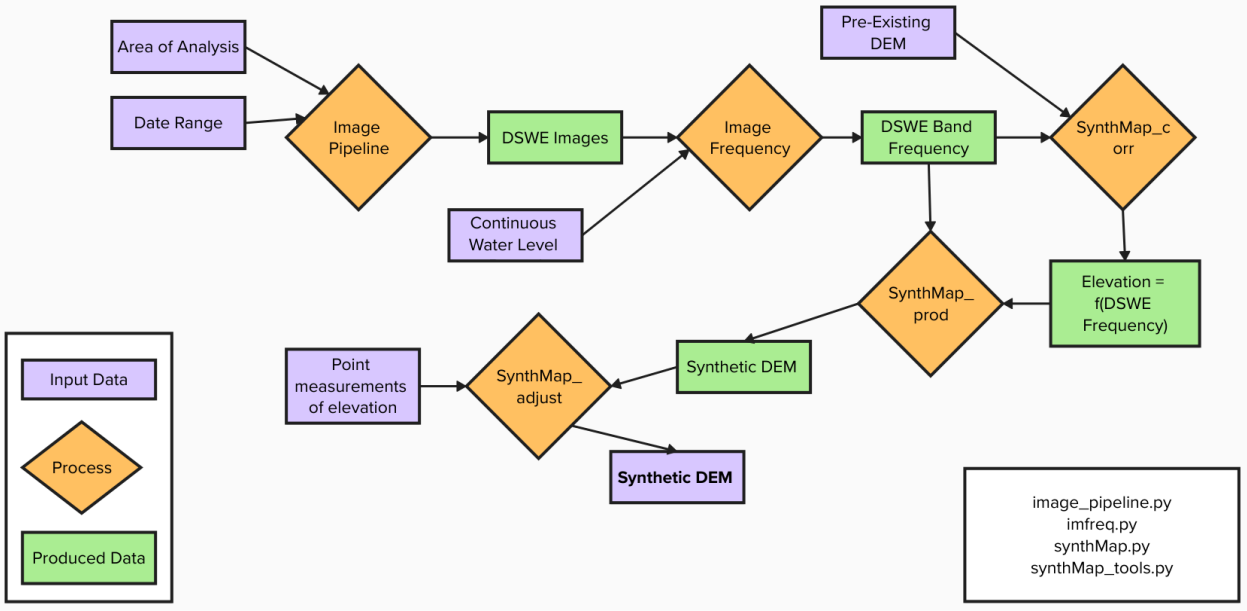

Figure A-1. Flow chart showing image processing and synthetic DEM creation workflow.

APPENDIX B. DATA DELIVERY

The data delivery consists of a directory that contains three subdirectories, each representing data products in one coastal marsh geography. These files are the products of the code described in Appendix A. Further documentation on the processes used to produce them and their formats can be found in the linked github repository.

APA: Apalachicola, FL
GRB: Grand Bay, MS
BRE: Breton Sound, LA

Within the subdirectory for each geography, the \imfreq folder contains maps of wetland inundation frequency for each decade from 1980 to 2020. The subfolder for each decade contains
- an inundation frequency map for each band of the Landsat Dynamic Surface Water Extent product. Images are in geotiff format.
- an index of Landsat DSWE imagery that was used to produce the inundation frequency maps
- diagnostic imagery in .png format

The \synth_maps folder contains synthetic digital elevation models (DEM's) for each decade from 1980 to 2020. Each map is in geotiff format.

APPENDIX C. UNSUITABILITY OF VEGETATION AS A PREDICTOR OF ELEVATION

The initial approach taken in this project was to mine historical vegetation data from in-situ and from remotely sensed data products, with the intent that changes to the spatial distribution of vegetation could indicate changes in relative elevation. The Water Institute project team and partners from NOAA investigated this concurrently, and both groups came to the conclusion that vegetation is not a sensitive enough indicator of elevation to be helpful in the process of constructing historical DEMs.

The NOAA team attempted to use vegetation classifications from the National Wetlands Inventory as elevation predictors. Figure C-1 shows the result of their investigation, that several of the relevant vegetation communities occupy an elevation distribution of multiple meters, so they cannot be sufficiently precise indicators of vertical gradients in coastal wetlands.

The Water Institute team attempted to use vegetation species composition data from the Plum Island Estuary in Massachusetts to conduct a point-based analysis. The approach here was to use a Self-Organizing Map clustering algorithm to find clusters of vegetation that could meaningfully be related to specific elevations. This approach was used productively by Snedden (2019) to map vegetation communities to salinity, but it did not perform as well for elevation. As with NOAA's investigation, The Water Institute team found that the identified species composition clusters often occupied multiple meters of vertical relief, so could not be used as predictors (Figure C-2).

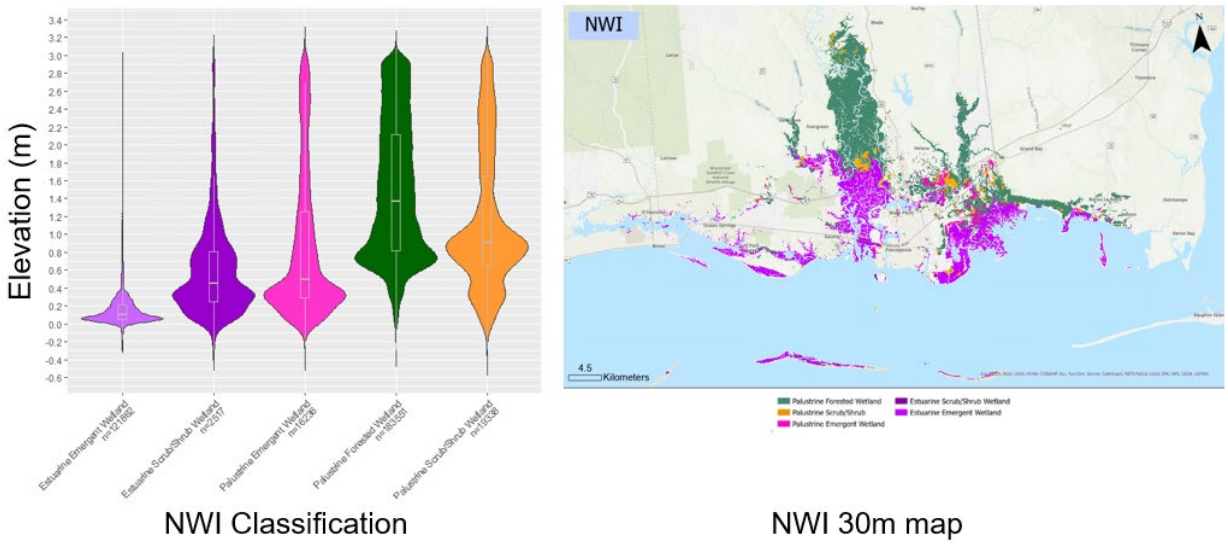

Figure C-1. Spatial distribution of vegetation communities in the National Wetlands Inventory (right), and their distribution as elevation predictors (left). Image courtesy of Christina Cuttshaw, NOAA.

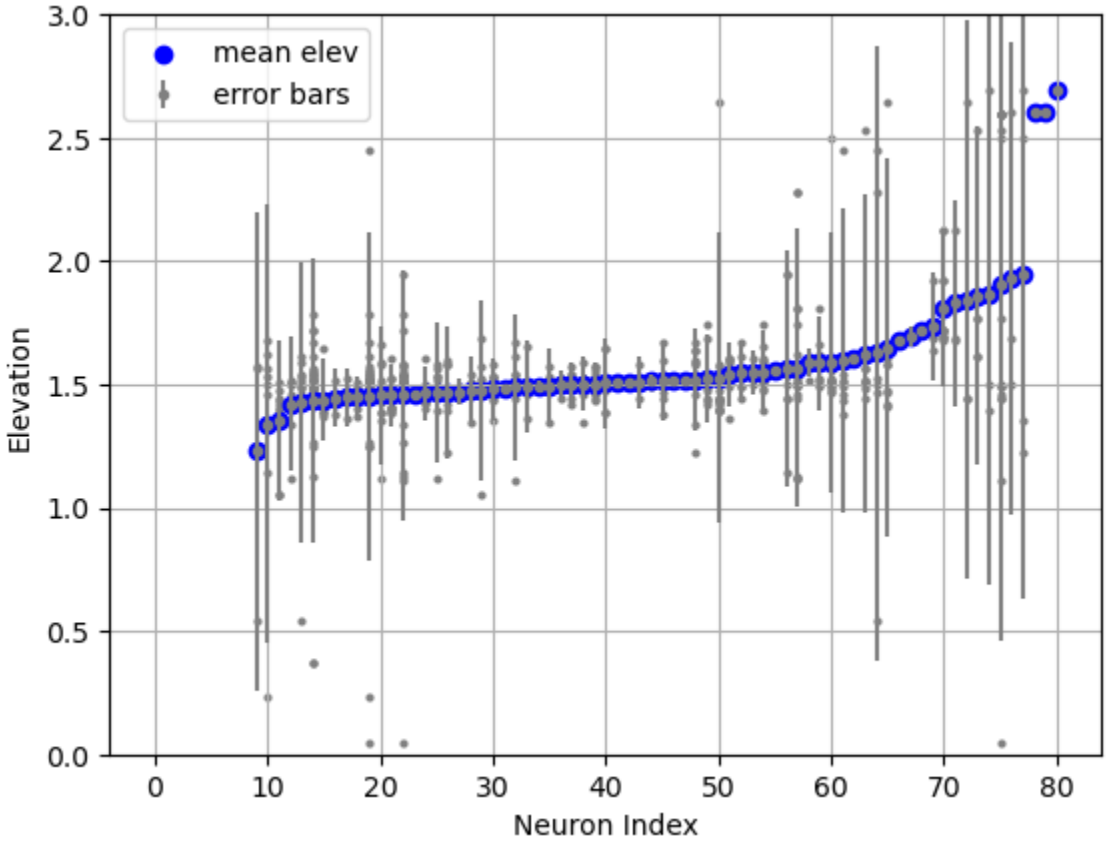

Figure C-2. Neurons representing clusters of similar vegetation species compositions, with mean and error bars of elevation where the sample was collected. From the Plum Island Estuary, Massachusetts.

APPENDIX D. STAKEHOLDER ENGAGEMENT MEETINGS

As part of the project *Advancing Capacity for Marsh Modeling Retrospective Analyses in in the Gulf of Mexico*, four virtual engagement events were held between January 2024 and September 2025, organized by Nina Davis of the Program for Local Adaptation to Climate Effects (PLACE). These events fulfilled the project's deliverables of convening two briefings with marsh modelers and two marsh managers, ensuring iterative input on technical development and clear communication with end users. Each meeting was well attended, generated constructive dialogue, and advanced both technical progress and stakeholder engagement.

D.1 MARSH MODELER KICK-OFF MEETING (JANUARY 2024)

This working session initiated the technical component of the retrospective analysis. Modelers and the project team reviewed the proposed methodology for developing Digital Elevation Models (DEMs), examined data mining efforts since the 2022 workshop, and flagged potential data gaps and methodological issues. Participants left with a shared understanding of the DEM development pathway and its connection to the broader Coastal Ecosystem Prediction System (CEPS) effort.

D.2 COASTAL ECOSYSTEM PREDICTION SYSTEM BRIEFING WITH MARSH MANAGERS (JUNE 2024)

The first marsh manager briefing provided an early project update and an overview of how the retrospective analysis connects to regional and national marsh modeling initiatives. Marsh managers learned about the Community of Practice structure, working groups, and opportunities for engagement. The session ensured managers were well informed about next steps and how their input could shape the project.

D.3 FINAL MODEL MEETING (AUGUST 2025)

The second marsh modeler meeting revisited DEM progress once the products were produced. While DEM construction proved challenging, modelers raised concerns (e.g., uncertainties in Grand Bay, limits of Landsat-based inputs) and suggested refinements. These discussions strengthened alignment among the technical team and helped define clear paths forward for producing robust DEMs across the three sites.

D.4 FINAL MARSH MANGER BRIEFING: DEMS AND MARSH CHANGES (SEPTEMBER 2025)

The final briefing provided marsh managers and partners with an overview of DEM results and practical guidance on their application. The rationale, process, and broad outcomes of DEM development were presented. Following the DEM presentation, recommended and not recommended uses were shared. Participants learned how DEMs can inform regional planning, prioritization, and communication, while recognizing their limitations for permitting, engineering, or site-scale design. The session concluded with discussion on how to stay connected through the Marsh Model Community of Practice.

D.5 OVERALL OUTCOMES

Together, these events created a clear, iterative engagement cycle where modelers helped shape technical products, and marsh managers gained the guidance needed to apply these products effectively. The meetings advanced the creation of the DEM time series, built capacity for retrospective analysis, and strengthened the foundation for future marsh modeling and coastal resilience planning across the Gulf.

1110 RIVER ROAD S., SUITE 200
BATON ROUGE, LA 70802

(225) 448-2813
WWW.THEWATERINSTITUTE.ORG